The Effect of Aluminium Industry Effluents on Sediment Bacterial Communities

Hardeep Gill

Thesis submitted to the

Faculty of Graduate and Postdoctoral Studies

in partial fulfillment of the requirements for the

Master of Science, Biology with Specialization in Chemical and Environmental Toxicology

Ottawa-Carleton Institute of Biology

and

Faculty of Science, University of Ottawa

Thèse soumise à la

Faculté des études supérieures et postdoctorales

dans le cadre des exigences du programme de

Maîtrise ès sciences, Biologie avec spécialisation en chimie et toxicologie de l'environnement

Institut pour la Biologie Ottawa-Carleton

et

Faculté des sciences, Université d'Ottawa

Abstract

The goal of this project was to develop novel bacterial biomarkers for use in an industrial context. These biomarkers would be used to determine aluminium industry activity impact on a local ecosystem. Sediment bacterial communities of the Saguenay River are subjected to industrial effluent produced by industry in Jonquière, QC. *In-situ* responses of these communities to effluent exposure were measured and evaluated as potential biomarker candidates for exposure to past and present effluent discharge.

Bacterial community structure and composition between control and affected sites were investigated. Differences observed between the communities were used as indicators of a response to industrial activity through exposure to effluent by-products. Diversity indices were not significantly different between sites with increased effluent exposure. However, differences were observed with the inclusion of algae and cyanobacteria. UniFrac analyses indicated that a control (NNB) and an affected site (Site 2) were more similar to one another with regard to community structure than either was to a medially affected site (Site 5) (Figure 2.4). We did not observe a signature of the microbial community structure that could be predicted with effluent exposure.

Microbial community function in relation to bacterial mercury resistance (Hg^R) was also evaluated as a specific response to the mercury component present in sediments. Novel PCR primers and amplification conditions were developed to amplify *merP*, *merT* and *merA* genes belonging to the *mer*-operon which confers Hg^R (Table 5.6). To our knowledge, the roles of *merP* and *merT* have not been explored as possible tools to confirm the presence of the operon. Hg^R gene abundance in sediment microbial communities was significantly correlated ($p < 0.05$) to total mercury levels (Figure 3.4) but gene expression was not measurable. We could not solely

attribute the release of Hg^0 from sediments in bioreactor experiments to a biogenic origin. However, there was a 1000 fold difference in measured Hg^0 release between control and affected sites suggesting that processes of natural remediation may be taking place at contaminated sites (Figure 3.7).

Abundance measurements of Hg^R related genes represent a strong response target to the mercury immobilized in sediments. Biomarkers built on this response can be used by industry to measure long term effects of industrially derived mercury on local ecosystems. The abundance of *mer*-operon genes in affected sites indicates the presence of a thriving bacterial community harbouring Hg^R potential. These communities have the capacity to naturally remediate the sites they occupy. This remediation could be further investigated. Additional studies will be required to develop biomarkers that are more responsive to contemporary industrial activity such as those based on the integrative oxidative stress response.

Résumé

L'objectif de ce projet était de développer de nouveaux biomarqueurs bactériens en vue de déterminer l'impact des activités de l'industrie de l'aluminium sur l'écosystème environnant. Les communautés bactériennes des sédiments de la Rivière Saguenay sont exposées à des effluents provenant des établissements industriels de Jonquière, QC. Nous avons mesuré les changements, in-situ, des communautés microbiennes exposées aux effluents afin d'évaluer leur potentiel en tant que biomarqueurs d'exposition aux activités présents et passés.

Nous avons évaluer la structure et la composition des communautés bactériennes entre les sites contrôles et les sites affectés. Les différences observées entre les communautés ont été utilisées comme indices de réponse à l'activité industrielle. Nous n'avons pas observé de différence significative entre les indices de diversité des sites affectés par le complexe industriel et les sites contrôles. Les analyses UniFrac ont démontrées que la structure de la communauté du site de contrôle (NNB) et d'un des sites affecté (Site 2) avait une plus grande similarité entre elles qu'avec un site moyennement affecté (Site 5) (Figure 2.4). Nous n'avons pas observé de signal distinct de la communauté microbienne qui pouvait être attribué à l'exposition aux effluents.

Nous avons aussi étudié l'impact du mercure présent dans les sédiments sur la résistance microbienne au mercure (Hg^R). De nouvelles amorces de PCR ainsi que des nouvelles conditions d'amplification ont été développé afin d'amplifier les gènes *merP*, *merT* et *merA*, tous faisant parti de l'opéron *mer* qui confère la Hg^R (Table 5.6). À notre connaissance, le rôle de *merP* et *merT* en tant qu'outil permettant l'étude de la distribution de l'opéron *mer* dans l'environnement n'avait, jusqu'à cette étude, jamais été exploré. L'abondance des gènes de Hg^R parmi les communautés microbiennes était corrélée de façon significative ($p < 0.05$) avec les

concentrations en mercure total (Figure 3.4) mais l'expression des gènes n'a pu être quantifiée. La production de Hg^0 estimée à l'aide d'expérience conduites en bioréacteurs contenant des sédiments n'a pu être attribué uniquement à une source biogénique, malgré une différence d'un facteur de 1000 entre l'émission de Hg^0 des sites affectés et du site contrôle. Ceci nous porte à croire qu'un assainissement naturel pourrait avoir lieu aux sites contaminés (Figure 3.7).

L'abondance des gènes de résistance au mercure représente un bon indice du mercure immobilisé dans les sédiments. Des biomarqueurs qui exploitent ce principe pourraient servir à l'industrie afin de mesurer les effets à long terme du mercure contenu dans les effluents sur les écosystèmes locaux. L'abondance des gènes de l'opéron *mer* dans les sédiments des sites contaminés indique la présence d'une communauté microbienne prospère ayant un potentiel de résistance au mercure. Ces communautés ont la capacité d'assainir leur environnement et cette capacité pourrait être étudiée davantage. Des études supplémentaires sont nécessaires pour développer des biomarqueurs qui sont plus sensibles à l'activité industrielle contemporaine telle que ceux basées sur la réponse intégrative au stress oxydatif.

Acknowledgements

"It was the best of times, it was the worst of times…"

– Charles Dickens, *A Tale of Two Cities* (1859)

I find these words best represent my experience as a graduate student. Over these past two years it has indeed been the best and worst of times. This thesis is the crystallization of the work that was done during my time at the University of Ottawa. The efforts put forth have not been solely my own but also belong to those whom I have had the privilege to work with. First among these individuals is Dr. Alexandre Poulain. Alex, without your guidance, mentorship and above all patience this work could not have been completed. I am deeply indebted to you for your help. You fostered an environment that helped teach me the meaning of true excellence.

Lab work could not have taken flight were it not for the technicians I had the pleasure of working with. Dr. Emmanuel Yumvihoze and Philip Pelletier, thank you for your help in matters related and unrelated to the scientific endeavour. Emmanuel, I knew I could always count on your calm and steady demeanour when I came asking for help regarding the chemical analyses. Thank you for answering all of my questions and processing a great majority of those samples we brought back from the Saguenay. Phil, you always had an upbeat attitude. I found within your tenacious, indomitable work ethic and pleasant nature an example by which to operate. I thank you for all of the shared coffee breaks, conversation and help with the molecular work.

In light of the current circumstances regarding the political apathy towards environmental science, it will become all the more important to foster contacts with the private sector to support research. My project reflects such a collaboration, thus I must acknowledge our industrial contact, RioTinto Alcan for their support of my research. Furthermore, I am very grateful to our

industry contacts, Hélène Pinard, Amiel Boullemant and their team for their help in coordination of field work and logistics.

To my fellow students, Michelle, Charlotte, Dima, Maggie, Felix and Julien, throughout all of the trials and tribulations considered normal in science, I found solace in our shared experiences. Thank you for all of the random favours, explanations and crazy field trips. To Maggie in particular, without whom a chapter of this thesis would not have materialized, your energy and vibrant spirit I always found uplifting. Thank you for helping me with the sequence work. I'm happy to have had the opportunity to work with all of you.

To my friends and roommates, thank you for helping me to keep things in perspective. When times became rough, I knew I could always find good company in which to temporarily find retreat. Adam and Nigel, I'm happy to have had you with me in this journey. Brendan, Andrew, Arthur, Mariam, Dave, Rohan and Gabe, all of the time spent in the lab during weekends did not feel so gruelling knowing I had your company to share.

And finally to my family, Mom, Dad and Darcie, I would not be the person I am today were it not for your undying love and support through some of the most trying times in my life. I am so blessed to have you behind me in whatever endeavour I find myself pursuing. I dedicate this thesis to you, with my fullest gratitude and appreciation for creating some of the best of times, while helping me through the worst.

Sincerely,

Hardeep Gill

Ottawa, ON – May 2012

Table of Contents

List of Abbreviations

16S rRNA	gene encoding the 16S ribosomal RNA component of prokaryotic ribosomes
ArsC	arsenate reductase
bp	base pair
Ca^{II}	divalent ionic calcium
Cd^{II}	divalent ionic cadmium
cDNA	complimentary deoxyribonucleic acid
CVAAS	cold vapour atomic absorption spectrometer
CVAFS	cold vapour atomic fluorescence spectroscopy
DEPC	diethylpyrocarbonate
DNA	deoxyribonucleic acid
EC	enzyme classification number
GDP	Gross Domestic Product
glnA	gene encoding glutamine synthetase (GlnA)
HDPE	high density polyethylene
HEPA	high efficiency particulate air
Hg^{0}	volatile elemental mercury
Hg^{I}	monovalent ionic mercury
Hg^{II}	divalent ionic mercury
Hg^{R}	bacterial mercury resistance
ICP-MS	inductively coupled plasma mass spectrometry
IJC	International Joint Commission
katG	gene encoding catalase-peroxidase (KatG)
LB	*Luria-Bertani* medium (lysogeny broth)
merA	gene encoding mercuric reductase enzyme (MerA)
merB	gene encoding organomercurial lyase (MerB)
merP	gene encoding periplasmic mercury binding protein (MerP)
merR	gene encoding Hg^{II} responsive *mer*-operon regulator protein (MerR)
merT	gene encoding cytosolic membrane mercury transport protein (MerT)
MGE	mobile genetic element
mRNA	messenger RNA

NADPH	Nicotinamide adenine dinucleotide phosphate
NB	North Beach
NmerA	mercuric reductase variant
NNB	New North Beach
NSB	New South Beach
OSR	oxidative stress response
OTU	operational taxonomic unit
PAH	polycyclic aromatic hydrocarbon
Pb^{II}	divalent ionic lead
PCR	polymerase chain reaction
PLFA	phospholipid fatty acid
QA/QC	quality assurance/quality control
qPCR	quantitative polymerase chain reaction (real-time PCR)
RDP	Ribosomal Database Project
RNA	ribonucleic acid
ROS	reactive oxygen species
rpoB	gene encoding the β subunit of RNA polymerase (RpoB)
SB	South Beach
SPL	spent pot-lining
THg	total mercury
US EPA	United States Environmental Protection Agency
Zn^{II}	divalent ionic zinc

List of Tables

List of Figures

1.0 Introduction

1.1 Industry and the Environment

The industrial revolution brought with it advances in manufacturing, mass production and economic growth (Clark, 2007). Manual labour was replaced with automated machinery, plant material was replaced by coal as a fuel source, and the growth of GDP surged (Clark, 2007). Arguably, the expansion of industrial practice proceeded to improve the living standards of people due to the benefits of increased household income and access to affordable commercial goods (Clark, 2007). Industry and related processes have continued to grow since the dawn of the revolution. The effects of such growth have influenced a multitude of factors, both positively and negatively. Environmental integrity is one factor that has been negatively affected.

The environmental consequences of unrestrained industrialization have been brought to light in the past half century. Public awareness of environmental degradation was generated in part due to social environmental movements. Literary titles such as *Silent Spring* (Carson, 1962) bolstered public outcries against the destruction of the environment for economic and financial gain. Ultimately, these vocal protests led to the establishment of government agencies and departments charged with the protection of the environment (Costa, 2007). In the United States, the Nixon administration founded the United States Environmental Protection Agency (US EPA) in 1970. One year later, the federal government of Canada established its own department of the environment (Environment Canada).

Agencies and departments of the environment upheld new regulations enacted to protect the natural environment from future harm. To that end, it was necessary to characterize the shape and form of the damage inflicted. Initially, the damages characterized pertained chiefly to the human perspective using classical toxicology as a guide (Van-Straalen, 2003); *ecotoxicology*, as originally defined by René Truhaut, encompassed effects upon humans (Truhaut, 1977).

Contemporary definitions take a holistic approach in determining the effect of industrial activity on the entire ecosystem (Di-Giulio & Newman, 2007). Ultimately, regulatory efforts serve to prevent future degradation using the descriptives of past oversight. For historically perturbed contexts, reclamation and renewal of the ecosystem is the primary objective.

Endeavours to protect the environment are facilitated when industry and controlling corporations themselves enthusiastically take part in the process. Public pressure, once directed at government, is now targeting private enterprise. Success has been generated in the push for an agenda of corporate social and environmental responsibility; many industrial companies are now seeing environmental protection and the sustainable use of natural resources as a necessary component of their business model. This project represents a collaborative effort between academia and industry. Together with our partners, we sought to determine and characterize the effects of aluminium industry processes on the local environment.

Our industrial partners belong to the mineral processing industry in Canada. Their operations focus on the production of primary aluminium through the refinement of ores and smelter operations. It is understood that industrial undertakings do not come without an element of environmental disturbance. The collaboration was established for this reason and we worked to develop biological markers of exposure to effluent by-products.

1.2 Canadian Mining & Mineral Processing Industries

Mining, mineral processing and metal manufacturing represent a significant portion of the Canadian economy. In 2009 the industry employed over 300 000 individuals and had production activity valued at over $32 billion, or roughly 2.7% of total Canadian GDP (Trelawny & Pearce, 2009). Despite the negative impacts of the global recession and a strong Canadian dollar the industry still accounts for 17% of total Canadian trade (import and export) with metal

exports alone totalling $49 billion in 2009 (Trelawny & Pearce, 2009). With worldwide demand for raw material resources increasing, most notably from China, the world's fastest growing and second largest economy, Canada is solidifying its role as a global resource producer. Of Canadian exports to China, minerals and metals comprise nearly one-third of the total (Trelawny & Pearce, 2009). As such, industry growth is projected to increase by 6.4% year-over-year from 2010 to 2013 (Trelawny & Pearce, 2009).

1.2.1 Canadian Aluminum Industry

Aluminum is the third most abundant element in the Earth's crust after oxygen and silicon (Turekian & Wedepohl, 1961). It is used extensively by society due to its ready availability, high strength, good conductivity, light weight, malleability, ductility, resistance to corrosion and ease of recycling. Its use can be seen in many industries seeking to exploit these favourable properties, including building and construction, automotive, aeronautics and aviation (Jones & Haynes, 2011). At the close of 2009, world production of primary aluminum stood at over 36 million tonnes (Mt) with Canada contributing roughly 12%, through a national production capacity of over 3 Mt per annum (Sass, 2009). This placed Canada as the third largest producer of aluminum in the world after China (13.3 Mt) and Russia (3.3 Mt) (Jones & Haynes, 2011). The Canadian aluminum produced during that year accounted for approximately 15% of the $32 billion total-mineral-industry production value (Sass, 2009, Jones & Haynes, 2011). Of national production capacity, over 90% of Canadian aluminum was produced in the province of Quebec with one-third of national output being further situated in the Saguenay Fjord region (Figure 1.1) (Sass, 2009). The industry has been attracted to the Saguenay region due to its relatively cheap hydropower capacity (RéseauTransAl, 2007, Hydro-Québec, 2011) which has

been able to meet the requirements of the aluminum smelting industry - primary aluminum production requires a large supply of electric power.

1.3 Industrial Processes

The production of primary aluminum begins with the extraction of bauxite, the mineral form of aluminum, from bauxite mines. These mines are located in close proximity to the equator (Mimna*, et al.*, 2011). Bauxite, a heterogeneous mixture of alumina and other oxides of aluminum, silica and iron, among other impurities, is used as the feedstock to generate alumina (Al_2O_3) by the Bayer Process (Jones & Haynes, 2011, Mimna*, et al.*, 2011). The purified alumina is then subsequently processed via the Hall-Héroult Process, producing the primary aluminum metal (Habashi, 2005).

1.3.1 Bayer Process

The Bayer Process serves to dissociate aluminum oxide from bauxite ore impurities through alkaline chemical digestion which solubilizes aluminum oxide. Caustic soda (NaOH) is applied to milled bauxite at high temperatures (~175°C). This produces aqueous aluminum hydroxide ($[Al(OH)_4]^-$) and separable non-soluble ore impurities, known collectively as "red mud" (Jones & Haynes, 2011). After the red mud has been removed by filtration, aluminum oxide is precipitated in the form of alumina trihydrate ($Al_2O_3 \cdot 3H_20$) by cooling the solution and seeding it with pure alumina which aids crystallization (Habashi, 2005). The crystals are then dehydrated via calcination at temperatures greater than 1,100°C leaving pure alumina – a fine, dry, white powder (Trelawny & Pearce, 2009).

The Bayer Process produces approximately one to two tonnes of red mud waste for each tonne of alumina produced (Mimna*, et al.*, 2011). Thus, the remnant can pose a problem due to its alkalinity and composition. Industrial treatment of red mud usually consists of storing the

waste slurry in tailings ponds adjacent to refineries. Here they are allowed to dry prior to disposal.

1.3.2 Hall-Héroult Process

The Hall-Héroult Process involves reductive electrolysis of alumina dissolved in cells of molten cryolite (Na_3AlF_6) which conducts electricity at roughly 970°C (Habashi, 1998). The electron flow is introduced into the cell through a carbon anode and propagates through the cryolite solution to the cathode (Habashi, 1998). Alumina in the solution then reacts with the anode forming aluminum and carbon dioxide (CO_2) which volatilizes out (Habashi, 1998). The molten aluminum sinks to the bottom of the reduction cell to be subsequently siphoned, transported and cast into final primary metal products (Habashi, 1998).

Reduction cells are lined with material rich in carbon and during the electrolytic process the lining is penetrated with sodium fluoride and cyanide (Agrawal*, et al.*, 2004). After some time, the pot lining becomes exhausted as penetration of these noxious chemicals becomes sufficiently high (Agrawal*, et al.*, 2004). The spent-pot-lining (SPL) is then dug out and replaced. Depending on the facility, 20 to 40 kg of sodium fluoride and cyanide rich SPL waste is generated for each tonne of aluminum produced (Jones & Haynes, 2011). Other waste products from this process include hydrogen fluoride gas, polycyclic aromatic hydrocarbons (PAHs) and fluorocarbons (Agrawal*, et al.*, 2004, Friesen*, et al.*, 2007).

1.3.3 Castner-Kellner Process

As caustic soda digestion of bauxite ore is scaled up to industrial level operations, production of sodium hydroxide (NaOH) to meet industry needs follows suite. NaOH stocks are replenished by chlor-alkali plants. These plants are often located in close proximity to bauxite refineries to facilitate the replenishment of caustic soda stocks. The preferred method of

production is through the mercury-cell process – otherwise known as the Castner-Kellner Process – which works similarly to the Hall-Héroult electrolytic process (Habashi, 1998). A sodium chloride (NaCl) brine solution is subjected to an electric current; electrons flow from the anode, where chlorine is oxidized forming chlorine gas, to the mercury (Hg) cathode where reduced sodium forms an amalgam with Hg (Habashi, 1998). The amalgam is reacted with water producing hydrogen gas, NaOH and Hg to be recycled in the process once more (Habashi, 1998).

The mercury-cell process is preferred as it yields a caustic soda mix with fewer chlorine impurities (Habashi, 1998). However, as a result of the industrial use of Hg, the risk of exposure to this toxic element in an environmental context is ever present (Gagnon*, et al.*, 1997) and proper management is required to mitigate release. An example of poor management can be found in the area of the St. Lawrence River near Cornwall, Ontario, Canada. Cornwall once hosted pulp and paper mills and a chlor-alkali plant (Delongchamp*, et al.*, 2009). Here, industrial activities contaminated the local watershed with mercury ultimately forcing the zone to be classified as an "Area of Concern" by the International Joint Commission (IJC) in 1985 (Delongchamp*, et al.*, 2010).

1.4 Project Context

There exist many industrial by-products of aluminum smelting and bauxite refining, such as PAHs, fluoride, aluminium and other metals (Legault, 1996, Mimna*, et al.*, 2011). While proper safeguards and measures are usually implemented to mitigate the production and release of these chemicals, accidents have occurred in the past (Gelencser*, et al.*, 2011, Ruyters*, et al.*, 2011). Some facilities may see accidents consisting of caustic soda spillage, release of untreated water and hydrocarbon leakage. These events seriously disrupt the health of both the local ecosystem and the local population. This project will focus on the past and present-day activities

of the Jonquière smelter and refinery complex of the Saguenay River region (Figure 1.2). Because of the nature of past operations some contaminants still remain in river sediments and may influence the findings of this project (Gagnon*, et al.*, 1997).

The river stretches approximately 165 km and drains waters from Lac Saint-Jean into the Saint Lawrence River at Tadoussac, QC. The Saguenay-Lac Saint-Jean region is home to approximately 275 000 people (StatsCan, 2012) spread across various townships and cities around the lake and along the river. In 1926 the smelter plant became operational in Arvida (now Jonquière). As production was scaled-up a chlor-alkali plant was constructed on site in the late 1940s to meet the growing demand for caustic soda. However, the plant was later decommissioned in 1976 (Gagnon*, et al.*, 1997). Thus, any Hg within effluents derived from current industrial activity is no longer attributed to this process.

Presently, industrial effluent produced by the Jonquière complex is discharged through channels that empty into Saguenay River (Figure 1.2). While the effluent is either treated or recirculated within the industrial process, the region has seen accidental spills from red mud tailings ponds. Spills can arise due damage in piping systems or technical errors resulting in overflows. Additionally, the effluent treatment process may not be entirely efficient at removing all traces of remaining contaminants. Because of the accidents, and because contaminants may still be released from contemporary activities, the presence of these by-products (*e.g.* Hg) within the sediments and water column of the river is suspected (Loring*, et al.*, 1983, Gagnon*, et al.*, 1997). It should be noted that the aluminium industry currently operates within established provincial regulations. Any trace contaminant release in effluents should be at concentrations under the level put forth by environmental guidelines.

1.5 Project Rationale

The use of aluminum is not forecasted to decline in the near future. Thus, the mitigation of any negative environmental impact of aluminum production will not consist of diminished industrial activity. Rather, improved environmental stewardship, safe practice and responsible safeguards to prevent spills will serve to this end. Appropriate environmental monitoring of the local environment will ensure that the health of the ecosystem and its inhabitants are maintained.

Contaminant release into watersheds often triggers the oxidative stress response (OSR) of aquatic organisms residing there (Valavanidis*, et al.*, 2006). The OSR is characterized by the inability of cellular antioxidant systems to cope with the imbalance of reactive oxygen species (ROS). Currently, fish-based biomarkers of the OSR are used for aquatic toxicological assessments of industrial impact (Miller*, et al.*, 2009). This approach in ecotoxicological assessment is well established. However, limitations arise in experiments using fish. Handling of these organisms requires costly holding facilities, rigorous maintenance and strict adherence to established ethics associated with animal care and use. For these reasons, the development of an alternative approach to assess the influence of industrial activity on local ecosystems is desired. In this project, the effect of past and present industrial activity on the Saguenay River ecosystem was assessed using environmental microbe derived biomarkers. Contemporary activity signifies alumina refining and aluminium smelting while past activities relate chiefly to processes related to the Castner-Kellner Process.

1.6 Project Objectives

The development of novel microbe-based biomarker alternatives carries great potential for industrial use. Bacterial biomarkers offer lower operational costs compared to fish and a wide variety of reporting signals. For example, responses can be derived from the characterization of

gene expression (Schaefer, *et al.*, 2004) or from the changes observed at a microbial community level (Frostegard, *et al.*, 1993). Bacteria also parallel fish in their ability to exhibit the OSR when exposed to heavy metals and polycyclic aromatic hydrocarbons (PAHs) (Farr & Kogoma, 1991, Orell, *et al.*, 2010).

1.6.1 Bacterial Heavy Metal Resistance Mechanisms

Metals are required in trace amounts for normal bacterial growth, development and vitality. However, problems arise when cellular concentrations of micronutrients exceed certain thresholds. For instance, divalent zinc cations (Zn^{II}) are essential enzyme metal cofactors (Sugarman, 1983) but too much Zn^{II} disrupts aerobic respiratory chain metabolism (Hynninen, 2010). Thus, in order to maintain cellular homeostasis for zinc or other micronutrients, mechanisms to equilibrate cellular concentrations are necessary. This is especially true for microorganisms inhabiting environments with elevated metal levels ($Silver_b$ & Phung, 2005, Gough & Stahl, 2011).

Toxic metal ions have damaging effects on cellular function and health. Divalent cadmium and lead (Cd^{II} and Pb^{II}) are essential trace metal "lookalikes" and displace metalloprotein micronutrient ions such as calcium (Ca^{II}) and Zn^{II} (Nies, 1999). This disrupts enzymatic functionality that could harm cellular wellbeing. Toxic heavy metals such as Cd^{II} and Pb^{II} enter cells using the same transport systems used for essential divalent cations (Hynninen, 2010). Many cellular mechanisms used to control essential trace metal concentrations in cells are also used to resist toxic heavy metal equivalents.

A variety of metal tolerance and resistance mechanisms have been previously described (Osborn, *et al.*, 1997, Nies, 1999, Hynninen, *et al.*, 2009). Intracellular complexation of toxic metal ions with cellular peptides is a primary eukaryotic defence mechanism (Perales-Vela, *et*

al., 2006). Peptide metallothioneins that sequester toxic heavy metals are found in higher plants, algae and fungi (Class II and Class III) as well as most vertebrates (Class I) (Perales-Vela*, et al.*, 2006). Metallochaperone proteins buffer cellular concentrations of essential micronutrients through sequestration and release (Hynninen, 2010).

Prokaryotes primarily detoxify intracellular heavy metals through active efflux channels (Nies, 2003, Hynninen*, et al.*, 2009). While active efflux of toxic heavy metals is the most common metal resistance mechanism among prokaryotes, other mechanisms involve enzymatic reduction-oxidation reactions that transform toxic metal ions into less toxic or more easily transportable forms. Bacterial arsenate reductase (ArsC) of the *ars*-operon facilitates the reduction of arsenate (AsO_4^{-3}), which has an oxidation state of +5 (As^{V}), to arsenite (AsO_2^{-}) with an oxidation state of +3 (As^{III}) (Silver$_a$ & Phung, 2005). This enzymatic reaction is followed by the active efflux of arsenite to the cellular exterior (Hynninen, 2010). Mercuric reductase (MerA) and organomercurial lyase (MerB) of the *mer*-operon respectively transform toxic Hg ions and organic mercurials into the ultimate detoxified and volatile form, elemental Hg (Hg^0) (Barkay*, et al.*, 2003).

In environmental settings, bacterial isolates that hold metal resistance systems range from a few percent in pristine settings to nearly all isolates in metal contaminated contexts (Silver$_b$ & Phung, 2005).

1.6.2 Community Level Response Biomarkers

Community level bacterial responses to toxic metals and other contaminants have been extensively described. Cell macromolecular components are used to "fingerprint" individual species and lineages within community assemblages. This can be useful for determining changes in community structure and composition due to toxicant exposure (Frostegard*, et al.*, 1993,

Muller*, et al.*, 2002, Case*, et al.*, 2007). The Saguenay River hosts aluminium industries that have introduced chemicals to the river system in the form of effluent by-products. Sediment microbial communities along the banks of the Saguenay River are exposed to these complex and dynamic chemical mixtures. The response of these bacterial communities, as assessed through changes in community structure and composition, can yield a response marker to whole-effluent mixture exposure.

1.6.3 Mercury Exposure Response Biomarkers

A component of the chemical by-product mixture is mercury (Hg). In the past, the aluminium industry subjected the surrounding aquatic ecosystem to higher than ambient levels of Hg due to the operation of the chlor-alkali plant (Loring*, et al.*, 1983, Gagnon*, et al.*, 1997). With the closure of the plant, the industrial complex currently operates within the guidelines set by the provincial government. Yet trace amounts of Hg may escape the effluent treatment and recirculation process (Figure 1.3). Additionally, the Hg released in the past is still present in the receiving sediments.

The biological response to the Hg component of past and present effluents can be used to indicate the extent of industrial influence over the Saguenay River through released effluent by-products. The enrichment of bacteria harbouring the ability to detoxify mercurial compounds from their surroundings is considered a biological response specific to Hg exposure (Muller_{a}*, et al.*, 2001). Thus, enzymatically based bacterial mercury resistance (Hg^{R}) was used as a biomarker targeted in this project to evaluate the influence of industrial activity.

Hg was chosen as the specific toxicant of interest because: (i) it is an excellent model to test for microbial responses to anthropogenic activities in the environment; (ii) it is emitted from

the alumina extraction process and hence acts as a tracer of this activity; (iii) the analytical facilities used to measure Hg speciation at trace levels are accessible at the University of Ottawa.

1.6.4 Bacterial Mercury Resistance (Hg^R)

Terrestrial and aquatic microorganisms are exposed to ambient concentrations of Hg which has been present in these mediums since the formation of the Earth. Not all Hg is easily accessible by biological systems. Terrestrial Hg forms complexes with organic molecules that limits its bioavailability (Osborn*, et al.*, 1997). In saline seawaters, mercuric chloride anions ($HgCl_3^-$ and $HgCl_4^{-2}$) dominate over the more bioavailable form $HgCl_2$ (Barkay*, et al.*, 2010). Particular environmental parameters such as redox potential, pH and salinity influence the speciation of Hg and by extension alter its bioavailability (Barkay*, et al.*, 2010). For instance, in environments with high reduction potential Hg exists either as Hg^0 or soluble and insoluble sulfur complexes (Barkay*, et al.*, 2010). These forms of Hg exhibit limited toxicity to biological systems. Hg typically exists in its most toxic oxidative state (Hg^{II}) in oxygenated freshwaters, soils and sediments (Barkay*, et al.*, 2010).

Bacteria have adapted mechanisms to tolerate or detoxify Hg compounds (Osborn*, et al.*, 1997, UNEP, 2002, Barkay*, et al.*, 2003, Barkay & Wagner-Dobler, 2005). Five methods of bacterial mercury resistance (Hg^R) have been identified (Osborn*, et al.*, 1997).

1. **Reduced uptake**: Cellular permeability to Hg^{II} was reduced in *Enterobacter aerogenes* preventing the entry of Hg into the cytoplasm (Pan-Hou$_b$*, et al.*, 1981).
2. **Demethylation of organomercurials followed by sequestration with sulfides**:

Hg from demethylated organomercurials was sequestered through reactions with hydrogen sulfide forming insoluble mercuric sulfide (Pan-Hou$_a$ & Imura, 1981).

3. **Sequestration of methylmercury with sulfate**:

   Concentrations of methylmercury were kept at subtoxic levels in *Desulfovibrio desulfuricans* through production of hydrogen sulfate (Baldi*, et al.*, 1993). Sulfate reacts with methylmercury to form insoluble dimethylmercury sulfide.

4. **Hg methylation**: Methylation of mercury can be a protective mechanism for some bacterial strains, although methylmercury is considered more toxic than Hg^{II} (Osborn*, et al.*, 1997).

5. **Enzymatic Hg^R**: Divalent Hg^{II} cations are reduced to the less toxic and volatile Hg^0.

Enzymatic Hg^R is the focus of this study. Enzymatic Hg^R is controlled by the genes of the *mer*-operon that encode various proteins involved the detoxification pathway (Barkay*, et al.*, 2003, Barkay & Wagner-Dobler, 2005). The *mer*-operon is found in both gram-positive and gram-negative bacteria (Osborn*, et al.*, 1997). Most *mer*-operons hold a regulatory gene (*merR*) which encodes the MerR protein. MerR binds to an operator region (MerO) preventing transcription of *mer*-operon functional genes (Barkay*, et al.*, 2003). When in the inactive state, MerR attracts RNA polymerase to the promoter region and bends DNA of the region away from the polymerase forming a pre-initiation complex (Barkay*, et al.*, 2003). Hg^{II} present in cells binds to MerR causing an allosteric change in the protein that liberates MerO and improves

access of the RNA polymerase to the functional gene transcription start site (Barkay, *et al.*, 2003).

The process of Hg^{II} reduction begins in the extracellular or periplasmic space. Here, Hg^{II} is scavenged by the periplasmic mercury binding protein (MerP) encoded by the *merP* gene. Hg^{II} is sequestered by two cysteine amino acids of MerP which have thiol R groups (Osborn, *et al.*, 1997). Through a redox exchange mechanism, Hg^{II} is transferred from MerP to two cysteine groups of the cytosolic Hg transmembrane transport protein (MerT), which is encoded by *merT* (Barkay, *et al.*, 2003). Hg^{II} is transferred to a cysteine pair on the cytoplasmic face of MerT. Mercury resistance protein MerC is also mediates Hg^{II} transport across the cellular membrane (Barkay, *et al.*, 2003). The gene encoding MerC (*merC*) is found in *mer*-operons from bacteria isolated from polluted environmental contexts (Osborn, *et al.*, 1997). From the cysteine groups of transporter proteins Hg^{II} is transferred to the amino terminal cysteine pair of the mercuric reductase enzyme (MerA: EC 1.16.1.1) encoded by the *merA* gene (Osborn, *et al.*, 1997). Hg^{II} is then moved to the MerA carboxyl terminal cysteine pair where association with active site cysteine residues leads to Hg^{II} reduction using NADPH (Barkay, *et al.*, 2003). Not every observed variant of the *mer*-operon shares the same gene profile but each operon must encode for MerA in order to be fully functional (Liebert, *et al.*, 1997). Other genes observed in *mer*-operons include: *merB* which encodes the organomercurial lyase enzyme (MerB: EC 4.99.1.2); *merE* and *merF* which encode additional membrane transport proteins; and *merG*, which encodes a protein providing organomercurial resistance to gram-negative bacteria lacking *merB* in the operon (Barkay, *et al.*, 2003).

The enzymatic Hg^{R} detoxification pathway is primordial and widespread given the ubiquity of Hg in the lithosphere (Barkay & Wagner-Dobler, 2005, Fritsche, *et al.*, 2008, Harris-

Hellal, *et al.*, 2009). The *mer*-operon sequences have been identified in bacterial chromosomes, plasmids, transposons (Class II) and other mobile genetic elements (MGEs) (Osborn, *et al.*, 1997, Barkay, *et al.*, 2010). Physicochemical and biological parameters that determine Hg bioavailability and toxicity also influence *merA* gene sequence distribution and evolution (Barkay, *et al.*, 2010). Oxic environments typically favour Hg^{II} (Barkay, *et al.*, 2010). This would increase its bioavailability and toxicity in these particular contexts. Lineages of bacteria inhabiting these environments undergo horizontal gene transfer (HGT) more extensively when compared to other lineages inhabiting environments which do not induce greater Hg bioavailability (Barkay, *et al.*, 2010). Thus distribution through HGT is localized to where Hg is most toxic such as oxygenated freshwaters or mercury contaminated soils and sediments.

The evolution of *merA* is driven further by intracellular thiol capacity. As mentioned above, Hg disrupts cellular antioxidant levels. Bacteria having the capacity to replenish and maintain high levels of thiol containing antioxidants would be able to tolerate Hg toxicity (Barkay, *et al.*, 2010). The MerA enzyme has a variant with a 70 amino acids appended to the amino terminal (NmerA). This residue is similar in structure to MerP and improves the effectiveness of Hg^{II} reduction (Barkay, *et al.*, 2010). In lineages where thiol antioxidant levels are high leading to increased Hg tolerance (Gram-negatives), the NmerA mercuric reductase variant is not common (Barkay, *et al.*, 2010). However, in bacteria where thiol levels low (Firmicutes), NmerA is seen at greater frequencies (Barkay, *et al.*, 2010).

1.7 Project Hypotheses

Initially, the collaboration between our laboratory and our industrial partners focused on the oxidative stress response (OSR) of both microbes and fish. However, the work presented in this thesis emphasizes the sediment microbial community response to effluent exposure from

past and present discharges. Consequently, my hypotheses related to the influence of industrial activity on the local ecosystem are as follows:

H1: Sediment microbial communities exposed to effluent discharge will exhibit a difference in community structure and composition when compared to unexposed sediment communities.

H2: Sediment microbial communities exposed to effluent discharge will be enriched with microbes possessing enzymatic mercury resistance (Hg^R) potential.

Through the outcome of this work it is expected that novel biomarkers based on the microbial community responses mentioned above will be developed. The efforts detailed here pertain to in-field biomarker experiments, built using molecular tools tracking *in-situ* responses. It is anticipated that industry will find use in these biomarkers as tools to track their ecological footprint. **Chapter 2** of this thesis focuses on the first hypothesis related to the response of sediment bacterial communities to industrial activity. **Chapter 3** details results concerning Hg^R mediated by the *mer* operon as a specific response of exposure to past and present industrially derived Hg.

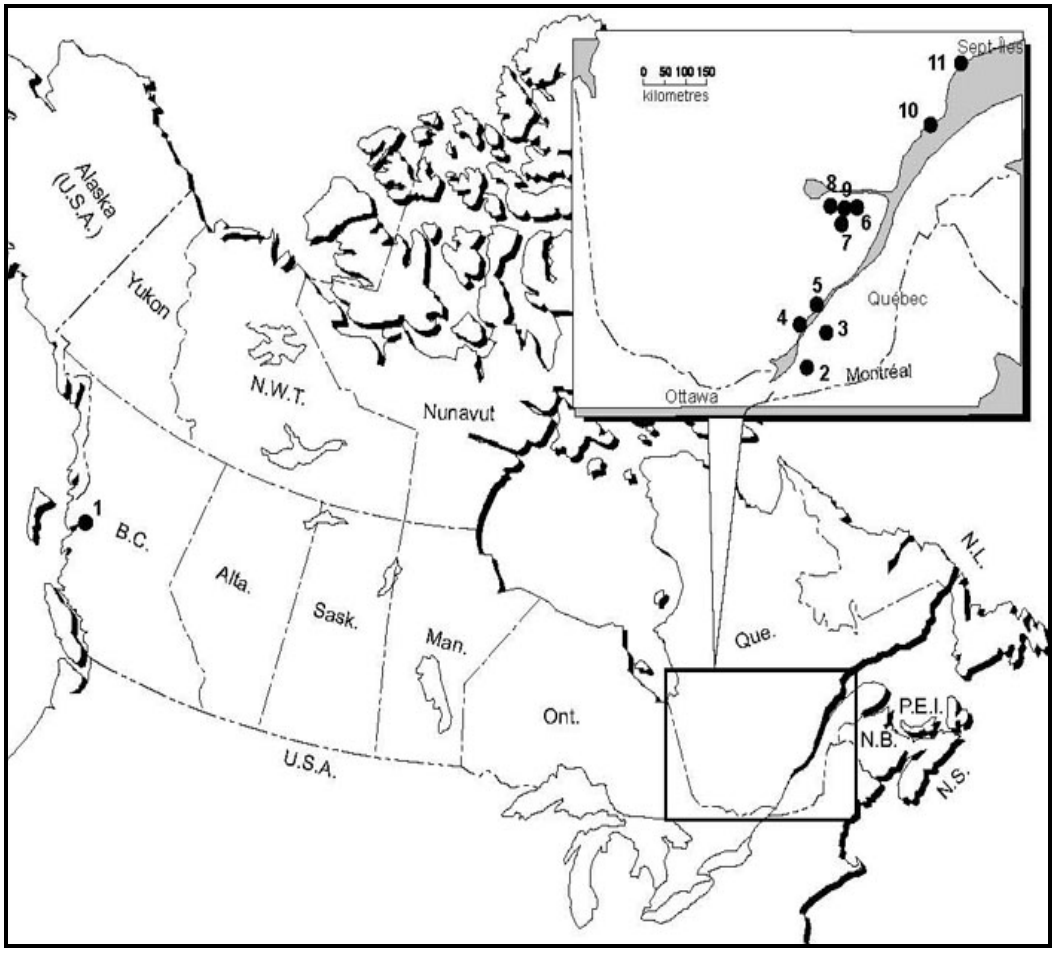

Figure 1.1: Locations of Canadian aluminum smelter plants. Facilities 6 through to 9 are situated in the Saguenay Fjord region. The image was taken from P. Sass (2009).

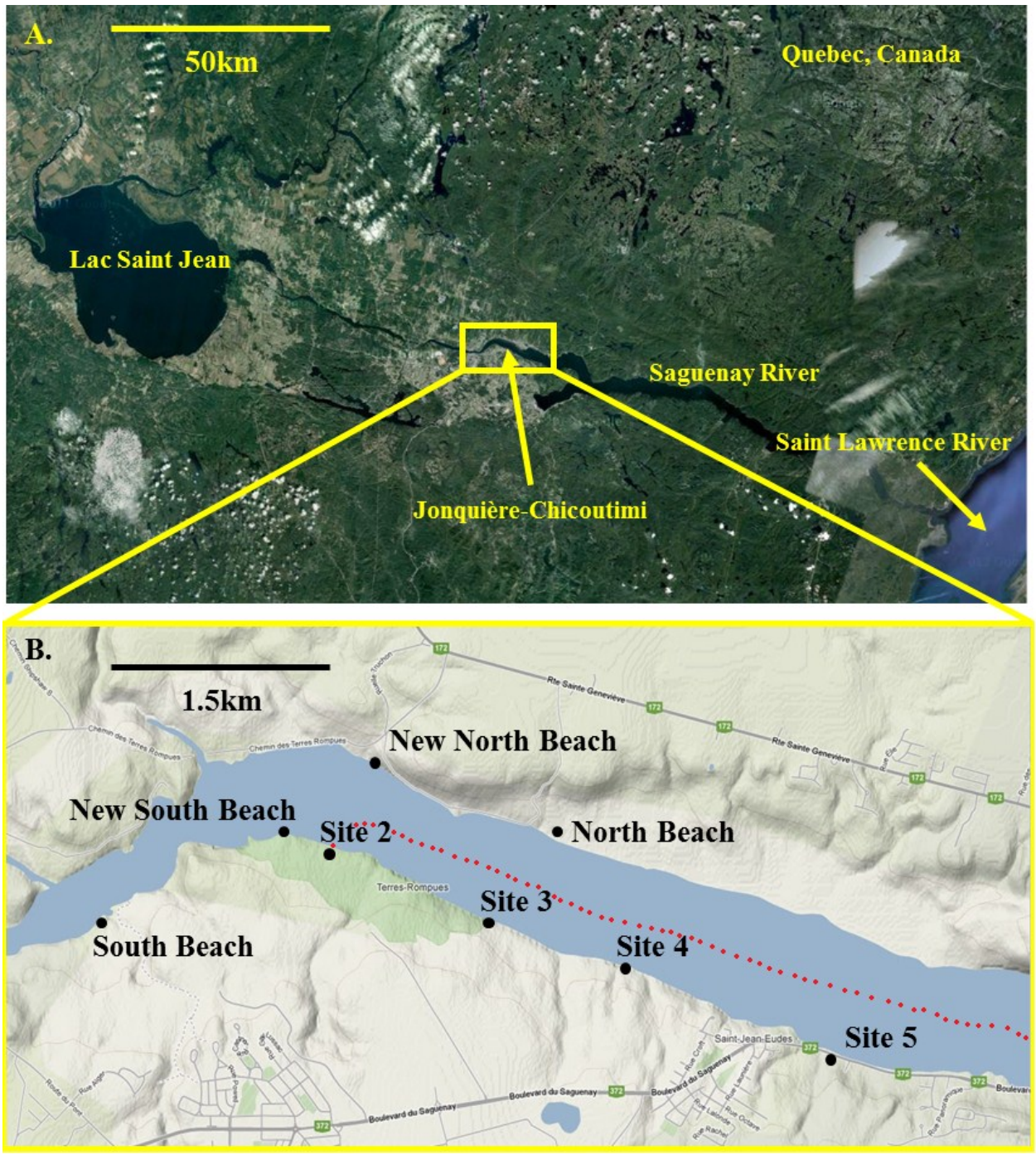

Figure 1.2: Project location within the regional context (A.). Associated sampling sites along the Saguenay River are listed in the local map schematic (B.). Project control sites are listed as: North Beach (NB), New North Beach (NNB), South Beach (SB) and New South Beach (NSB). Sites adjacent to smelter effluent discharge points are listed from 2 to 5. The estimated extent of the effluent discharge plume is indicated using a dotted red line. Google Maps was used to generate the image (©2012 TerraMetrics, ©2012 Google)

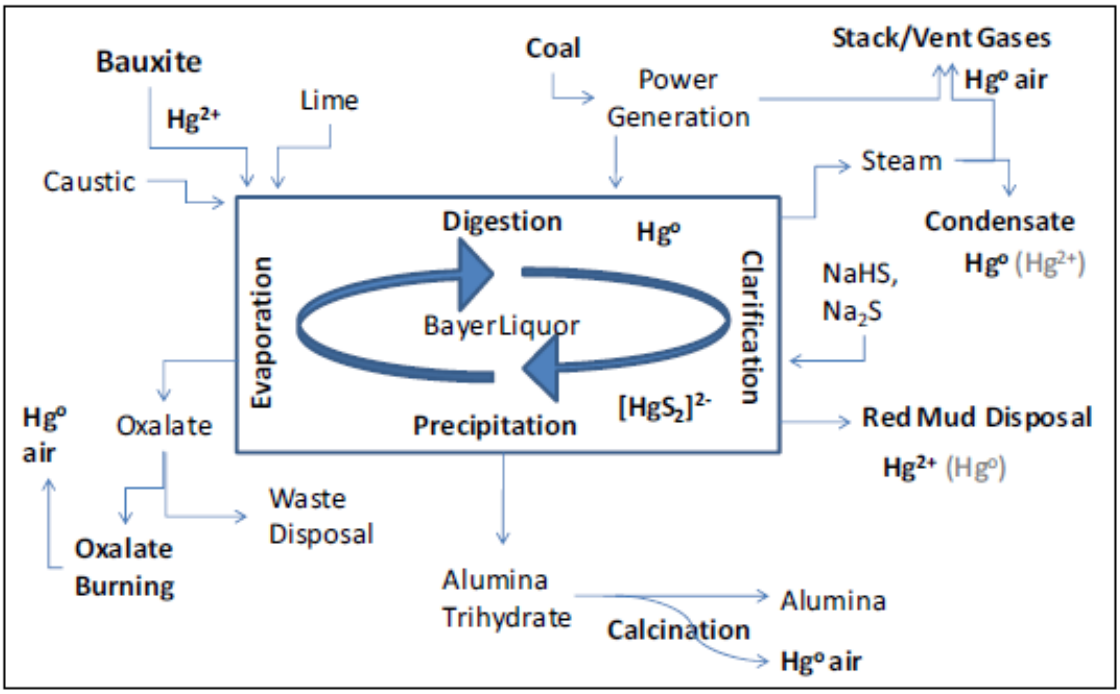

Figure 1.3: Mercury outputs in the Bayer Process. Environmental controls mitigate the release of mercury in alumina refining. Waste products can be recirculated in the process. Oxalate burning is not performed at the facility that this project concerns. Instead, it is filtered and shipped for disposal off-site. The image was taken with permission from Mimna, *et al.* (2011).

2.0 The effect of aluminium industry activity on the microbial community structure of downstream river sediments.

2.1 Abstract

Measures of microbial community richness, diversity and structure and were used to assess the influence of aluminium industry activities on biological systems that receive effluent by-products. Hyper variable regions V1 through V5 of the bacterial *16S rRNA* gene were amplified from sediment community metagenomes. Sediments from three sites along the Saguenay River were used to capture changes across a geographical range and across a gradient of effluent exposure. Clone libraries were constructed using the gene fragments taken from affected (Site 2), medially affected (Site 5) and control (NNB) sites. It was estimated that approximately half of each community was covered using the clone library methodology. Library sequences were used to determine measures of community richness (Chao1, ACE) and diversity (Shannon's Entropy, Simpson's Index) at each site using the MOTHUR program calculators. Richness estimates did not exhibit any significant trend across experimental sites. The diversity indices decreased across sites with increased effluent exposure. However, this trend is attributable to the greater presence of algae and cyanobacteria. Chloroplast *16S rRNA* gene identity markers were found in high proportional abundance at Site 2 which deflated diversity indices. A global phylogenetic tree of all sequences was used in UniFrac analyses to determine if and how the three sites differed through the lineages found at each. Community structures at Sites NNB and 2 were more similar than either was with the medially affected Site 5. Changes in community diversity, estimates of community richness and changes in community structure were not indicative of industrial influence. It is concluded that a better indicator of anthropogenic disturbance to microbial communities may lie in the measurement of bacterial community function over community richness, diversity or structure.

2.2 Introduction

Microbes can be used as sensitive monitors of environmental perturbation from anthropogenic activity. Parameters such as bacterial respiration and the mineralization-fixation of carbon and nitrogen have been used to monitor the influence of metal pollution on bacterial communities (Brookes, 1995). Microbes equipped with recombinant reporter gene constructs sensitive to specific stimuli have been used to test the quality of aquatic ecosystems and arable soils (Barkay*, et al.*, 1998, Rasmussen*, et al.*, 2000). Additionally, changes in diversity, richness and structure of bacterial communities may come as a result of exposure to pollutants. These changes can be considered a microbial community level response to pollution. Sediments, which have been traditionally considered a sink for pollutants released into aquatic systems (Gagnon*, et al.*, 1997, Avramescu*, et al.*, 2011), host these microbial communities. Their response to contaminant release is used as a measure of the impact that these chemical mixtures may have on the greater ecosystem (Jordan*, et al.*, 1995).

Cellular macromolecules used to "fingerprint" individual species and lineages within community assemblages have been analyzed to estimate bacterial species richness and community structure (Muller*, et al.*, 2002). Cell membrane phospholipid fatty acid (PLFA) profiles or genetic material can be used as the biochemical targets for determining the identities of bacteria in a particular community (Frostegard*, et al.*, 1993, Case*, et al.*, 2007). In environmental community contexts, these targets grant flexibility and sensitivity when analysing bacterial assemblages as they are culture-independent. Only a small fraction of microbial communities found outside of the laboratory setting are culturable in the lab: 0.01 to 10% (Bruce*, et al.*, 1995). Thus the use of culture-dependent techniques to determine community structure and richness is limited (Rasmussen*, et al.*, 2008).

Environments which host industrial activity often see acute or chronic chemical stress applied to soil microbial communities from effluent by-products (Bouskill*, et al.*, 2010, Gough & Stahl, 2011). While changes in structure and diversity due to contaminant exposure are measurable, it is often difficult to predict which pattern of change will be observed. Drops in diversity are expected when chemical stressors affect all community actors equally (Giller*, et al.*, 1998). Conversely, if stressors only impede competitive members of a community that are already established within a niche, diversity could increase as competition for resources decreases (Giller*, et al.*, 1998). Situations where community structure does not change in light of toxicant exposure may involve the transmission of mobile genetic elements (MGEs) associated with heavy metal resistance (Liebert*, et al.*, 1997, Barkay*, et al.*, 2003, Hynninen, 2010). For instance, a newly identified metal resistance gene *mrdH* was found to be flanked by MGEs induced by cadmium, nickel, and zinc (Haritha*, et al.*, 2009). Presumably, the horizontal transfer of genetic determinants of resistance between bacterial lineages would promote survival among community members. Thus, community functional potential is changed while identity remains consistent.

Experimental observations involving toxic metal contamination have seen instances where exposed communities change in structure (Baath, 1989, Frostegard*, et al.*, 1993, Diaz-Ravina & Baath, 1996) and others where they do not (Gough & Stahl, 2011). Community richness has been seen to decrease (Muller*, et al.*, 2002) and even increase (Bouskill*, et al.*, 2010) in light of contaminant exposure. Predictions of changes to structure and richness ultimately require insight into how the chemical or effluent mixture will effect individual community members, the functions they perform and the magnitude of deleterious effect that pollutants such as metals have on them (Barkay, 1987, Giller*, et al.*, 1998). Additionally,

community diversity and structure analyses using different biochemical markers may conflict. In a bioremediation study involving soils contaminated with oil, it was found that PLFA profiles indicated the microbial community returned to a pre-exposure structure over time; however, PCR-denaturing gradient gel electrophoresis (DGGE) analyses of a gene based identity marker (*16S rRNA*) indicated that an adapted microbial community different from the pre-exposed had taken hold (MacNaughton*, et al.*, 1999).

Despite limitations in a predictive capacity, the use of bacterial community structure, diversity and richness are still good measures of the biological response to complex chemical mixture exposure. The Saguenay River, QC has accommodated the aluminium industry for over 80 years. Three sites along the river were characterized: a control site (NNB); one site in direct contact with effluent by-product (Site 2); and, a site roughly 1 km downstream from an effluent discharge point, in contact with dilute effluents (Site 5). Patterns of community structure between sites were assessed to determine if any major differences could be seen and thus related to the impact of effluent exposure.

2.3 Material and Methods

2.3.1 Sampling Sites

Please refer to Figure 1.2 for a project site schematic map. Site NNB was located on the opposite shore of the industrial zone and was not exposed to the effluent plume. This site is considered a control. Tracer experiments were performed by our industrial partners to identify the extent of the plume range downstream of the various sites (data not shown). These results confirmed that the north shore of the river is not currently exposed to the plume. Two sites were located on the south shore. Site 2 is directly downstream of an effluent discharge point. Site 5 was located *ca.* 1 km downstream of another effluent discharge point. Sites 2 and 5 were classified as possible affected sites.

2.3.2 Physicochemical Measurements of River Water

Water temperature, pH and conductivity were recorded using the YSI 556 Multiparameter System (YSI Environmental Inc., Yellow Springs, OH, USA) between July 22nd, 2011 and July 28th, 2011. Daily measurements were taken at NNB and Site 2. At Site 2, parameters for the effluent stream as well as the effluent discharge-river water mixing zone were recorded. The sonde was calibrated daily prior to use with calibration solutions for pH and salinity. Access to Site 2 was not possible on July 27th, 2011 due to weather-related conditions.

2.3.3 Sediment and Water Sample Collection

River sediments and water samples were collected from the banks of the Saguenay River in July and August of 2011. Sediment samples were obtained at low tide owing to the greater ease of access to riverbed sediments. For sites in contact with effluent discharge streams (Site 2 and Site 5), low tide accessible sediments were collected from points where the effluent stream

and river water formed a mixing zone at high tide. At each sampling site, sediments taken from 1-3 cm depths from the surface were mixed together from an area of roughly 3 m^2. Sediment samples were partitioned into multiple sterile DNase/RNase free 50 mL Falcon® tubes. Falcon® tube sediments were frozen in liquid nitrogen and stored at -20°C prior to transport. Falcon® tube sediment samples were transported to the University of Ottawa (Ottawa, ON, Canada) on dry ice and stored at -80°C until processed.

Water samples were collected according to methods described by the US EPA for trace metal analyses in water (EPA, 1996). River water was collected in acid washed 1 L fluorinated high-density polyethylene (HDPE) bottles from two of the three project sites: NNB and Site 2. Water was sampled at three different time points between July 21st and August 6th, 2011 to characterize temporal changes in water column chemistry. Site 2 water was collected where effluent flow mixed with river water. Bottles were rinsed with site specific water three times prior to collection. Thereafter, water samples were preserved by acidification with trace metal grade 69-70% nitric acid (HNO_3) (OmniTrace® NX0407-2) to a final concentration of 0.7% (v/v). Preserved samples were kept at 4°C prior to processing. For laboratory quality assurance and control (QA/QC), *travel*, *laboratory* and *field* water sample blanks were prepared in acid washed 1 L HDPE bottles using deionized Milli-Q water (MilliPore, Billerica, MA, USA). The blanks were brought to their respective locations to determine baseline concentrations for metals measured in water samples (EPA, 1996). The blank samples were acidified in the same manner as experimental samples.

2.3.4 Chemical Analysis of River Water

Water concentration of metals (Be, Na, Mg, Al, K, Ca, V, Cr, Mn, Fe, Co, Ni, Cu, Zn, As, Se, Sr, Mo, Cd, Sb, Ba, Tl, Pb, Th, U) were analysed in water using the Agilent Tech 7700

Series ICP-MS (Agilent Technologies, Mississauga, ON, Canada). General instrument methodology followed previously published protocols (Lewen*, et al.*, 2004). Calibration standards (Environmental Calibration Standard – Part#5183-4688) and internal standard mixes (Agilent Internal Standard Mix – Part# 5188-6525) were purchased from Agilent Technologies (Mississauga, ON, Canada). Internal standard elements (Se, Ge, Rh, Ln, Tb, Bi, Er) were analysed for matrix recovery rates. Calibration standards along with blank samples were run intermittently throughout the course of the procedure.

Total mercury (THg) levels in river water were measured using a separate protocol. THg concentration was measured using methods described by US EPA Method 1631 (EPA, 2002). Prior to analysis, bromine chloride (BrCl) was used to oxidize all Hg in water samples to Hg^{II}. Following the subsequent reduction of the water samples by hydroxylamine, stannous chloride ($SnCl_2$) was applied to convert Hg^{II} to volatile Hg^0. Hydroxylamine is used to destroy free halogens (Br) in water samples which may damage instrumentation. Hg^0 was purged from water samples using argon gas and was collected onto a gold trap. Hg^0 was thermally desorbed from this gold trap and carried via inert gas to a second (analytical) gold trap. Again, Hg was thermally desorbed from the analytical trap and carried to the cold-vapour atomic fluorescence spectrometer (CVAFS) for detection. The Tekran® 2600 (Tekran®, Toronto, ON, Canada) was used for CVAFS analysis. Standard checks were performed for every 10 samples processed. The Tekran 2600® was calibrated with Hg Reference Solution 1000 ppm ±1% (Fisher CSM114-100). Detection limits followed those put forth by US EPA 1631 (minimum level of quantitation = 0.5 ng/L; method detection limit = 0.2 ng/L).

2.3.5 Statistical Analyses

Statistical analyses of metal concentrations in river water were performed using JMP Software (JMP® 10.0.0, SAS Institute Inc., Cary, NC, USA). Water data was generated for two of the three sampling sites (NNB and Site 2). Data was collected from replicate readings taken from each of the three sample collection time points. Data sets were defined by grouping the measurement replicates from all collection time points by site. The distribution of metal concentrations was tested for normality using the Shapiro-Wilk test. Homoscedasticity of the data sets was evaluated using Levene's test. Where normality and homoscedasticity were achieved, a two-tailed Student's T-test was performed to determine if there were significant differences between NNB and Site 2 data sets. Where normality could not be achieved – arising from sample variability or insufficient sample number – the Wilcoxon non-parametric T-test was used. When the data was normally distributed and the variances were not homogenous, Welch's T-test was used. Results from statistical tests were considered significant for $p < 0.05$.

2.3.6 Preparation of Laboratory Reagents and Materials

All laboratory aqueous stock and working solutions were formulated using Milli-Q water (MilliPore, Billerica, MA, USA) that was autoclaved after treatment with diethylpyrocarbonate (DEPC) to a final concentration of 0.1% (v/v) following protocols detailed in literature (Hurt*, et al.*, 2001). DEPC is used to inactivate RNase enzymes which can compromise sediment sample RNA extracts but must be decomposed by autoclaving prior to using treated water. All glassware and utensils used for nucleic acid extraction were thoroughly washed, rinsed with DEPC-water and subsequently autoclaved for 1 h at 128°C.

2.3.7 Sediment Sample Preparation and DNA Extraction

Sediments used in DNA extraction protocols were separated into 5 g partitions, each within sterile DNase/RNase 50 mL Falcon® tubes. Samples were washed with two to three volumes of a salt buffer (0.5 M EDTA, pH 8; 1 M Tris-HCl, pH 8.0; 0.5 M Na_2HPO_4, pH 8.0) adapted from literature (Zhou*, et al.*, 1996) and subsequently centrifuged at 9000 *g* at 4°C. Washing was performed three times prior to processing. The wash was performed to chelate metals and mitigate the co-extraction of soil humic substances (Figure 5.1). These chemicals inhibit downstream enzymatic analyses of nucleic acid extracts (Fortin*, et al.*, 2004). Moreover, high concentrations of divalent metal cations are known to prematurely precipitate DNA which may diminish extraction yield and efficiency (Gough & Stahl, 2011).

Washed sediments were immediately processed with the commercial PowerSoil® DNA Isolation Kit (MoBio Laboratories Inc., Carlsbad, CA, USA). Total DNA (metagenome) from sediments was extracted according to the manufacturer specifications. All extractions were performed under a laminar flow hood supplied with HEPA filtered air flow. Surfaces and instruments were sterilized with UV-C light, 70% ethanol and 10% bleach solutions. Following the isolation procedures, DNA extract concentration was determined through absorption spectra analysis with the NanoDrop Spectrophotometer 2000. Extracts were stored at -20°C until further use.

2.3.8 PCR Assays

PCR reactions targeting the *16S rRNA* gene were performed using the Eppendorf MasterCycler ProS (Eppendorf Canada, Mississauga, ON, Canada) and the Biometra T Professional Basic Gradient (Biometra, Goettingen, Germany). *16S rRNA* gene PCR assays used the 27F (5'-AGA GTT TGA TCM TGG CTC AG-3') and the 907R (5'-CCG TCA ATT CAT

TTG AG-3') primer combination. 880 bp amplicon fragments of the *16S rRNA* gene were generated from sediment DNA (metagenome) extracted from NNB, Site 2 and Site 5. The amplicon product encompasses hyper variable regions 1 to 5 (V1-V5) on the *16S rRNA* gene (Kim*, et al.*, 2011). Commercial enzyme Platinum® Taq Polymerase (Invitrogen, San Diego, CA, USA) was used to generate these PCR amplicons. PCR reactions were carried out according to the commercial kit recommendations with final per reaction reagent concentrations being: 1X PCR buffer, 2.5 mM $MgCl_2$, 0.2 μM forward/reverse primers, 0.2 mM dNTPs, 0.625 U Platinum® Taq Polymerase. For the determination of optimal PCR conditions in generating specific amplicon products with maximized yields, $MgCl_2$ concentrations varied from 1.5 mM to 3.5 mM. The thermo cycling protocol began with an initial denaturation step at 94°C (10 min) followed by a temperature cycle of 94°C (30 s), 50°C (30 s) and 72°C (60 s) for a total of 35 cycles. The final elongation step was held at 72°C (5 min). Once generated, amplicons were separated by agarose gel electrophoresis and visualized under UV light.

2.3.9 Cloning and Sequencing of 16S rRNA Gene Fragments

After separation by gel electrophoresis, PCR amplicons were extracted from agarose gels using the Qiagen QIAEX II Gel Extraction Kit (Qiagen, CAT #20021). The extracted amplicon samples were used to generate clone libraries using the StrataClone PCR Cloning Kit (StrataClone, CAT#240205) according to manufacturer protocols. To summarise, amplicons were ligated into the kit cloning vector (pSC-A-amp/kan). The vectors – each holding a copy of the *16S rRNA* gene fragment – were used to transform StrataClone competent *E.coli* cells. Competent cells were screened using X-gal in β-galactosidase colour screening assays (blue-white screening). Positive clones were selected for growth in LB-kanamycin broths. For every clone library, each representing one of the three sampling sites, 96 clones were randomly

selected for growth in LB-kanamycin broths. Broth growths were used in PCR assays targeting the vector insert as seen previously. The PCR amplicons from each clone library (96 clones) were shipped to Beckman Coulter Genomics (Danvers, MA, USA) for sequencing in accordance with the commercial service requirements.

2.3.10 Sequence Analysis

Sequences generated from clone libraries were trimmed for vector and primer based flanking sequences using the Ribosomal Database Project (RDP) Pipeline function (Cole*, et al.*, 2009). This function also reoriented sequences in preparation for alignment. The Orientation Checker program was used to determine where individual sequenced fragments fit along the 880bp *16S rRNA* gene amplicon stretch (Ashelford*, et al.*, 2006). Sequences were separated into 5' and 3' flanking groups based upon where they fit. Putative chimeric sequences were identified and removed from groupings using Mallard and Pintail programs (Ashelford*, et al.*, 2005, Ashelford*, et al.*, 2006). Sequence alignments were performed thereafter using the RDP Alignment tool (Cole*, et al.*, 2009). The RDP Classifier function was used to determine major groups of bacterial phyla and classes represented by operational taxonomic unit (OTU) (Cole*, et al.*, 2009). OTUs were defined based on 97% sequence identity.

The jModelTest program (v0.1.1) was used to determine the best model of evolution between sequence alignments (Posada, 2008). The selected models were used to construct phylogenetic trees through the FastTree program using maximum likelihood (Price*, et al.*, 2010). Distance matrices for sequence alignments were made using these trees in the PAUP program (v4.0). These matrices were imported into MOTHUR for richness (Chao1 and ACE) and diversity estimates of samples (Shannon's Entropy and Simpson's Index) (P. D. Schloss*, et al.*, 2009). Good's coverage was also calculated (Good, 1953) and rarefaction curves were

constructed (Figure 5.2) to further investigate the proportion of diversity covered by clone libraries from each sample site (Hughes*, et al.*, 2001).

A batch sequence alignment containing all sequences not separated by clone library was analysed for its model of evolution (jModelTest) in order to build a global tree (FastTree) encompassing all sequences generated in this project. The tree was built using Generalized Time Reversible model of sequence evolution (GTR) (Lanave*, et al.*, 1984) with gamma rate heterogeneity distribution (G) (**GTR+G**) (Shapiro*, et al.*, 2006). GTR models assign a separate substitution rate for all possible nucleotide changes: A↔C; A↔G; A↔T; C↔G; C↔T; G↔T. The tree was rooted using the *16S rRNA* gene sequence of *Aquifex pyrophilus* as an out-group. This species represents an early phylogenetic branch-off in domain Bacteria (Huber*, et al.*, 1992).

The global tree was used in UniFrac analyses to determine if differences between sampling sites existed by the types of bacterial lineages found at each (Lozupone & Knight, 2005). The UniFrac Significance tool was used to analyse the significance ($p < 0.05$) of the difference observed between site pairs. A p-value matrix detailing pair-wise comparison significance was generated. The reported p-values for the UniFrac Significance pair-wise comparison represented the fraction of permuted trees that have a UniFrac value equal to or higher than the true observed tree. Reported p-values were multiplied by the total number of pair-wise comparisons being made (Bonferroni Correction).

The UniFrac Jackknife Environmental Clusters tool was used to visually represent the pattern of differences observed between sites. The Lineage-Specific analysis tool was performed to determine which lineages of bacteria contributed significantly to differences observed between

environments. Individual sequence identity was determined using the BLAST function on the NCBI website.

2.3.11 Description of Richness Estimators and Diversity Indices

MOTHUR richness and diversity calculators were used to determine characteristics of community diversity (P. D. Schloss*, et al.*, 2009). The extent of diversity covered in each clone library was calculated using the Good's coverage (C). The formula for coverage is as follows:

$$(1)\ C = 1 - (\text{Number of OTUs sampled once}) \bullet (\text{Total number of sequences})^{-1}.$$

Thus the greater the number of singletons – OTUs represented by just one sequence in a library – the lower the coverage would be. If each sequence in a sample represented distinct OTUs, Good's coverage would equate to zero. Intuitively, this would imply that based on the sampling effort – the total number of sequences – the population from which the sample was derived was of high richness and that the scope covered using clone libraries was low.

Richness was evaluated using the Chao1 and ACE (Abundance-base Coverage Estimator). Chao1 was calculated using the following formula:

$$(2)\ \text{Richness} = \text{Observed OTU Number} + (\text{Number of singletons})^2 \bullet (2(\text{Number of doubletons}))^{-1}$$

where doubletons are OTUs represented by two sequences in the sample (Hughes*, et al.*, 2001). Richness increases with an increasing number of singletons. High doubleton counts in a sample could deflate the Chao1 richness estimate. Therefore, Chao1 is strongly influenced by the number of rare OTUs in a sample, with rare OTUs being defined as singletons and doubletons

(Hill, 1973). OTUs represented by three or more sequences are not incorporated into this estimator. The ACE richness estimator is similarly influenced by rare OTUs but has a broader definition of rarity: representation by 10 or fewer sequences in a sample. The equation for the ACE estimation is described in literature (Hughes*, et al.*, 2001).

Richness estimators use the number of rare OTUs in making estimates for the expected total number of OTUs. No direct inference can be made of the dominant OTUs observed in a sample. Shannon's Entropy (H) and Simpson's Index (D) are sensitive to the relative abundance of OTUs in a library sample. Shannon's Entropy is related to sample identity predictability. The greater the number of OTUs, each found in equivalent relative abundances, the greater the uncertainty in predicting the identity of the next sampled sequence (Hill, 1973). Simpson's Index of diversity measures the concentration of dominance exhibited across observed OTUs – the evenness of relative abundance. The index D-value represents the probability of sampling two sequences from the population which represent the same OTU. Should proportional dominance be concentrated in a single OTU within a community, the probability of sampling two sequences from this dominating OTU becomes high. If dominance is shared, or if there is a high degree of richness with no one OTU presiding over others in relative abundance, the probability of sampling sequences from the same OTU diminishes (Hill, 1973).

Richness estimates and diversity indices measure two different properties of a sampled community. Therefore it is important to consider both when characterising community structure in an effort to make comparisons between different communities.

2.4 Results & Discussion

2.4.1 Water and sediment chemistry

Chemical analysis of river water taken from NNB and Site 2 was performed to determine if differences existed in water column chemistry between the two sites. Increased concentrations of metals in Site 2 river water would be attributed to industrial effluent discharge. Significantly increased metal concentrations ($p < 0.05$) in Site 2 river water for beryllium, copper, zinc, selenium, cadmium, antimony, mercury and lead were found when compared to NNB (Table 2.1). Values were averaged over the three separate collection days and separated by site. The greatest differences between control and affected site average metal concentrations were seen for mercury (56.88 ng/L) and lead (1187 ng/L). However, the quantities observed did not exceed levels permitted by Health Canada. Maximum acceptable concentrations in drinking water are 10000 ng/L for lead and 1000 ng/L for mercury (HealthCanada, 1986, HealthCanada, 1992). Higher metal concentrations at Site 2 river water arose either from discharged effluents or resuspension from the sediments.

2.4.2 Coverage of Community Diversity

Clone libraries consisting of 96 randomly selected clones were constructed for each project site (NNB, Site 2 & Site 5). Elimination of putative chimeric sequences yielded workable *16S rRNA* gene sequences: 79 (NNB), 72 (Site 2) and 63 (Site 5). Chimeric sequences are corrupt artificial anomalies formed during PCR amplification (Ashelford*, et al.*, 2005). The estimated percentages of the bacterial community captured at all sites (Good's coverage) were 52% (NNB), 53% (Site 2) and 54% (Site 5). The rarefaction curves generated for each library are presented as supplementary information in Chapter 5. The curves represent the average number

of OTUs expected to be observed after resampling. Rarefaction curves that reach a stable OTU sampling plateau would indicate that a sufficient number of sequences were obtained from the community population. No rarefaction curves reached a visible plateau (Figure 5.2). This supports estimates made from Good's coverage (Table 2.2) and indicates that sediment bacterial communities were not sampled to exhaustion. It is very likely that rarer community members were not incorporated into the UniFrac analyses. Thus, in describing how industrial effluents affect whole community structure caution must be used.

2.4.3 Community Richness

Observed OTU numbers were 42 at Site 2, 44 at Site 5 and 58 at NNB using the 97% sequence similarity definition. Estimates of OTU richness were highest at Site 2 with 136 and 145 OTUs, estimated using the Chao1 and ACE indices, respectively. OTU richness was lowest at Site 5 with 75 and 82 OTUs, estimated using the same respective indices (Table 2.2).

Site 2 experiences the highest concentration loading of effluents as it is directly downstream of a discharge point. Site 5 is in contact with more dilute effluent. As Chao1 and ACE estimations are sensitive to the occurrence of rare species (Hughes*, et al.*, 2001), these richness analyses may signal that greater exposure to industrial effluent yields a greater number of rare OTUs. However, the 95% confidence intervals overlap between all sites. Moreover, NNB richness estimates – 93 and 112 OTUs from Chao1 and ACE, respectively – fall between those of Site 2 and Site 5. NNB is considered a control site with no current exposure to effluents. Therefore, no significant trend in richness can be discerned from these results.

If it was observed that richness estimates increased significantly in conjunction with increased exposure to effluents, it could be argued that industrial activities have opened up new niche spaces. These new niche spaces could promote the growth of a greater variety of microbes

increasing community richness. Moreover, dominant community members may be hindered due to deleterious effects of greater effluent exposure. This would reduce competition for resources allowing rarer players to flourish (Giller*, et al.*, 1998). The pattern of increasing species richness in light of metal contamination has been observed before (Bouskill*, et al.*, 2010).

2.4.4 Community Diversity

Shannon's Entropy (H) values were highest at NNB (3.99 ± 0.15), lowest at Site 2 (3.14 ± 0.33) and intermediate at Site 5 (3.69 ± 0.19). Reciprocal values for Simpson's Index (1/D) followed the same significant trend (Table 2.2). Thus, bacterial community diversity, as defined by the respective indices (see Section 2.3.11), declined with increased exposure to industrial effluent. However, this trend may be influenced by the inclusion of algae whose presence and abundance are related to non-industrial activities. A large fraction of total sequences in the Site 2 clone library were *16S rRNA* gene markers belonging to chloroplast organelles (Figure 2.2). The inclusion of these sequences in diversity analyses deflated the Site 2 diversity indices (data not shown). This generated a false decreasing trend in bacterial community diversity.

The Site 2 effluent discharge point lies adjacent to a private golf course (Club de Golf – Saguenay, Arvida) and water from the greens is drained into the Saguenay River. The use of fertilizers and pesticides on the golf course is likely to influence the nutrient flux of Site 2 sediments. A boost in primary production would be triggered with increased nutrient loads (Goldman, 1988). This in turn has influenced the proportion of the clone library that represents ribosomal identity markers from the chloroplast of primary producers. Therefore, it is not industrial activity influencing the diversity indices at Site 2 but a secondary external factor.

Without the addition of more sediment sampling sites along the Saguenay River, it is difficult to determine if declining community diversity is indicative of increased exposure to

industrial effluent. In this experiment it cannot be said that the observed declining trend is directly related to the activity of the aluminium industry.

2.4.5 Phyla Observed at Project Sites

The relative abundance of phyla observed at each site was taken as the percentage of total sequence numbers they represent. Figure 2.1 to Figure 2.3 detail the types of phyla observed and their proportional abundance. Exact percentages of each phylum out of the total number of sequences observed are listed in Chapter 5 (Table 5.1).

Proteobacteria, represent the largest and most diverse division among prokaryotes (Gupta, 2000). It was the most abundant phylum at all sites with *β-Proteobacteria* as the dominant class. Sequences corresponding to phyla Acidobacteria, Bacteroidetes and Chloroflexi were also observed at each site at comparable levels. Gram-positive phyla (Actinobacteria, Firmicutes) and the Nitrospirae phylum were observed only at NNB site. Cyanobacteria and sequences representing chloroplast *16S rRNA* sequences were seen at NNB and Site 2 but not at Site 5. The chloroplast sequences were seen in the highest proportional abundance at Site 2. Gemmatimonadetes was not observed at Site 2 but was seen at the remaining two sites.

Patterns of phyla extant at particular sites but not at others may be attributable to influences exerted by industrial activity via effluent exposure. For instance, gram-positive phyla (Actinobacteria, Firmicutes) were only observed at NNB site. Metal contaminated soils have been observed as having a greater abundance of gram-negative bacteria (Frostegard*, et al.*, 1993, Sandaa*, et al.*, 1999, Hynninen, 2010). Deficiency in representation by gram-positives at Sites 2 and 5 may have come due to metal contaminants released into the environment through effluent by-products. Gram-positive Actinobacteria represent one of the largest taxonomic units within domain bacteria (Ventura*, et al.*, 2007). Finding no representatives of this phylum in sediments

of Sites 2 or 5 maybe indicative of the influence industry has on sediment microbial communities. With this said, underrepresentation by gram-positive bacteria in these clone libraries may have come simply as a result of the greater difficulty in DNA extraction from cells of gram-positive bacteria when compared to gram-negatives. A thicker peptidoglycan layer provides gram-positive cell walls with greater resilience against standard DNA isolation techniques.

Sequences belonging to phylum Armatimonadetes were only observed at Site 2. *16S rRNA* gene sequences belonging to this phylum have been observed in diverse environments and certain species are associated with the degradation of halogenated aromatic compounds (Tamaki*, et al.*, 2011). Hydrocarbon contamination of Site 2 sediments as a result of industrial activity has been observed (data not shown) and may contribute to this observation.

Bacteroidetes were observed at all sites. This phylum is known for having malleable genomes allowing for horizontal gene transfer among its members (Thomas*, et al.*, 2011). Some genetic determinants of metal resistance, Hg^R for example, are found on mobile genetic elements (MGEs) (Haritha*, et al.*, 2009, Barkay*, et al.*, 2010). It is possible that members of this phylum at contaminated sites all share these mobile genetic resistance elements. This would allow Bacteroidetes to be found across control and affected sites, even though functional capabilities exhibited by phylum members maybe very different.

2.4.6 Community Structure Analyses

UniFrac was used to compare the community structure among the sites sampled. These metrics represent the branch length in a phylogenetic tree that is unique to a given environment. According to the UniFrac definitions of significance, the pairwise comparison p-value matrix showed a *suggestive significant probability* ($0.05 < p < 0.1$) between NNB and Site 2 in the true

phylogenetic tree. Pair-wise comparisons with Site 5 yielded a *marginal significance* ($0.01 < p < 0.05$) (Figure 2.4).

Clustering of environments, visualized using the UniFrac Jackknife tool, were based on the p-value distance matrix generated from pair-wise comparisons. The robustness of cluster nodes was tested using jackknife based resampling (Figure 2.4). Node A, signifying the clustering of Site 5 sequences, away from both NNB and Site 2, was recovered at a rate of 100% despite smaller sampling sizes. The recovery rate of node B, representing the split between NNB and Site 2, became smaller as the resampling size was decreased. However, Node B recovery from jackknife resampling tests did not fall below 87%. The resampling sizes were chosen to be equal to or less than the minimum number of sequences generated at a sampling site (Site 5: 63 sequences).

Chloroplast *16S rRNA* gene sequences contributed most to the observed clustering of sites. The difference between the expected and observed number of chloroplast *16S rRNA* sequences for all sampling sites was significant ($p < 0.05$) (Figure 2.4). Chloroplast sequences were removed from a subsequent UniFrac analysis to determine if the same pattern of site clustering would arise. Chloroplast *16S rRNA* sequences are derived from autotrophic eukaryotes. Inclusion of these sequences may conflict with the bacterial nature of this study. Additionally, as mentioned in Section 2.4.4, chloroplast sequence abundance may reflect the influence of a separate anthropogenic activity besides industry. This separate factor may have affected attempts to characterize the influence of the aluminium industry at Site 2. UniFrac analysis excluding chloroplast sequences yielded the same pattern of site clustering (data not shown).

Studies of community structure suggested that NNB and Site 2 were more closely related than either was to Site 5. This is counter to what was expected. NNB and Site 2 represent extreme cases with regard to the chemical relationship each site has with effluents released from industry. NNB is a control site with no detectable contact with effluent by-product while Site 2 is in close proximity to an effluent discharge point. The strong relatedness of NNB and Site 2 was found to be significant even after analyses using jackknife resampling from reduced sample pools (Figure 2.4). River water at Site 5 was not analysed for total metals but water column chemistry should represent a diluted influence of industry when compared to Site 2.

2.5 Conclusion

Results from richness estimates show no significant trend across sites. Diversity indices showed a declining trend with increased effluent exposure across sites. However, this was due to the inclusion chloroplast sequences that are found in high proportional abundance at Site 2. The presence and abundance of chloroplasts here are likely influenced by higher nutrient loads introduced by an adjacent private golf course (Club de Golf – Saguenay, Arvida). The inclusion of chloroplast sequences has thus deflated diversity indices at this site. Incorporating more sediment samples from sites along the effluent exposure gradient in later studies would confirm potential trends seen here.

UniFrac analyses indicated that structural differences between a control site (NNB) and affected site (Site 2) were minimal. Comparisons with Site 5 community structure yielded the greatest difference among sites. Thus, exposure to industrial effluent does not appear to influence sediment bacterial community structure. Because bacterial communities are known to differ at even small spatial scales (Hughes*, et al.*, 2001) it is possible that any observed differences community structure may simply reflect natural variations independent of industrial activity.

Once again, the incorporation of more sediment samples along the effluent exposure gradient could illuminate community structure differences derived from industrial activity. Additionally, boosting community coverage in UniFrac analyses would integrate the rarer members of each community. This would grant greater sensitivity in elucidating community differences. Improved coverage of OTUs could be achieved by boosting sequencing output. Sampling effort would see a 100 fold increase through pyro-sequencing of *16S rRNA* gene tags from a particular site, over traditional Sanger sequencing methods (Margulies*, et al.*, 2005). However the use of this technique is not without its faults as high sampling effort has been shown to bias richness estimates and diversity indices (Gihring*, et al.*, 2012).

Despite these additional efforts, it is possible that no change in community structure may be observed. In a recent publication, no variation in bacterial community structure was seen across a wide range of zinc concentration in anoxic waters (Gough & Stahl, 2011). In these instances the functionality of different communities may be more representative of the changes brought on by contaminant exposure (Liang*, et al.*, 2011). For example, mercury (Hg) exposure selects for bacteria holding a genetic determinant of mercury resistance, the *mer*-operon (Barkay*, et al.*, 2003). This genetic determinant can be found on mobile genetic elements that allow its transfer between bacterial lineages and species (horizontal gene transfer) (Haritha*, et al.*, 2009, Barkay*, et al.*, 2010). Thus, in Hg contaminated settings, no change in bacterial community structure may be seen, as measured by *16S rRNA* gene markers. Differences between communities would be discernable through their functionality in the form of Hg^R as conferred by mobile *mer*-operons.

From this work, community richness, diversity and structure analyses by themselves lack the resolution required to relate industrial influence upon sediment bacterial communities.

Greater resolution may be afforded by delving deeper into the functional capabilities of these communities as opposed to strictly looking at the identities of their members.

2.6 Tables

Table 2.1: Metal concentrations in NNB and Site 2 river water. Samples taken from three separate time points were analyzed. Three day averages (+SD) were calculated using daily means. Mercury concentration was determined using separate protocols. Ratios of Site 2 to NNB average concentrations are listed. Significant differences ($p < 0.05$) in concentration between sites are marked in bold print.

Element	Site								Site 2:NNB
	NNB				Site 2				
	Sampling Day			Mean	Sampling Day			Mean	
	1	2	3	(SD)	1	2	3	(SD)	
Be (ng/L)	19.9	13.7	6.7	13.4 (6.6)	17.3	43.6	29.6	30.2 (12.1)	**2.25**
Na (mg/L)	2.12	11.24	2.6	5.32 (4.06)	3.47	15.0	15.6	11.4 (6.12)	2.14
Mg (mg/L)	1.33	3.17	1.43	1.98 (0.899)	0.992	1.82	2.06	1.63 (0.483)	0.823
Al (mg/L)	0.968	0.723	0.345	0.679 (0.303)	0.344	1.14	0.755	0.745 (0.367)	1.09
K (mg/L)	0.385	1.41	0.718	0.838 (0.471)	0.400	1.09	1.28	0.925 (0.418)	1.10
Ca (mg/L)	5.13	14.7	7.28	9.03 (4.36)	5.66	13.4	16.5	11.8 (4.82)	1.31
V (µg/L)	1.33	1.41	0.781	1.17 (0.341)	0.853	2.77	2.58	2.07 (0.945)	1.77
Cr (µg/L)	0.897	0.964	0.489	0.783 (0.235)	0.525	1.47	1.06	1.02 (0.427)	1.30
Mn (µg/L)	33.5	24.4	13.7	23.88 (9.10)	14.6	37.5	32.0	28.0 (10.8)	1.17
Fe (mg/L)	0.972	0.702	0.381	0.685 (0.291)	0.361	1.14	0.826	0.776 (0.341)	1.13
Co (µg/L)	0.449	0.418	0.137	0.334 (0.173)	0.141	0.483	0.338	0.302 (0.155)	0.904
Ni (µg/L)	1.19	0.968	0.563	0.908 (0.309)	0.705	1.88	1.37	1.32 (0.530)	1.45
Cu (µg/L)	1.31	1.40	0.829	1.18 (0.356)	2.35	12.0	12.6	8.99 (5.16)	**7.62**
Zn (µg/L)	6.08	5.19	4.30	5.19 (1.04)	5.70	11.5	9.60	8.91 (2.67)	**1.72**
As (µg/L)	0.176	0.203	0.164	0.181 (0.023)	0.147	0.250	0.233	0.210 (0.051)	1.16
Se (ng/L)	41.4	37.9	32.5	37.3 (4.1)	52.9	64.2	63.9	60.3 (6.6)	**1.62**
Sr (mg/L)	34.5	159.1	44.5	79.37 (62.08)	23.94	50.72	59.42	44.7 (16.58)	0.563

Mo (ng/L)	89.6	370.9	164.5	208 (133.1)	159.4	350.1	418.4	309.3 (121.4)	1.49
Cd (ng/L)	10.2	11.9	8.4	10.2 (1.9)	11.7	23.6	21.4	18.9 (5.7)	**1.85**
Sb (ng/L)	14.1	17.8	14.2	15.3 (1.9)	26.4	45.4	41.1	37.6 (9.1)	**2.46**
Ba (µg/L)	16.4	20.6	12.5	16.5 (4.03)	11.7	23.7	22.5	19.3 (5.96)	1.17
Hg (ng/L)	2.27	2.29	2.17	2.24 (0.064)	21.36	78.84	70.43	56.88 (31.04)	**25.4**
Tl (ng/L)	27.9	22.2	15.1	21.7 (6.2)	53.3	25.0	16.9	31.8 (22.2)	1.47
Pb^{206} (ng/L)	313.0	224.7	96.7	211.5 (99.1)	403.8	1905	1252	1187 (680.5)	**5.61**
Pb^{207} (ng/L)	278.4	207.2	88.5	191.4 (88.0)	370.6	1719	1164	1085 (612.6)	**5.67**
Pb^{208} (ng/L)	293.8	214.0	91.7	199.9 (93.1)	380.7	1767	1183	1110 (629.6)	**5.55**
Th (ng/L)	39.9	43.1	24.5	35.8 (9.4)	33.9	131.0	79.1	81.3 (43.9)	2.27
U (ng/L)	51.4	120.0	62.7	77.9 (33.9)	50.1	94.3	117.0	87.1 (30.6)	1.12

Table 2.2**:** Data derived from the MOTHUR program without the removal chloroplast sequences. Total *16S rRNA* gene clone numbers generated from clone libraries are listed with chimeric sequences removed. OTUs derived from these gene clones are listed. Richness estimates and diversity indices are shown with respective 95% lower confidence intervals (LCIs) and upper confidence intervals (UCIs).

Site	Total # of Sequences	Number of OTUs	Coverage (%)	Species Richness Estimates & Indices of Community Diversity			
				Chao1 Estimate (LCI, UCI)	*ACE* Estimate (LCI, UCI)	*Shannon's Entropy*, H (LCI, UCI)	Reciprocal *Simpson's Index*, 1/D (LCI, UCI)
NNB	79	58	52.00	93 (74, 137)	112 (98, 130)	3.99 (3.84, 4.15)	142.86 (250, 100)
Site 2	72	42	53.00	136 (78, 286)	145 (82, 310)	3.14 (2.81, 3.48)	10.53 (29.41, 6.45)
Site 5	63	44	54.00	75 (56, 122)	82 (59, 135)	3.69 (3.50, 3.87)	83.33 (166.67, 52.63)

2.7 Figures

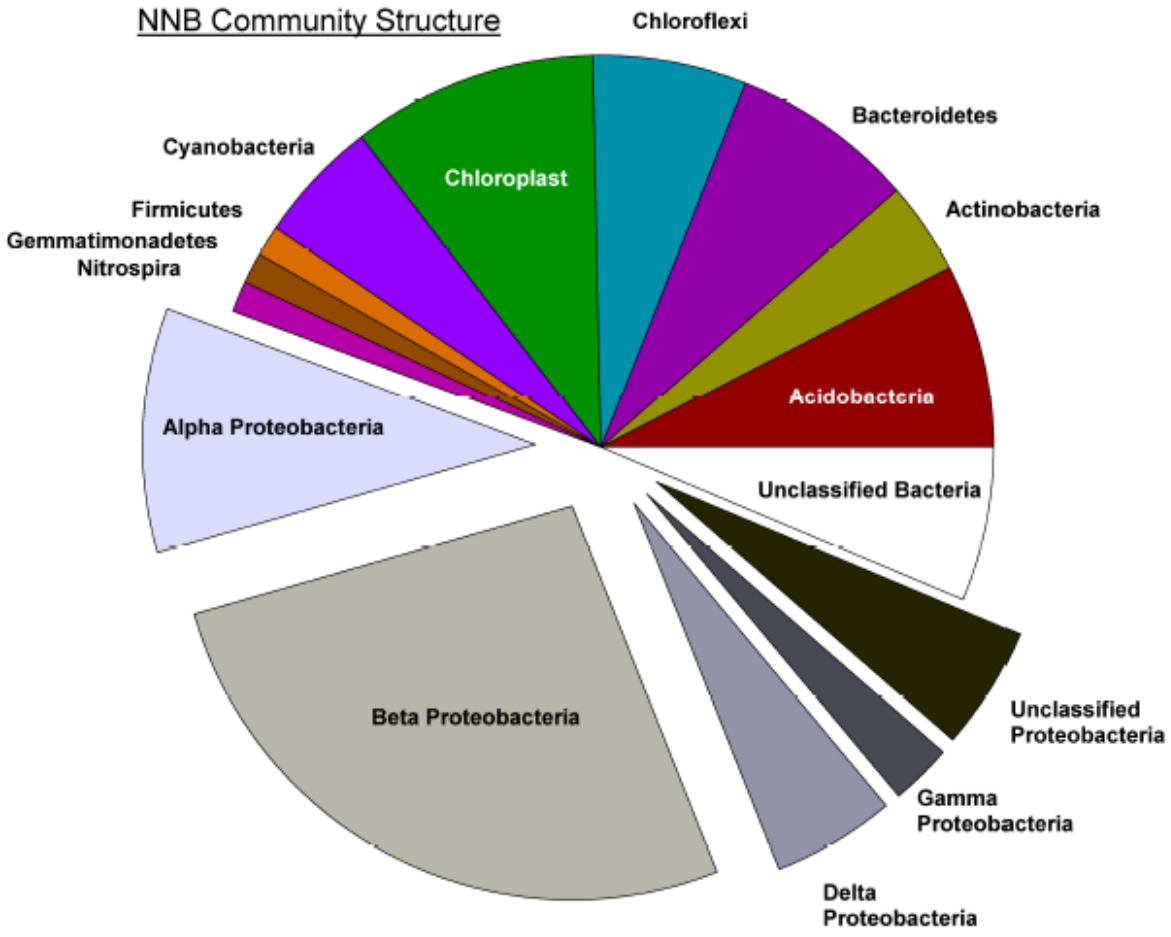

Figure 2.1: Graphic representation of the bacterial community phyla observed in New North Beach sediments. Phylum abundance is represented by the fraction of total sequences which fall under each phylum. Expanded slices correspond to observed classes of Phylum Proteobacteria.

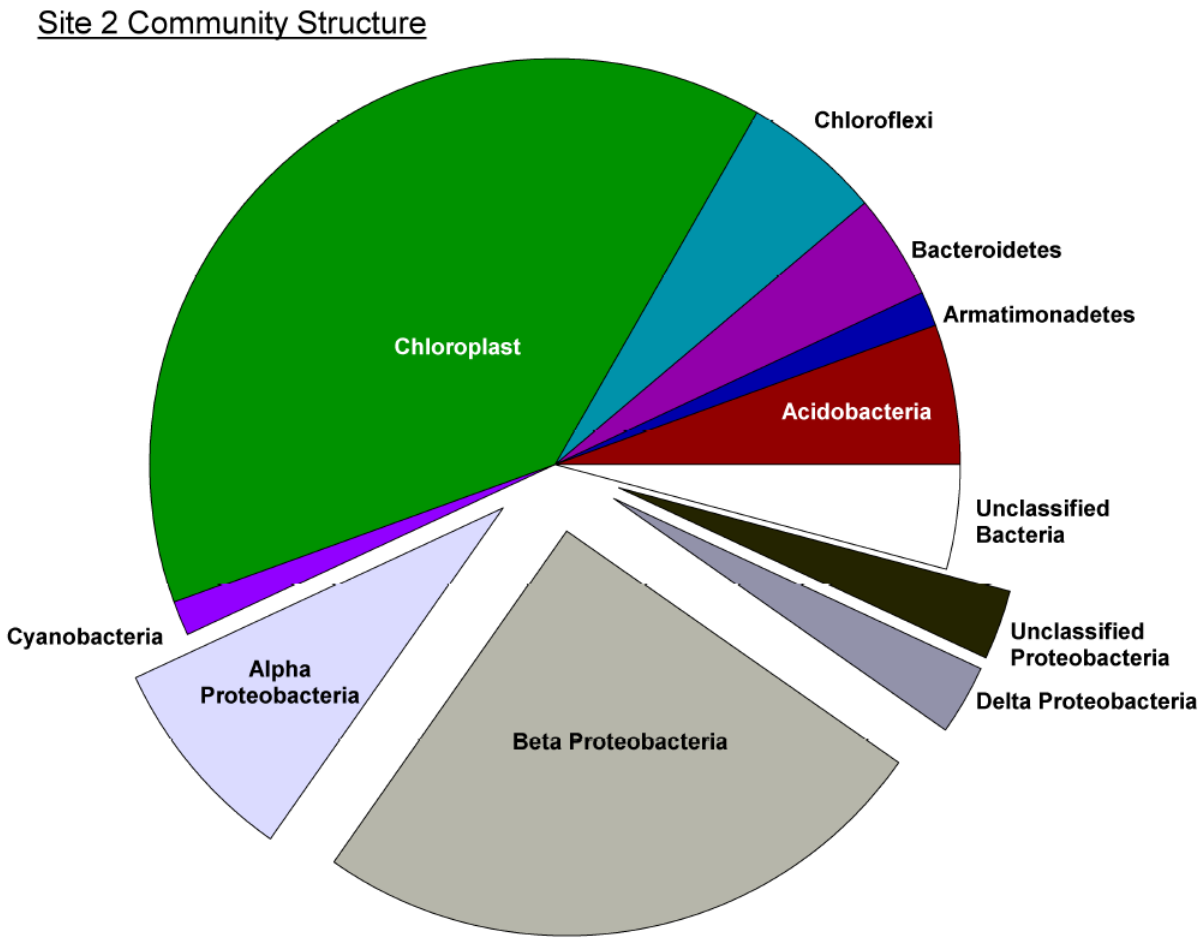

Figure 2.2: Graphic representation of the bacterial community phyla observed in Site 2 sediments. Phylum abundance is represented by the fraction of total sequences which fall under each phylum. Expanded slices correspond to observed classes of Phylum Proteobacteria.

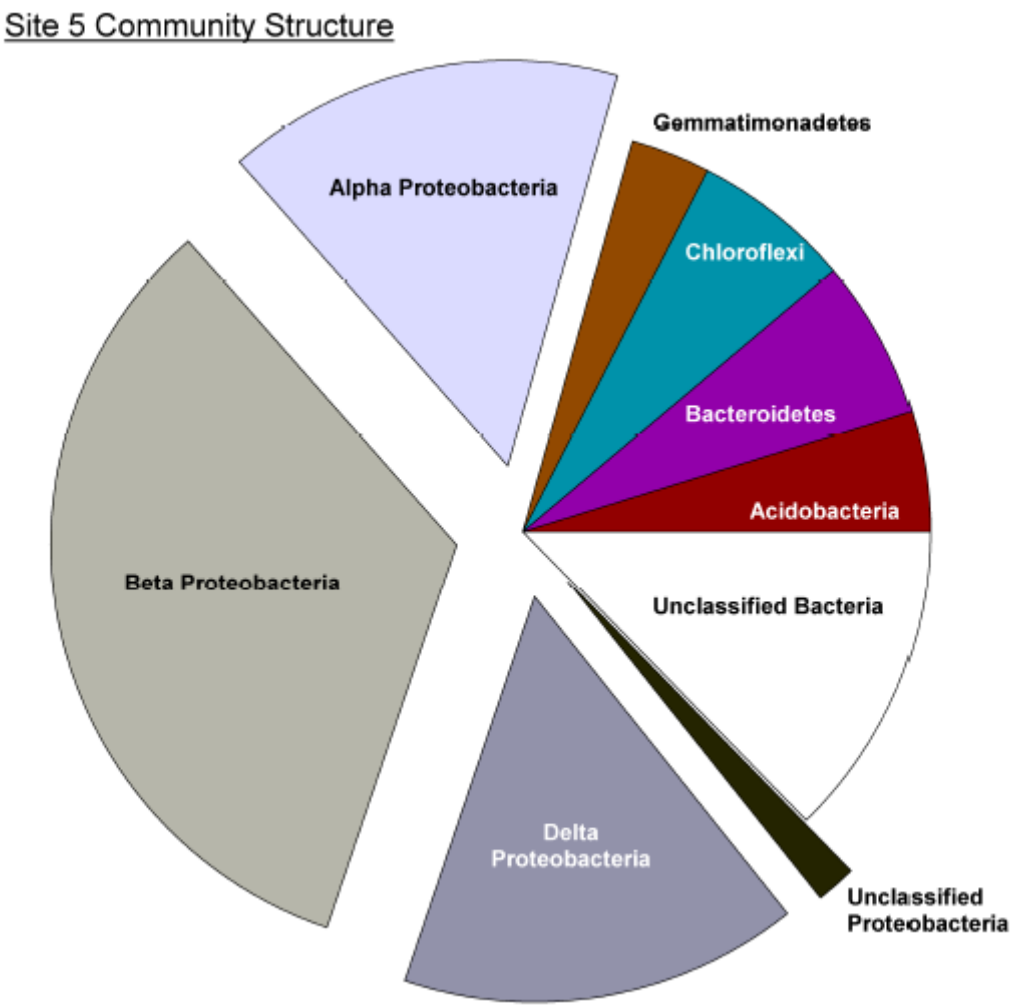

Figure 2.3: Graphic representation of the bacterial community phyla observed in Site 5 sediments. Phylum abundance is represented by the fraction of total sequences which fall under each phylum. Expanded slices correspond to observed classes of Phylum Proteobacteria.

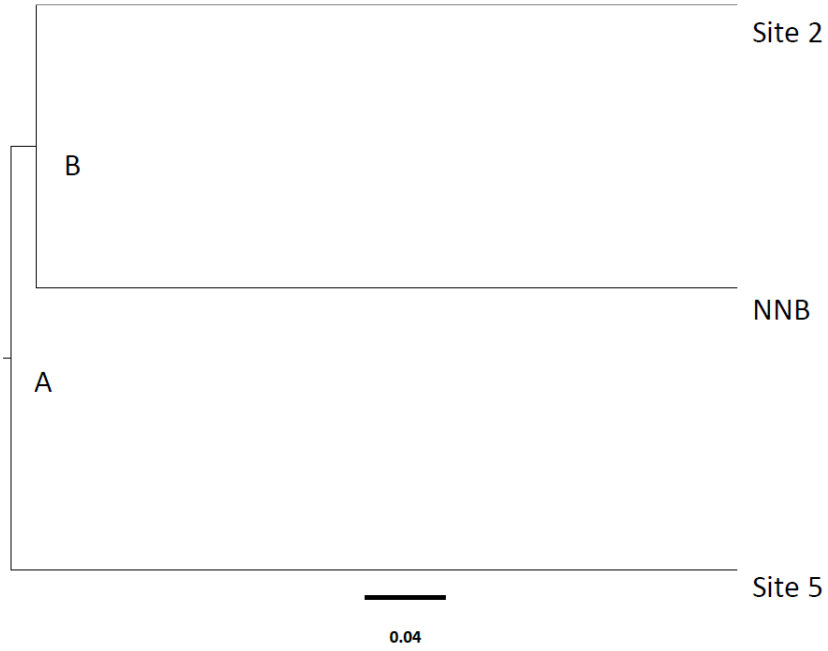

UniFrac Significance Distance Matrix				*UniFrac* Cluster Analysis				Lineage-Specific Analysis			
Site	**NNB**	**Site 2**	**Site 5**	Node	**n = 63**	**n = 55**	**n = 50**	Chloroplast Node	**NNB**	**Site 2**	**Site 5**
NNB	-	0.06	≤ 0.03	**A**	1.0	1.0	1.0	Observed	8	28	0
Site 2		-	≤ 0.03	**B**	0.94	0.90	0.87	Expected	13.29	12.11	10.60
Site 5			-					p-Value		8.63×10^{-8}	

Figure 2.4: Visual representation of UniFrac environmental clustering. Clusters were constructed using the UniFrac Significance Distance Matrix values. Results from Jackknife analysis of cluster significance with varying sample sizes (n) are listed. Lineage specific analyses concerning chloroplast OTUs are indicated.

3.0 Bacterial *mer*-operon genes as a tool to probe the response of microbial communities to mercury exposure from aluminum industry effluent.

3.1 Abstract

Genes of the *mer*-operon are involved in the enzymatically-based bacterial mercury resistance (Hg^R) redox pathway. The *mer*-operon genetic determinant of Hg^R was used to probe microbial community responses to sediment mercury (Hg) exposure. Immobilized sediment Hg was derived from past aluminium industry effluent. Hg may represent a component of currently discharged effluents. Operon gene abundance and expression, and the activity of the mercuric reductase enzyme (MerA) were assessed. It was hypothesized that the degree to which bacteria with enzymatic Hg^R dominate a community reflects the magnitude at which these communities are exposed to bioavailable forms of Hg. Sediment total mercury (THg) levels of effluent affected sites were significantly higher when compared to control sites ($p < 0.05$). Using newly designed primers, genes of the *mer*-operon genes *merP*, *merT*, and *merA* were quantified through qPCR. Operon gene abundances correlated strongly to the distribution of Hg over the project sites. Linear regression models indicate that THg was a good predictor of *mer*-operon gene abundance. The *merA* gene showed the strongest relationship ($R^2 = 0.849$, $p = 0.003$). Transcripts associated with the *mer*-operon in the sediments were neither detectable nor quantifiable even in sediments exhibiting high Hg concentrations. Control site and affected site sediments were assessed for their biological capacity of reducing Hg^{II} to volatile Hg^0 with enzyme MerA. Hg^0 is the final product in enzymatically-based Hg^R. Hg^0 released from affected sediments was 1000 fold higher than in control site sediments but the biological basis of this release could not be confirmed.

3.2 Introduction

Bacterial life can be detected in most if not all environments found on Earth (Fredrickson, *et al.*, 1988, Jordan, *et al.*, 1995, Liebert, *et al.*, 1997, Frias-Lopez, *et al.*, 2008, Niederberger, *et al.*, 2010, Sylvan, *et al.*, 2012). Bacteria have evolved many mechanisms from which they are able to sustain themselves within their immediate environment (Brock & Gustavson, 1976, Compeau & Bartha, 1985, Raphael, *et al.*, 2011). In addition, bacteria are able to transform elements in their immediate environment at various spatial scales: fermentative metabolism in milk by *Lactobacillus sp.* yields lactic acid reducing pH levels (Larsen & Anon, 1989); the quality of aquatic ecosystems can be heavily disrupted through the production of toxins originating from cyanobacterial blooms (Yoshida, *et al.*, 2008); and, the contemporary oxygen rich atmosphere was established through oxygenic photosynthesis carried out by microbes (Holland, 2006). These biologically mediated changes can arise either as an indirect result of bacterial activity (Holland, 2006, Yoshida, *et al.*, 2008) or as a direct result of creating an environment better suited to their survival (Larsen & Anon, 1989, Lovley, 2001, Orell, *et al.*, 2010). The biological detoxification of xenobiotics and toxic metals like mercury (Hg) are examples of how bacteria carrying resistance determinants are able to change the chemical composition of their environment to improve cellular survival and viability (Barkay, 1987, Rasmussen, *et al.*, 2000, Lovley, 2001, Poulain, *et al.*, 2007, Orell, *et al.*, 2010).

3.2.1 Industrially Derived Mercury

Mercury (Hg) is a constituent element in the crust of the earth with natural concentrations ranging anywhere between 21 to 56 $ng \cdot g^{-1}$ in the lower and upper portions of the crust, respectively (Wedepohl, 1995). In an average soil between 20 and 150 $ng \cdot g^{-1}$ of Hg can be expected (Osborn, *et al.*, 1997). A large fraction of terrestrial Hg is not bioavailable because it is

bound as organic molecule complexes (Osborn*, et al.*, 1997). Hg bioavailability is dependent on its oxidation state (Barkay*, et al.*, 2003). Abiotic and biotic processes transform Hg between the three most common states: divalent Hg (Hg^{II}), monovalent Hg (Hg^{I}) and volatile elemental Hg (Hg^{0}) (Smith*, et al.*, 1998, Barkay*, et al.*, 2003, Steffen*, et al.*, 2008). Elemental Hg (Hg^{0}) exhibits low vapour pressure and is easily transported over large geographical scales through the atmosphere (Steffen*, et al.*, 2008).

In certain environmental contexts, local Hg concentrations are found well beyond naturally occurring levels due to anthropogenic activity (Barkay*, et al.*, 2003). Coal fired power plants incinerate fossilized organic matter liberating Hg bound to it (UNEP, 2002, Barkay*, et al.*, 2003, Mimna*, et al.*, 2011). The Hg within coals has been observed at concentrations between 20 to 1000 $ng \cdot g^{-1}$ (Mimna*, et al.*, 2011). Unlawful gold mining techniques that use Hg to extract the precious metal account for roughly 23% of global anthropogenic Hg emissions (UNEP, 2008). Chlor-alkali plants use Hg as an industrial scale chemical catalyst for the production of sodium hydroxide and accidental spill-over of Hg may occur as a result of its use (UNEP, 2002, Barkay*, et al.*, 2003). Alumina refineries produce red mud tailings as a by-product of processing bauxite ores. These tailings contain Hg (Figure 1.3) with actual concentrations dependent on the origin of source bauxite ores that can vary from 20-2000 $ng \cdot g^{-1}$ (Mimna*, et al.*, 2011). However, environmental quality controls established at particular alumina refining plants prevent major outputs of tailing based Hg.

3.2.2 Cellular Effects of Hg Exposure

Hg harms biological systems by disrupting protein structure and enzyme functionality, as well as through inducing oxidative stress (Clarkson, 1997, Ercal*, et al.*, 2001, Valko*, et al.*, 2005). Hg is a redox-inactive metal with an affinity for thiol groups (Ercal*, et al.*, 2001).

Antioxidants such as glutathione (GSH) contain thiol groups. Enzymes are involved in maintaining the balance between cellular pro-oxidants and antioxidants levels (Farr & Kogoma, 1991). Thus, Hg induces oxidative stress by depleting cellular antioxidant stores and by rendering enzymes involved in the oxidative stress response (OSR) non-functional (Ercal*, et al.*, 2001).

3.2.3 Bacterial Community Exposure to Mercury

Community level responses to increased Hg exposure exhibited by soil bacteria have been previously documented (Barkay, 1987, Rasmussen & Sørensen, 1998, Rasmussen*, et al.*, 2000, Muller$_a$*, et al.*, 2001, Muller*, et al.*, 2002). For instance, ephemerally exposed communities may experience a drop in diversity (Rasmussen*, et al.*, 2000, Muller*, et al.*, 2002). Community diversity may recover in certain instances (Rasmussen & Sørensen, 1998, Rasmussen*, et al.*, 2000), while in others it remains at a reduced level (Muller$_b$*, et al.*, 2001). This phenomenon is related to the selective pressure Hg exerts on the community favouring bacteria holding Hg^R (Rasmussen & Sørensen, 1998, Rasmussen*, et al.*, 2000, Muller$_a$*, et al.*, 2001, Muller$_b$*, et al.*, 2001, Barkay & Wagner-Dobler, 2005). Thus, recovery in community diversity may only reflect an increase in richness among bacteria holding Hg^R factors (*mer*-operon) (Rasmussen & Sørensen, 1998, Barkay & Wagner-Dobler, 2005). In environments where Hg exposure is low and fluctuates, the fraction of the community holding *mer*-operon elements can reduce its toxicity to other microbes (Barkay, 1987, Rasmussen*, et al.*, 2000). Presumably, consistent exposure to high Hg concentrations will select for the Hg^R bacteria in the community.

3.2.4 Objectives

The objective of this study is to test whether the by-products of past and present aluminium industry activities released to the environment contribute to shape microbial

communities in the receiving ecosystems, particularly through enrichment in microbes resistant to mercury. The Hg present in sediments along the river banks has historically been derived from a now retired chlor-alkali plant within the smelter complex. While environmental guidelines are respected in this industrial context, residual amounts of Hg in effluents may originate as a result of processing bauxite (Mimna*, et al.*, 2011).

The *mer*-operon was used as a model to probe the response of the microbial community to Hg exposure. Gene marker abundance and expression of *merP*, *merT*, and *merA* were measured along with MerA enzyme activity. It was hypothesized that the degree to which bacteria holding Hg^R dominate a community will reflect the magnitude to which these communities are exposed to bioavailable forms of Hg.

3.3 Materials and Methods

3.3.1 Sampling Sites

Sampling sites were situated along the northern and southern banks of the Saguenay River in Jonquière (Québec, Canada) proximal to aluminium industry effluent discharge points (Figure 1.2). Two control sites were located on the opposite shore (northern shore) of the industrial complex and were not exposed to the industrial effluent plume (NB and NNB). Tracer experiments were performed by our industrial partners to identify the extent of the plume range downstream of the various sites (data not shown). These results confirmed that the north shore of the river is not currently exposed to the plume. Six sites were located on the south shore with three directly downstream of industrial effluent discharge points (Site 2, Site 3, and Site 4). Site 5 was located *ca.* 1 km downstream of an effluent discharge point. Sites 2 to 5 were classified as affected sites. Control sites SB and NSB were located upstream of and effluent discharge point.

3.3.2 Physicochemical Measurements of River Water

Water temperature, pH and conductivity were recorded using the YSI 556 Multiparameter System (YSI Environmental Inc., Yellow Springs, OH, USA) between July 22nd, 2011 and July 28th, 2011. Daily measurements were taken at two control sites (NNB and NSB) and two effluent discharge sites (Site 2 and Site 3) (Table 5.2). At each affected site, measurements of the effluent stream and the effluent discharge-river water mixing zone were recorded. The sonde was calibrated daily prior to use using calibration solutions for pH and salinity. Access to NSB and Site 2 was not possible on July 27th, 2011 due to weather-related conditions.

3.3.3 Sediment and Water Sample Collection

River sediments and water samples were collected in July and August of 2011. Sediment samples were obtained at low tide owing to the greater ease of access to riverbed sediments. For sites in contact with smelter effluent discharge streams (Site 2, Site 3, Site 4, and Site 5), low-tide accessible sediments were collected from points where effluent stream and river water formed a mixing zone at high tide. At each sampling site, sediments taken from 1-3 cm depths from the surface were mixed together from an area of roughly 3 m^2. Sediment samples were partitioned either into multiple sterile DNase/RNase free 50 mL Falcon® tubes or into four ounce polyethylene sterile specimen cups. Falcon® tube sediments were frozen in liquid nitrogen and stored at -20°C prior to transport. Specimen cup sediments were kept at 4°C at all times prior to laboratory use. Falcon® tube sediment samples were transported to the University of Ottawa (Ottawa, ON, Canada) on dry ice and stored at -80°C until processed.

Water samples were collected according to methods described by the US EPA for trace metal analyses in water (EPA, 1996). River water was collected in acid washed 1 L fluorinated high-density polyethylene (HDPE) bottles from two control sites and two affected sites (NNB, NSB, Site 2, and Site 3). Water was sampled at three different time points between July 21st and August 6th, 2011 to characterize temporal changes in total Hg (THg) concentration within the water column (Table 5.3). Site 2 and Site 3 waters were collected where effluent flow mixed with river water. Bottles were rinsed with site specific water three times prior to collection. Thereafter, water samples were preserved by acidification with trace metal grade 69-70% nitric acid (HNO_3) (OmniTrace® NX0407-2) to a final concentration of 0.7% (v/v). Preserved samples were kept at 4°C prior to processing. For laboratory QA/QC, *travel*, *laboratory* and *field* water sample blanks were prepared in acid washed 1 L HDPE bottles using deionized Milli-Q water

(MilliPore, Billerica, MA, USA). The blanks were brought to their respective locations to determine ambient baseline levels of THg measured in water samples (EPA, 1996). The blanks were acidified in the same manner as the experimental samples.

3.3.4 Preparation of Laboratory Reagents and Materials

All laboratory aqueous stock and working solutions were formulated using Milli-Q water (MilliPore, Billerica, MA, USA) that was autoclaved after treatment with diethylpyrocarbonate (DEPC) to a final concentration of 0.1% (v/v) following protocols detailed in literature (Hurt*, et al.*, 2001). DEPC is used to inactivate RNase enzymes which can compromise sediment sample RNA extracts but must be decomposed by autoclaving prior to using treated water. All glassware and utensils used for nucleic acid extraction were thoroughly washed, rinsed with DEPC-water and subsequently autoclaved for 1 h at 128°C.

3.3.5 Sediment Sample Preparation

Sediment samples used for Hg analyses were held in deep-freeze at -80°C and subsequently lyophilized under vacuum pressure (5 ATM) for 72 h at deep-freeze temperatures. Samples were homogenized prior to THg measurements. Sediments used in nucleic acid extraction protocols were separated into 5 g partitions each within sterile DNase/RNase 50 mL Falcon® tubes. These samples were washed with two to three volumes of a salt buffer (0.5 M EDTA, pH 8; 1 M Tris-HCl, pH 8.0; 0.5 M Na_2HPO_4, pH 8.0) adapted from literature (Zhou*, et al.*, 1996) and subsequently centrifuged at 9000 *g* at 4°C. Washing was performed three times prior to processing. The wash was performed in order to chelate metals and mitigate the co-extraction of sediment humic substances which inhibit downstream enzymatic analyses of nucleic acid extracts (Figure 5.1) (Fortin*, et al.*, 2004). Moreover, high concentrations of divalent

metal cations are known to prematurely precipitate DNA which may diminish extraction yield and efficiency (Gough & Stahl, 2011).

3.3.6 Total Hg Analysis

Lyophilized and homogenized sediments were processed for THg using the Mercury SP-3D Analyzer (Nippon Instruments Corp.). Samples were thermally decomposed releasing Hg vapour (Hg^0) which formed an amalgam with the instrument gold trap. Once liberated from the gold trap, THg concentrations were obtained via cold vapour atomic absorption spectrometry (CVAAS) (UOP Method 938-00; 0.01 ng Hg detection limit; range <1000 ng Hg). The Mercury SP-3D Analyzer was calibrated with the Hg Reference Solution 1000 ppm ±1% (Fisher CSM114-100). MESS-3 (91±9 ng/g) (NRC, Canada) was used as the reference sample.

THg levels in water were measured using methods described by US EPA Method 1631 (EPA, 2002). Prior to analysis, BrCl was used to oxidize all Hg to Hg^{II} in water samples. Following the subsequent reduction of the water samples by hydroxylamine, stannous chloride ($SnCl_2$) was applied to convert Hg^{II} to volatile Hg^0. Hydroxylamine is used to destroy free halogens in water samples which may damage instrumentation. Hg^0 was purged from the water sample using argon gas and was collected onto a gold trap. Hg^0 was thermally desorbed from this gold trap and carried via inert gas to a second (analytical) gold trap. Again, Hg was thermally desorbed from the analytical trap and carried to the cold-vapour atomic fluorescence spectrometer (CVAFS) for detection. The Tekran® 2600 (Tekran®, Toronto, ON, Canada) was used for CVAFS analysis. Standard checks were performed after 10 samples were processed. The Tekran 2600® was calibrated with Hg Reference Solution 1000 ppm ±1% (Fisher CSM114-100). Detection limits followed those put forth by US EPA 1631 (minimum level of quantitation = 0.5 ng/L; method detection limit = 0.2 ng/L).

3.3.8 Sediment Metagenome DNA Extraction

Sediment samples washed with salt buffer were immediately processed with the commercial PowerSoil® DNA Isolation Kit (MoBio Laboratories Inc., Carlsbad, CA, USA). Total DNA (metagenome) from sediments was extracted according to the manufacturer specifications. All extractions were performed under a laminar flow hood supplied with HEPA filtered air flow. Surfaces and instruments were sterilized with UV-C light, 70% ethanol and 10% bleach solutions. Following the isolation procedures, extract solution DNA concentration was determined through absorption spectra analysis with the NanoDrop Spectrophotometer 2000. DNA extracts were stored at -20°C until further use.

3.3.9 Sediment Metatranscriptome RNA Extraction

Initial attempts in total sediment RNA extraction were performed using RNA PowerSoil® Total RNA Isolation Kit (MoBio Laboratories Inc., Carlsbad, CA, USA) following salt buffer washing steps as implemented in sediment DNA extractions. A maximum of 5 g of sediment was processed per extraction to boost yields. All extractions were performed under a laminar flow hood supplied with HEPA filtered air flow. Surfaces and instruments were sterilized with UV-C light, 70% ethanol, 10% bleach and RNase Away (Molecular BioProducts Inc., San Diego, CA, USA) solutions. Following the isolation procedures, RNA extract concentration was determined through absorption spectra analysis with the NanoDrop Spectrophotometer 2000 (ThermoScientific, Nepean, ON, Canada). The 50 µL final extract volume was aliquoted by 25 µL into 0.5 mL Eppendorf tubes and stored at -80°C until further use.

RNA extractions using the RNA PowerSoil® commercial kit proved insufficient in obtaining high extract yield and quality. For this reason, sample preparation services provided by

the Norgen Biotek Corp. (Thorold, ON, Canada) were employed. Unaltered sediment samples (NNB, NSB, Site 2, Site 3, and Site 5) which were stored at -80°C were shipped to Norgen Biotek Corp. on dry ice. 10 g of sediment sample were processed. RNA extracts in a final volume of 2 x 100 µL per sample were shipped back to the University of Ottawa over dry ice and immediately stored at -80°C upon arrival until further use.

3.3.10 cDNA Synthesis

To eliminate DNA carried over during RNA extraction procedures, DNase treatments of RNA extracts were performed. The RQ1 RNase-Free DNase (Promega, Madison, WI, USA) commercial enzyme kit was used according to manufacturer specifications. DNA digestion effectiveness was verified by reference-gene targeted PCR assays. DNase digested RNA samples were subsequently purified using the RNeasy® MinElute® Cleanup Kit (Qiagen, Valencia, CA, USA) following listed protocols to remove salts from solution. Excess salts could interfere with cDNA synthesis. Once purified RNA extracts were deemed free from substantial carry-over DNA and excess salts, cDNA synthesis was executed via SuperScript™ III First-Strand Synthesis System for RT-PCR (Invitrogen, San Diego, CA, USA). RNA samples were processed according to kit specifications. Each sample was separated into two reaction vessels: one containing the reverse-transcriptase enzyme (+RT) and the other without (–RT). This measure was implemented to ensure that any enzyme-based signal generated using reverse transcribed RNA indeed represented cDNA and not carry-over DNA.

3.3.11 Conventional PCR Assays

PCR reactions were performed using the Eppendorf MasterCycler ProS (Eppendorf Canada, Mississauga, ON, Canada) and the Biometra T Professional Basic Gradient (Biometra, Goettingen, Germany). Commercial enzyme Platinum® Taq Polymerase (Invitrogen, San Diego,

CA, USA) was used to generate PCR amplicons. Results of conventional PCR assays were used to ensure assay specificity and quality prior to the application of PCR protocols in quantification assays (qPCR) (QA/QC).

PCR reactions were carried out according to the commercial kit recommendations with final per reaction reagent concentrations being: 1X PCR buffer, 2.5 mM $MgCl_2$, 0.2 μM forward/reverse primers, 0.2 mM dNTPs, 0.625 U Platinum® Taq Polymerase. For the determination of optimal PCR conditions in generating specific amplicon products with maximized yields, $MgCl_2$ concentrations varied from 1.5 mM to 3.5 mM. Once generated, amplicons were separated by electrophoresis, and visualized under UV light.

Genes targeted in PCR assays and their associated PCR primers with respective information on cycling conditions are presented in Table 5.6. The results of conventional PCR assays applied on extracted sediment metagenomes are presented from Figure 5.4 to Figure 5.15.

3.3.12 qPCR Assays

qPCR reactions were performed using the commercial enzyme kit SsoFast™ EvaGreen® Supermix (Bio-Rad Laboratories, Hercules, CA, USA) according to manufacturer recommendations. Final per reaction reagent concentrations were: 1X SsoFast EvaGreen Supermix and 0.2 μM Forward/Reverse primers. Samples and associated assay standards were assayed in triplicate with each replicate having a final volume of 20 uL. 60 μL sample master mix solutions were created to reduce variability between sample triplicates. Samples and associated assay standards were run using the Eco™ Real-Time PCR System (Illumina® Inc., San Diego, CA, USA). Machine user interface software used was the Eco™ Real-Time PCR system qPCR Software v2.0.6.0 (Illumina® Inc., San Diego, CA, USA). The software calculated

assay reaction efficiencies and the standard curve regression coefficient, y-intercept and slope. This information is listed in Chapter 5 (Table 5.7 and Table 5.11).

3.3.13 qPCR Assay Standard Development

qPCR standards were created using PCR amplicon products derived from laboratory pure cultures known to house the gene of interest (Bustin, 2000). After the successful amplification of the partial gene segment of interest, the amplicons were cloned within the vector pGEM-T Easy Plasmid (Promega, Madison, WI, USA) and used to transform a competent stock of laboratory culture (*E.coli* strain XL10). The transformed culture was grown overnight and the vector plasmid housing the amplicon of the gene of interest was extracted using the Wizard® Plus SV Minipreps DNA Purification System (Promega, Madison, WI). Extracts were stored at -20°C until further use.

The standard copy number was calculated by determining the molar mass of the cloned plasmid which was derived from known sequence data. Quantification of the plasmid extract was performed using the NanoDrop Spectrophotometer 2000 (ThermoScientific, Nepean, ON, Canada). Gene standard copy number per µL of plasmid extract was calculated as follows:

(1) Plasmid Concentration (g/µL) ÷ Molar Mass of the Plasmid (g/mol) = Molar Copies (mol/µL)

(2) Copies (mol/µL) x Avogadro's Number = **Copy Number·µL^{-1}**

Concentration values for standard copy number were entered into the Eco™ Real-Time PCR system qPCR Software based on the volume (µL) inputs in each reaction vessel. 10-fold based dilution series of the standard plasmid stock were generated to create a dilution curve for

the qPCR standards. Standard quantities used in the generation of standard curves ranged from 10 copies to 10^7 copies of gene specific amplicon.

3.3.14 Sediment Microcosms Analysis - Mercury Vapour (Hg^0) Release

Sediment samples that were stored at 4°C and never frozen were used to determine biogenic production potential of Hg^0. Biogenic production of Hg^0 is mediated through the MerA enzyme (EC: 1.16.1.1). Approximately 40 g of sediment was mixed with sterilized and Hg-free water up to a final volume of 600 mL. The sediment solution volumes were held in 1 L glass Erlenmeyer flasks and agitated with magnetic stir bars. The sediment solution was gassed with Hg-free air supplied by a Tekran® Model 1100 Zero Air Generator (Tekran® Instruments Corporation, Toronto, ON) through Teflon tubing. Gaseous output from the sediment slurry passed through a collector tube connected to a Tekran® Model 2537A/B (Tekran Instruments Corporation, Toronto, ON). Hg^0 released by the microcosm was pre-concentrated onto a gold-trap within the Tekran® Model 2537. The Hg^0 was detected by CVAFS methods. The sample volume from which Hg was collected onto the gold trap was 7.5 L and measurements of Hg^0 were performed every 5 min. To assess non-biogenic production of Hg^0, a second microcosm apparatus using the same sediments was treated with formaldehyde (Fisher BioReagents, Ottawa, ON, Canada) to a final concentration of 1% (v/v) in order to arrest bacterial activity. Formaldehyde treated microcosms were held at room temperature for 24 h prior to the initialization of Hg^0 measurements using the Tekran® Model 2537 A/B. Microcosm bioreactors were protected from light at all times using aluminium foil to prevent light-dependent Hg redox reactions (Zhang, 2006).

3.3.15 Statistical Analyses

Statistical analyses were performed using JMP Software (JMP® 10.0.0, SAS Institute Inc., Cary, NC, USA). Data sets (gene copy abundance, THg) were pooled by control site data (NB, NNB, SB, NSB) and affected site data (Sites 2 to 5). Data pools were tested for normality using the Shapiro-Wilk test. Where normality was achieved in data sets, the two-tailed Student's T-test was performed to determine if there was a significant difference between control and affected site pooled data. Where normality could not be achieved, arising from sample variability or insufficient sample number, the Wilcoxon non-parametric T-test was used. Homoscedasticity of the data sets was assessed using Levene's test. When variances were unequal between means within data sets, Welch's T-test was applied to determine if the means could be considered equivalent given differing standard deviations (SD) (Table 5.9).

Similar tests for normality and homoscedasticity were applied for data sets pertaining to individual project sites: NB, NNB, SB, NSB and Sites 2 to 5. A simple linear regression model was used to determine if sediment THg concentration could predict gene copy numbers. Data outliers in regression curves were determined using Dixon's Q-test. Results from statistical tests were considered significant for $p < 0.05$.

3.4 Results

3.4.1 Physicochemical Parameters in Water

Abiotic parameters such as temperature, pH and salinity can influence the mobility and toxicity waterborne toxicants (Lydy*, et al.*, 1990, Hamilton*, et al.*, 1995, Barkay*, et al.*, 2010). To determine if abiotic factors would come into play in this project, measurements of river water temperature, pH and conductivity were taken at two control sites (NNB and NSB) and two affected sites (Site 2 and Site 3). Control site waters had lower temperatures, pHs and conductivity readings when compared to affected site waters. The highest readings for each parameter were observed at Site 3. Higher temperatures, pHs and conductivity readings were observed in effluent streams of Site 2 and Site 3 when compared to respective readings taken in the effluent stream-river water mixing zones. At Site 3, conductivity measurements were approximately an order of magnitude higher than in the control sites. Site 3 pHs indicated that waters were more alkaline here than at the control sites. Mean values and ranges of measurement are detailed in Table 5.2.

3.4.2 Sediment THg Levels

Hg was used as an indicator of aluminium industry influence on the local watershed. Hg was released as a by-product of currently decommissioned chlor-alkali processes. At present, Hg may be emitted at trace levels due to bauxite processing. Sediments were collected from 8 sites along the Saguenay River (Figure 1.2). When grouped together, sediment THg concentrations were found to be significantly higher at affected sites (Sites 2 to 5) when compared to control sites (NB, NNB, SB, and NSB) (Figure 3.1). Differences between individual sites of each grouping were observed. One control site (NSB) exhibited higher THg concentrations than an affected site (Site 5).

3.4.3 Metagenome Data – The *mer*-operon

The enzymatic Hg^R genetic determinant was used as a tool to probe the response of microbial communities to the Hg component of industrial effluents. Conventional PCR assays targeted the *mer*-operon. Strong amplicon band signals were generated for affected sites when compared to control sites (Figure 5.8 to Figure 5.15). The same trend was not observed with PCR assays targeting housekeeping reference genes. Assays targeting these genes yielded gel bands of similar specificity and intensity across all project sites (Figure 5.4 to Figure 5.7). All gel based PCR results are listed in Chapter 5.

qPCR assays were used to confirm gel based results and quantify gene abundances. When pooled together as control or affected site, *mer*-operon gene abundances (*merT*, *merP*, *merA*) were found to be significantly higher at affected sites when compared to control sites (Figure 3.2). Differences between sites could be observed within each group. Individual affected sites typically exhibited the highest *mer*-operon gene abundance. Two different primer pairs were used to target *merP* and *merT* genes. With the merT2d primer pair individual affected sites all exhibited greater *merT* gene copy numbers compared to control sites. For the merT1d primer pair Site 4 was not significantly different than any of the control sites ($p > 0.05$, data not shown). Primer pair merP2d showed that Site 4 and Site 5 were not significantly different from control sites ($p > 0.05$, data not shown). Assays using primer pair merP3d displayed Site 5 not being significantly different from the control sites ($p > 0.05$, data not shown).

Abundances of genes not involved in Hg^R were quantified. Housekeeping genes are involved in core metabolic processes and are expected to be found in all bacterial genomes. Experiments focused on *glnA*, *katG* and *rpoB*. Whether mean values of gene copy numbers were pooled together as control or affected site, or when values were considered independently, no

significant difference between control site and affected site groups were found (Figure 3.3 and Table 5.9).

3.4.4 Regression Analyses – Gene Abundance and Hg Concentration

To test whether the differences observed between affected and control sites could be explained by THg concentration in sediments, simple regression models were constructed with log transformed THg as the independent variable. Regression coefficients and significance values are listed in Table 5.10. For all assays except merT1d and merP2d, significant relationships were found between log THg and log transformed mer-operon gene abundance (Figure 3.4). The strongest relationship and significance was observed between *merA* gene abundance and sediment THg. Log transformed reference gene (*glnA*, *katG*, *rpoB*) abundances were similarly compared to sediment THg (Figure 3.5). No significant relationships were observed between these variables (Table 5.10). For all regression curve constructions NSB site was determined to be an outlier using Dixon's Q-test ($p > 0.05$).

3.4.5 Metatranscriptome Analyses – Sediment RNA

Detection and quantification of expression was attempted for the genes of interest from each project site. Expression analysis was performed to determine if Hg^R gene expression paralleled the trend of Hg^R gene copy number to sediment THg concentrations. Initial attempts to determine transcript level signal response in sediments from each site proved unsuccessful. Difficulties were met in obtaining sediment RNA extracts of sufficient yield and quality. Sediments from control sites (NNB and NSB) and affected sites (Site 2, Site 3 and Site 5) were shipped to a commercial processing company. Sediment RNA was isolated using proprietary means. RNA quality was tested using synthesized cDNA as a template for *16S rRNA* qPCR assays. Reactions using reverse transcriptase (RT+) yielded a strong and specific signal (Figure

3.6). Reaction sets not appended with the reverse transcriptase enzyme (RT–) did not match the RT+ reaction in signal strength signifying low carry-over of contaminant DNA (Figure 3.6). All attempts to amplify functional gene messenger RNA from the environmental transcriptomes failed whether in-house or the commercially derived RNA extracts were used.

3.4.6 Sediment Microcosm Bioreactor

Sediments taken from NNB and Site 2 were analysed for their potential to biogenically produce Hg^0 as a measure of *mer*-operon mediated Hg^R in these sediments. Cumulative release of Hg^0 was roughly three orders of magnitude greater from Site 2 sediments when compared to NB microcosms (Figure 3.7). Despite a high degree of variability between daily measurements, an increasing trend of Hg^0 release per day could be seen in Site 2 sediment microcosms. To determine whether the Hg^0 released from sediment bioreactors was biogenic in nature, sediment microbial communities were treated with a 1% formaldehyde (v/v) solution to the final microcosm slurry volume. There was no difference in Hg^0 release between the 1% formaldehyde treated bioreactors and the non-treated bioreactors (Figure 3.7).

3.5 Discussion

3.5.1 Abiotic Factors at Project Sites – Hg Levels, Sources and Mobility

Hg was used as a tracer element of industrial activity as it can be detected at very low concentrations (EPA, 2002). This allowed us to track effluent release and the extent of its distribution in the sediments of the Saguenay River. Sediment Hg profiles showed an increase at sites which see the discharge of industrial effluent (Figure 3.1) indicating that Hg originated from released effluent. THg levels in water collected from effluent affected sites confirm the industrial source of released Hg. However, Hg in the water column could have also arisen from the resuspension of Hg previously deposited in sediments (Table 5.3).

One exception to the pattern of Hg emission lies at NSB. Here THg levels appeared to be higher than at affected Site 5. NSB lies upstream from the effluent discharge point at Site 2. Site 5 is located *ca.* 1 km downstream from the effluent discharge point at Site 3. THg levels in sediments at NSB and Site 5 were expected to be equivalent. A factor external to industrial activities likely affects THg levels seen in NSB sediments. This external factor may have caused NSB gene abundance data sets to be considered outlying in the regression curves analyses. The THg independent value in the regression curves is based on *industrially* derived Hg.

River water from affected sites (Sites 2 and 3) all showed increased temperatures, salinities and pHs when compared to control sites (NNB and NSB). Salinity was determined through water conductivity (μS/cm). Industrial outputs are the probable source of these physicochemical parameter increases. In aquatic settings, high temperature and salinity in conjunction with low pH may serve to mobilize contaminants such as Hg from sediments (Hamilton*, et al.*, 1995, Barkay*, et al.*, 2010). The mobility of Hg is diminished if adsorbed to sediments (Rasmussen*, et al.*, 2000). Increased mobility may elevate accessibility of the

bioavailable fraction of THg. The bioavailability of Hg present in sediments is an important factor to consider. Only a fraction of THg present in sediments may be biologically relevant. The influence of Hg on the microbial community would reflect exposure to this relevant fraction and not the total amount. It should be noted that in aquatic environments with high salinity Hg bioavailability is reduced. Chlorine anions sequester ionic Hg. $HgCl_3^-$ and $HgCl_4^{-2}$ dominate in seawater and have lower bioavailabilities compared to $HgCl_2$ (Barkay*, et al.*, 2010). The conductivity of seawater is approximately 50 000 µS/cm. No river water conductivity measurements reached this level of magnitude (Table 5.2).

3.5.2 Influence of Hg on Bacterial Communities

Industrially derived Hg appeared to shape the functional capabilities of sediment microbial communities where Hg was deposited. The effect of Hg exposure was tracked using the genetic determinants of Hg^R (*mer*-operon). Operon gene abundances were generally higher at affected sites (Figure 3.2) indicating an enrichment for bacteria holding Hg^R genetic determinants. When compared to *merP* and *merT*, copy numbers of *merA* exhibited the strongest and most consistent response signal across project sites. The *merA* regression curve coefficient and significance were greater than in curves built using *merP* and *merT* (Figure 3.4).

Dissimilarities in gene copy number between *mer*-operon gene assays were observed at particular sites. The *merP*, *merT* and *merA* genes represent typical constituent genetic elements of the generic *mer*-operon (Barkay*, et al.*, 2003). Therefore these genes were expected to be found in relatively equal amounts. Differences may be due to deficiencies in primer design. Unintended amplification of non-operational *merP* and *merT* gene sequences at control sites could result in inflated gene copy numbers. This would skew the linear regression curve. Furthermore, PCR amplification efficiency may not be uniform across DNA extracts taken of

project sites. PCR inhibitors that are extracted alongside nucleic acids deflate amplification yields (Fortin, *et al.*, 2004). These inhibitors may have been extracted in excess from affected site sediments and would diminish the qPCR derived gene copy number, again skewing the regression curve. Contaminated sediments also yield inhibitors of nucleic acid extraction, thus the pool of DNA extracted from affected project sites may not fully represent the actual conditions in the sediment metagenome (Zhou, *et al.*, 1996, Fortin, *et al.*, 2004). This misrepresentation influences the signal derived from these extracts. PCR amplification efficiency for DNA extracted from project sites was not assessed but assay efficiencies as determined using recombinant gene standards were deemed sufficient (>95%) (Table 5.7).

Inconsistencies in the association between *mer*-operon gene abundances to sediment THg arise because THg does not reflect the fraction of Hg that is biologically relevant. Microbial community responses to Hg exposure is generated from bioavailable Hg (Rasmussen, *et al.*, 2000). Using total sediment Hg concentrations may not be entirely effective for the characterization of Hg exposure. This could skew relationships drawn between Hg^R gene abundances and sediment THg.

Reference genes involved in core metabolic processes were also quantified (*glnA*, *rpoB*, *katG*). These genes are considered ubiquitous across environments due to the essential nature of their activity within cells. Thus, reference gene quantities were used to determine if *mer*-operon gene abundances across sampling sites were skewed due to differences in cellular abundance, nucleic acid extraction efficiency and PCR amplification efficiency (Figure 3.3). Differences in reference gene abundance across sites were unrelated to sediment THg levels (Figure 3.5). Bacteria are considered to have only one copy of the RNA polymerase subunit B (*rpoB*) gene per genome (Dahllof, *et al.*, 2000). Gene copy number of *rpoB* indicates the number of genomes and

by extension the number of cells present at each site. The *rpoB* gene quantification assay suggested that cell numbers were greater at NB sediments than at any other project site (Figure 3.3). This does not impact *mer*-operon analyses as Hg^R genes were at their lowest levels at NB site. Additionally, the catalase-peroxidase gene (*katG*) assay resulted in copy number differences between NSB and Site 3 (Figure 3.3). These discrepancies were assumed to be assay specific. No relationship between THg and *katG* abundance could be drawn. Moreover, amplification efficiency of *katG* standards indicates that assay design influences the copy number signal (Table 5.7). No trend between reference gene abundances and sediment THg levels were seen.

3.5.3 Modelling the Response of Bacterial Communities to Hg

Gene copy number results suggested that bacteria holding Hg^R had become established at affected sites due to exposure to industrially derived Hg. Dominance of microbial sub-communities holding Hg^R was reflected in abundances of Hg^R related genes. These gene markers are considered a biomarker of Hg exposure. This biomarker response was considered an indication of the extent to which industry effluents influence the local ecosystem.

The association between *mer*-operon gene abundances and sediment Hg exposure was modelled using linear regressions (Figure 3.4). Strengths of association were measured using regression coefficients and significance values. Correlations between the two variables were greatest for *merA* followed by *merP* and *merT*. This is likely due to discrepancies in PCR amplification efficiency, primer design efficiency, and the presence of inhibitor chemicals in DNA extracts. Reference gene abundances were also compared to sediment THg levels (Figure 3.5). This was done to determine if Hg exposure could predict the reference gene copy numbers. No significant association between reference gene copy number and THg concentration were observed.

Data sets from NSB were considered outlying and were not included in regression models. Correlations between *mer*-operon gene abundances to THg did not have strong regression coefficients and significance values when NSB data sets were included (Table 5.10). Results from Dixon's Q-test (data not shown) verified that NSB was an outlier in all regressions except for the *glnA* curve. In the interest of consistency, NSB *glnA* gene abundance data was omitted.

3.5.4 Gene Expression Study

It is possible to characterize the biological response of sediment microbial communities to Hg exposure when analysing the sediment metagenome. Determination of active *in situ* community responses required characterization of the sediment metatranscriptome. There is an inherent degree of difficulty when processing sediments for nucleic acid analysis (Roose-Amsaleg*, et al.*, 2001, Sessitsch*, et al.*, 2002), but success has been previously documented (Fortin*, et al.*, 2004, Schaefer*, et al.*, 2004, Poulain*, et al.*, 2007, Lee*, et al.*, 2008, DeCoste*, et al.*, 2011). While commercially extracted RNA of project site sediments were low in yield, RNA quality was determined to be sufficient based on the *16S rRNA* PCR assays using cDNA inputs and associated quality controls (Figure 3.6). Despite acceptable quality, no messenger RNA (mRNA) signals related to genes of interest were consistently identified. Target gene mRNAs were found in lower abundance compared to ribosomal RNA (rRNA). Therefore, the quantity of extracted RNA was insufficient to obtain the required resolution. Sediments afflicted with high metal and pollutant loads often see lower extraction yields and quality (Fortin*, et al.*, 2004). This may explain the difficulties encountered in this context for affected site sediments.

3.5.5 Hg^0 Production from Sediments

The potential for sediment microbial communities to enzymatically reduce Hg^{II} to Hg^0 was assessed in sediments taken from NNB and Site 2. The cumulative difference in Hg^0 release between the control site and affected site sediment microcosms was 100 to 1000-fold (Figure 3.7). The nature of the released Hg^0 remains unknown. Attempts to determine if the Hg^0 released was biogenic in origin proved inconclusive as microcosms that were chemically treated to arrest microbial activity released nearly the same amount of Hg^0 over time (Figure 3.7). The released Hg^0 may have already been present in the sediments. The magnitude of the difference in release between NNB and Site 2 is likely related to THg levels present sediments. Lyophilized sediment THg was three orders of magnitude higher at Site 2 when compared to the NNB (Table 3.1).

The daily release of Hg^0 increased in Site 2 sediment bioreactors with great variability over the course of the microcosm experiment. Due to the volatile nature of Hg^0 and the consistent agitation of sediment slurries in the microcosm chamber, it is conceivable that all volatile Hg was liberated early in the experiment. If no Hg^0 was being actively produced, a downward trend in daily production could be expected. As this was not the case it is plausible that Hg^0 was being produced over the course of the experiment. However, this increase is most likely due to changed chemical parameters in the bioreactors which liberated Hg^0 adsorbed to sediments.

While not directly indicative of enzymatic Hg^R, expression levels of *mer*-operon genes in the microcosm experiments could be used to determine the biogenic capacity of the microcosms to reduce Hg^{II}. As it stands, the greater release of Hg^0 in Site 2 sediments compared to NNB is only attributable to the THg levels already present at each site.

3.6 Conclusion

To address the influence of aluminium industry activity on the local ecosystem, the Hg component of industrial effluents was analyzed. Hg was used to trace the extent to which effluent by-products spread across the local aquatic ecosystem. To determine if a biological response to released Hg could be measured, the bacterial sediment communities that receive effluent by-products were probed. Bacterial function specifically related to the enzymatic detoxification of Hg was assessed. Community Hg^R was characterized using the *mer*-operon genetic determinant of Hg^R. Gene abundance and expression of enzymatic Hg^R genes (*merP*, *merT* and *merA*) as well as the final product of their activity (Hg^0) were measured. The strongest biological response signal to the levels of Hg immobilized in sediments was seen at the gene abundance level, particularly for the gene encoding MerA. Exposure to greater levels of sediment THg enrich for bacteria holding enzymatic Hg^R potential as measured by the abundance of the genetic Hg^R determinants. The abundance of *mer*-operon genes in affected sites indicates the presence of a thriving bacterial community harbouring Hg^R potential. These communities have the capacity to naturally remediate the sites they occupy.

The methods used in this study can be applied to other industrial contexts to determine the influence of pollution on receiving ecosystems. Analyses of specific effluent components in conjunction with respective biological responses represent a reductive approach in determining anthropogenic influences on ecosystems.

3.7 Tables

Table 3.1: Sampling site coordinates listed with sediment sample collection days. Sediment total mercury (THg) concentrations in dry weight are presented.

Site (Abbreviation)	Coordinates	Collection Date	THg (ng/g) (SD)
North Beach (NB)	48° 27' 05.80" N 71° 09' 17.87" W	August 1st, 2011	3.492 (0.216)
New North Beach (NNB)	48° 27' 26.76" N 71° 10' 32.15" W	August 1st, 2011	4.061 (0.498)
South Beach (SB)	48° 26' 54.16" N 71° 11' 43.62 W	August 4th, 2011	5.376 (0.06)
New South Beach (NSB)	48° 27' 04.61" N 71° 10' 26.16" W	August 5th, 2011	94.991 (5.50)
Site 2	48° 27' 01.57" N 71° 10' 15.85" W	August 1st, 2011	2951.272 (1068.05)
Site 3	48° 26' 41.37" N 71° 09' 08.15" W	August 2nd, 2011	608.248 (50.46)
Site 4	48° 26' 33.46" N 71° 08' 35.74" W	August 4th, 2011	2141.806 (246.90)
Site 5	48° 26' 16.95" N 71° 07' 30.21" W	August 1st, 2011	23.892 (10.19)

3.8 Figures

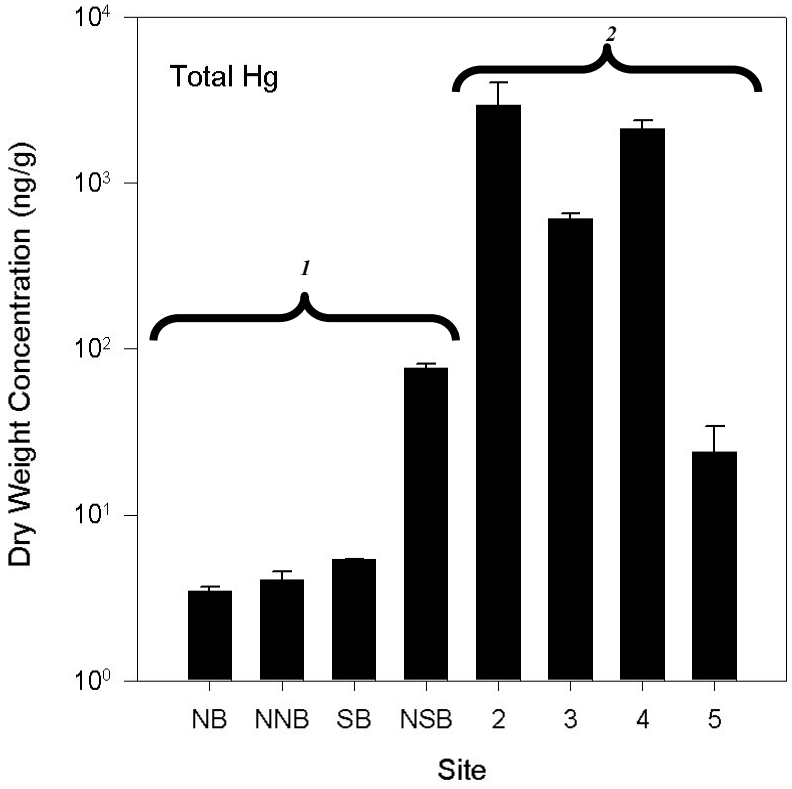

Figure 3.1: Log scale representation of total sediment Hg dry weight concentrations (+SD) across sampling sites. Significant differences between control and affect site pooled data are indicated by number (***1***, ***2***). See Table 5.9 for details regarding statistical analyses.

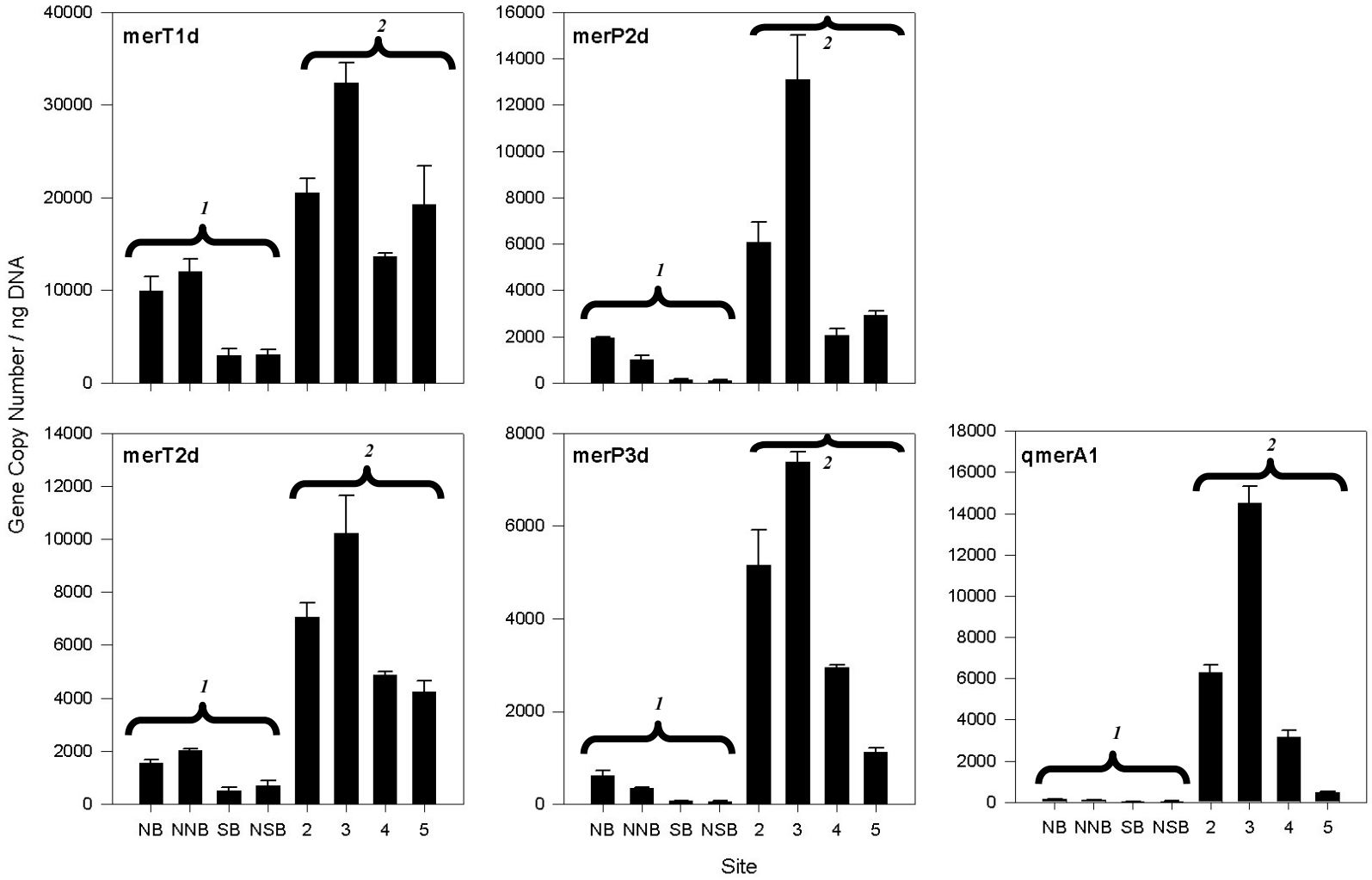

Figure 3.2: Sediment gene copy numbers (+SD) for the *mer*-operon quantified in qPCR assays using designated primer sets (in-set). Gene copy numbers were normalized by total DNA extracted from each site. Significant differences between control and affect site pooled data are indicated by number (***1***, ***2***). See Table 5.9 for details regarding statistical analyses.

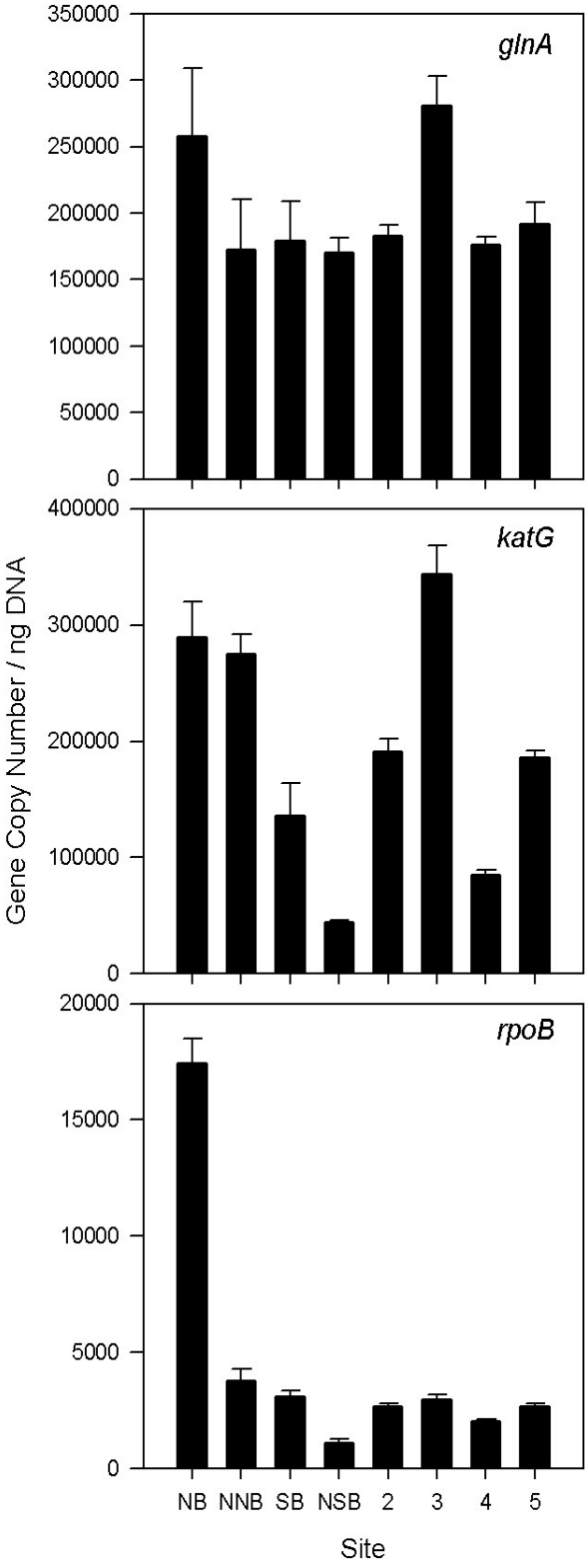

Figure 3.3: Reference gene copy numbers (+SD). Gene copy numbers were normalized by total DNA extracted from each site.

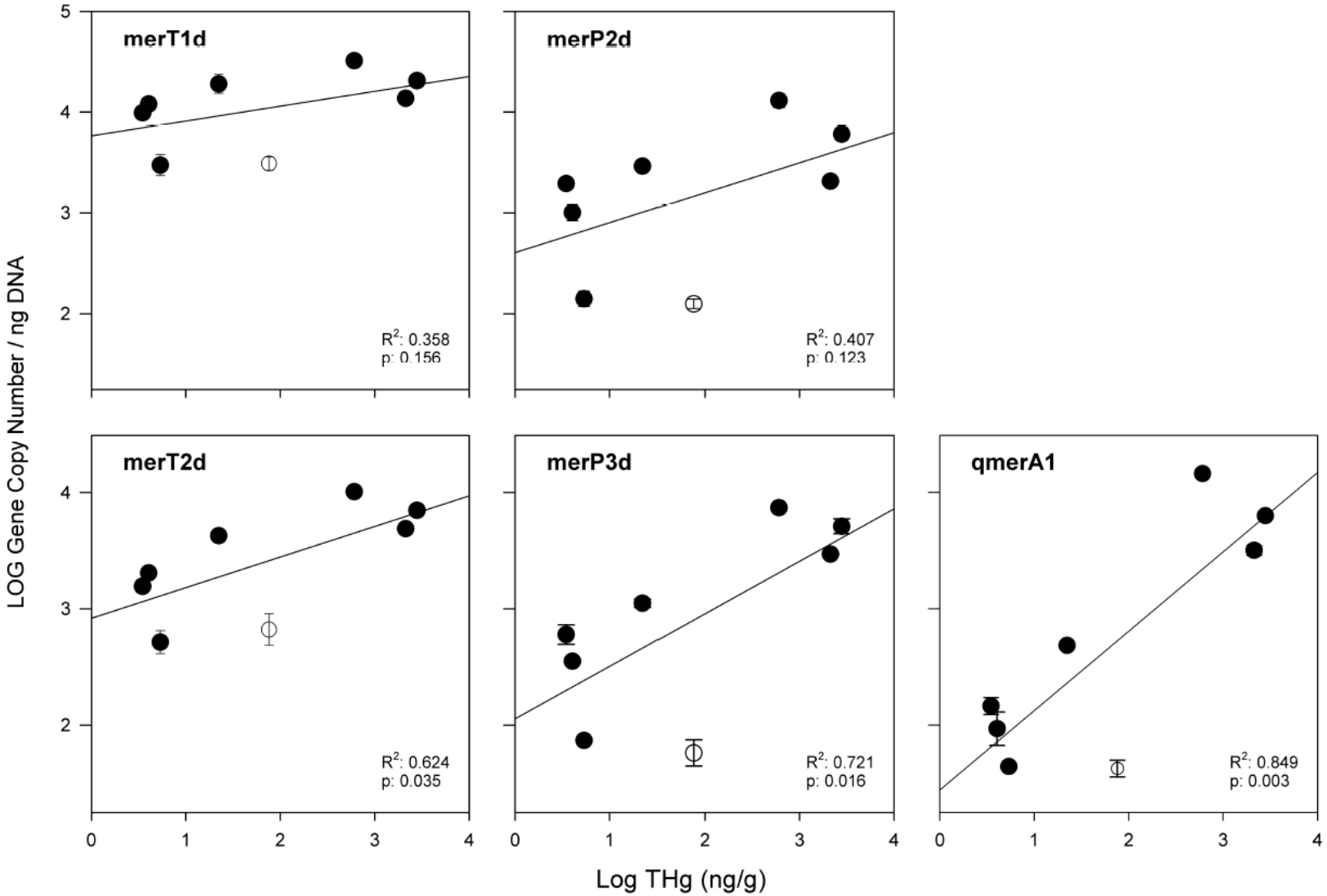

Figure 3.4: Regression analysis of Hg^R gene copy number to total sediment Hg concentrations. Regression curves for *merP* were constructed with qPCR assays using merP2d and merP3d primer sets. Curves for *merT* were constructed using merT1d and merT2d primer sets. The *merA* regression curve was built using the qmerA1 primer set. Regression coefficients (R^2) and significance values (p) are detailed in-set and exclude the NSB outliers indicated with hollow points.

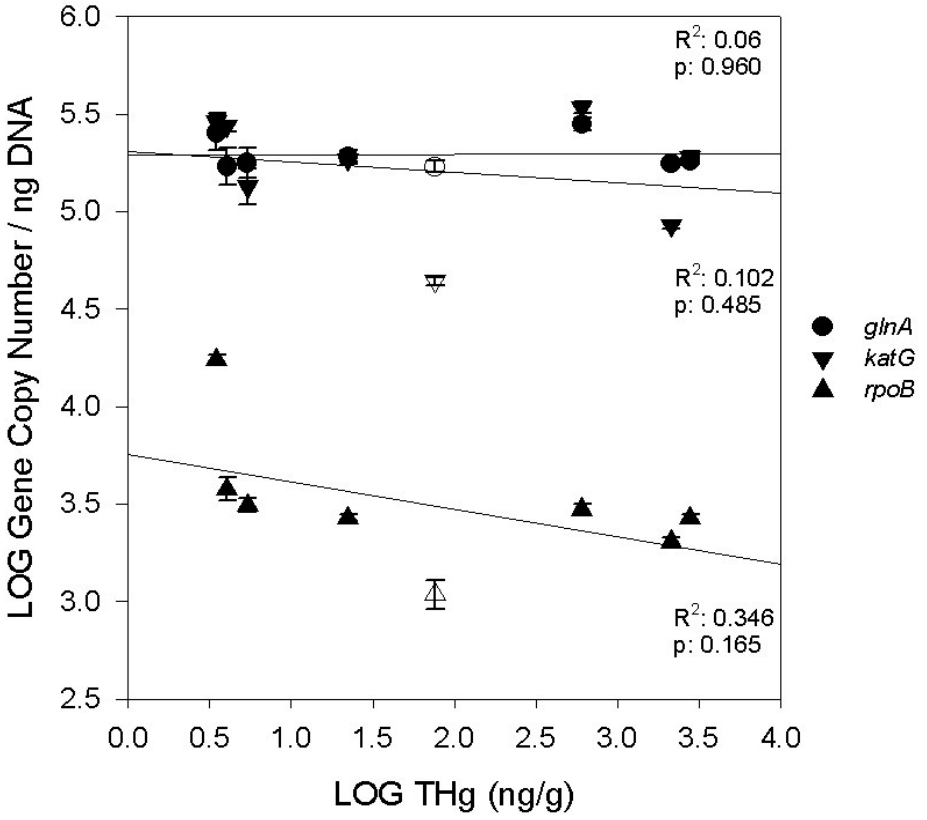

Figure 3.5: Regression analysis of reference gene copy number to total sediment Hg concentrations. Regression coefficients (R^2) and significance values (p) are detailed in-set and exclude the NSB outliers indicated with hollow points.

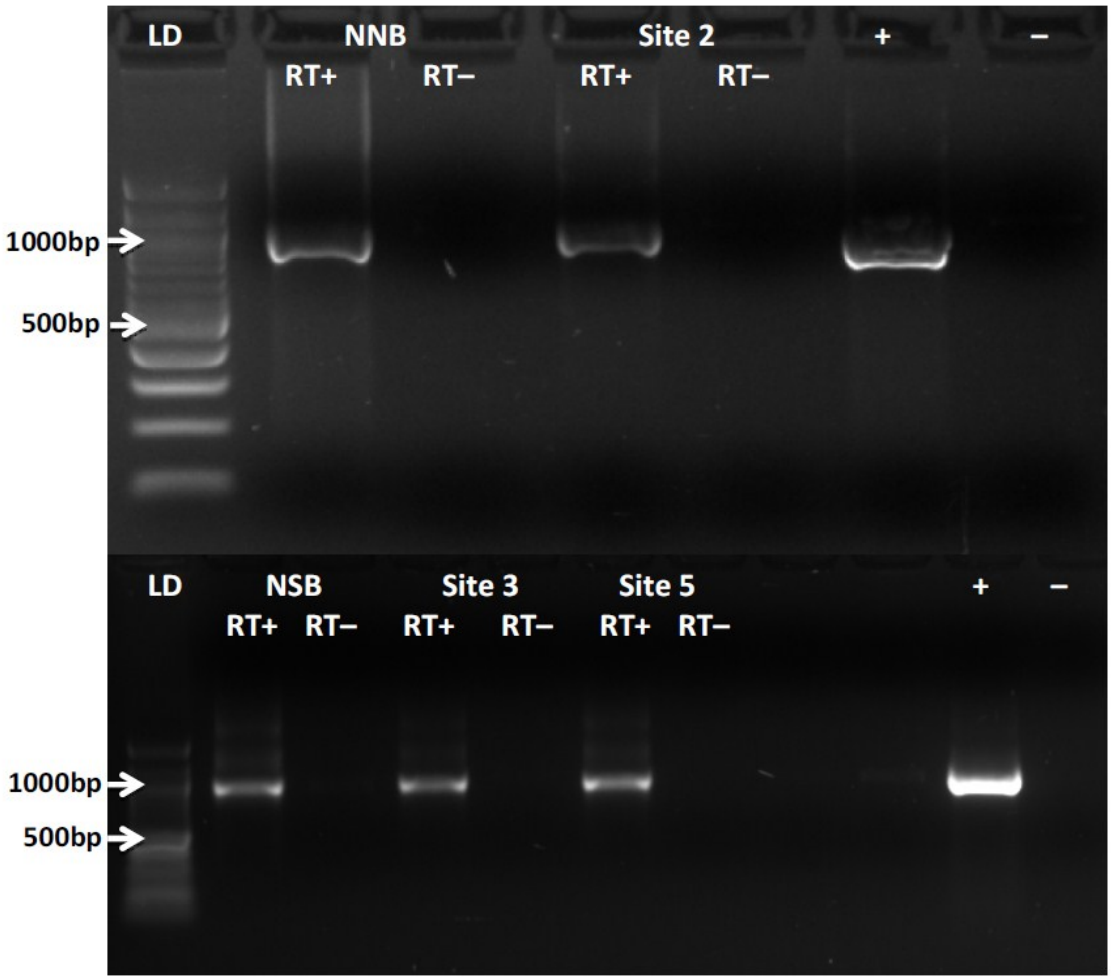

Figure 3.6: Electrophoretic gel image of *16SrRNA* gene targeted PCR products that used cDNA template synthesized from RNA extracted from experimental sites. Results from reverse transcriptase reactions (RT+) and reactions excluding reverse transcriptase (RT–) are indicated.

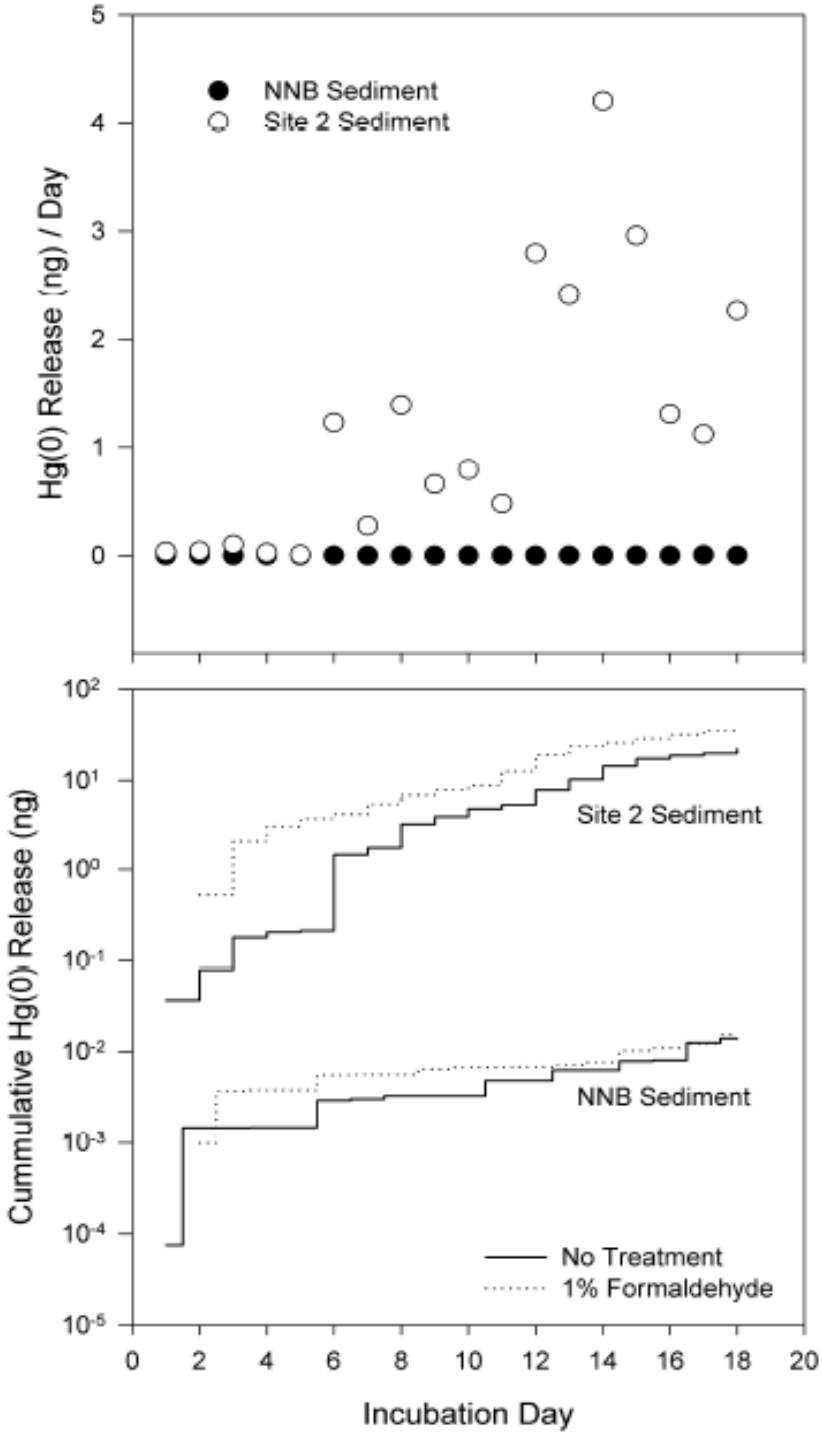

Figure 3.7: Sediment microcosm bioreactor results for daily Hg^0 release (top panel) and cumulative Hg^0 release (bottom panel) over the course of the experiment. Sediments from NNB and Site 2 were used in the microcosm experiments and are indicated by respective data plots.

4.0 Conclusions

In this project, the influence of past and current industrial activity upon the Saguenay River ecosystem was measured using novel *in-situ* biomarkers. Bacterially derived biomarkers were developed as potential tools for use by our industrial partners. Biomarkers were based on the responses exhibited by the sediment microbial communities of the Saguenay River that are exposed to aluminium industry effluent. Responses were characterized through changes in community structure and composition (Chapter 2) and function (Chapter 3). Differences in microbial community structure and composition do not reflect exposure to whole-effluent chemical mixtures (Chapter 2). Community function based on Hg^R reflected a responsive end-point of exposure to the Hg component of industrial effluent. The potential of bacteria to detoxify Hg indicates that affected sites are currently undergoing a process of biologically mediated remediation (Chapter 3).

The structure and composition of bacterial communities along the river did show differences across the sites analysed. Differences are expected regardless of the environmental context. Bacterial communities are observed as having different compositions even at small spatial scales (Hughes*, et al.*, 2001). However, these changes in structure and composition could not be explained through presence of the aluminium industry. Richness estimates did not display a significant trend across sites with increased effluent exposure (Table 2.2). Equally, diversity indices, corrected for by the exclusion of chloroplast sequences, could not place industrial activity as an influencing factor. In UniFrac analyses, community structure between a control (NNB) and an affected site (Site 2) were more similar to one another when compared to a medially affected site (Site 5) (Figure 2.4). This came as a surprise as it was believed that community composition and structure would be dictated by effluents released as by-products of

industrial activity. UniFrac results may have arisen due to the low percentage of community diversity covered in the analyses (Table 2.2). Greater sequencing effort may allow us to incorporate a greater percentage of total community diversity in the analysis. This may boost resolution required to derive a more complete picture of community structure and composition in the light of industrial activity. As it stands, Chapter 2 results indicate that the first hypothesis (**H1**) should be rejected. Community structure and composition were found to be more similar between a control and affected site when compared to a medially affected site.

Community functionality in response to Hg exposure was found to be a sensitive biomarker. A multitude of mechanisms for bacterial Hg resistance (Hg^R) have been described (Osborn*, et al.*, 1997, Barkay*, et al.*, 2003). The well-studied enzymatic-based Hg^R is mediated by the *mer*-operon (Barkay*, et al.*, 2003). Genes of the mer-operon are involved in the detoxification pathway that ultimately reduces ionic Hg (Hg^{II}) to the volatile and less toxic form (Hg^0) (Barkay*, et al.*, 2003). Community functionality in Hg detoxification via enzymatic Hg^R was assessed. Abundances of *mer*-operon genes, *mer*-operon gene expression levels, and the generation of the ultimate detoxified product (Hg^0) were measured. To our knowledge, the *mer*-operon genes encoding the periplasmic Hg scavenging protein (*merP*: MerP) and transmembrane Hg transport protein (*merT*: MerT) have remained understudied. Nor have their functions been characterized in an environmental context. Novel PCR primers were developed amplify *merP*, *merT* and *merA* gene targets. Operon gene abundances were generally higher at affected sites (Figure 3.2) indicating an enrichment for bacteria holding enzymatic Hg^R potential. The *merA* gene encodes for mercuric reductase (MerA), the core enzyme responsible for the reduction of

Hg^{II}. The qPCR assays targeting the *merA* gene yielded the strongest and most consistent signal with respect to sediment THg (Figure 3.4).

Gene expression experiments proved unsuccessful throughout the course of the project. Transcripts (mRNA) were deemed poor biomarker targets. The presence of organic and inorganic contaminants, more specifically trace metals, present in sediments may have hampered RNA extraction and cDNA synthesis (Fortin*, et al.*, 2004). However, Hg^0 release was 100 to 1000-fold higher affected site sediments (Site 2) when compared to those of a control site (NNB). While Hg^0 release could not be attributed to the activity of MerA, the abundances of *mer*-operon genes in affected sites indicate the presence of thriving bacterial communities harbouring Hg^R potential. The detection of *mer*-operon genes does not necessarily indicate *in-situ* activity; however, it does allude to the functional potential of sediment communities to naturally remediate ecosystems affected by industrial activity. Thus, the second hypothesis (**H2**) concerning the enrichment of Hg^R bacteria at sites influenced by industrial activity is supported.

The aluminium industry has been in operation for more than 80 years along the Saguenay River. The majority of Hg immobilized in sediments came as a result of past chlor-alkali activity (Gagnon*, et al.*, 1997). Environmental controls at the aluminium industrial complex in Jonquière/Arvida, QC are stringent yet trace levels of Hg can escape alumina refining (Figure 1.3). This is unavoidable as Hg is a natural component of bauxite source ores (Mimna*, et al.*, 2011). Thus, the possibility still exists of finding trace amounts of Hg in effluent by-products of this process. This study suggests that the sediment microbial communities have become enriched with bacteria holding enzymatically-based Hg^R due to exposure from industrial effluents containing Hg. Therefore, the environment can be seen as being naturally equipped with the

ability to remove Hg from contaminated sites by transforming it into the less toxic and volatile form (Hg^0). While Hg^0 released from affected site sediments cannot be directly attributed to the detoxification pathway of enzymatic Hg^R, it suggests that natural remediation of contaminated sites is an on-going process.

The detection and quantification of Hg^R genetic determinants in sediments are seen to be valid markers of biological responses to the industrial activities along the Saguenay River. To develop monitoring tools of greater practicality that can be standardized over many environmental contexts, future studies should involve the validation of sediment microbial community responses by using both bacterial and fish-based ecotoxicological tests. These tests would be carried out in controlled laboratory settings and would focus on the oxidative stress response (OSR). The OSR is a global measure of stress and would reflect the effect of whole-effluent complex chemical mixtures on biological systems. *In-vitro* analyses would use whole-cell bacteria isolated from the environment. These isolates could be tested for their ease of use in studies concerning engineered horizontal gene transfer (HGT) of metal resistance determinants. This would eventually provide our industrial partners with the tools to monitor their impact on the environment and possibly engineer natural mechanisms to remediate contaminated sites using cost effective and simple tools.

5.0 Supplementary Information

5.1 List of Supplementary Tables

5.2 List of Supplementary Figures

Table 5.1: Percentage of total clone library sequences falling under respective phyla. Libraries were constructed for three of the eight project site. Sequences belonging to the chloroplast *16S rRNA* gene are marked under Chloroplasts*.

Phyla	Site (Total Sequence Number)		
	NNB (n=79)	Site 2 (n=72)	Site 5 (n=63)
Acidobacteria	7.6	5.6	4.8
Actinobacteria	3.8	0.0	0.0
Armatimonadetes	0.0	1.4	0.0
Bacteroidetes	7.6	4.2	6.4
Chloroflexi	6.3	5.6	6.4
Chloroplasts*	10.1	38.9	0.0
Cyanobacteria	5.1	1.4	0.0
Firmicutes	1.3	0.0	0.0
Gemmatimonadetes	1.3	0.0	3.2
Nitrospirae	1.3	0.0	0.0
Proteobacteria			
α Proteobacteria	10.1	8.3	15.9
β Proteobacteria	26.6	25.0	33.3
γ Proteobacteria	2.5	0.0	0.0
Δ Proteobacteria	5.1	2.8	15.9
Unclassified	5.1	2.8	1.6
Unclassified Bacteria	6.3	4.2	12.7

Table 5.2: Sonde measurements of river water taken at sites along the Saguenay River. Measurements for temperature, pH and conductivity were recorded daily for seven days. Values between days were used to calculate a weekly mean. Standard deviations (SD) are listed. Minimum and maximum observed values are given by ranges.

Water Sonde Measurements	Site					
	NNB	NSB	Site 2	Site 2 Effluent	Site 3	Site 3 Effluent
Mean Temperature (ºC) (SD)	21.81 (1.1)	22.0 (1.0)	24.74 (2.2)	25.8 (1.9)	30.28 (3.5)	33.7 (1.3)
Temperature Range (ºC)	20.27 – 23.20	20.9 – 23.58	21.85 – 26.89	23.18 –26.89	22.9 – 33.33	31.08 – 35.0
Mean pH (SD)	6.64 (0.3)	6.2 (0.7)	7.03 (0.7)	7.4 (0.2)	7.69 (0.3)	8.0 (0.1)
pH Range	6.28 – 6.96	5.25 – 7.01	5.75 – 7.6	7.2 – 7.77	7.08 – 8.06	7.88 – 8.31
Mean Conductivity (µS/cm) (SD)	72 (42.5)	27.8 (2.1)	116.5 (64.1)	145.3 (48.5)	525 (236.7)	690.7 (69.4)
Conductivity Range (µS/cm)	37 – 149	24 – 30	45 –171	73 – 192	104 – 814	603 – 825

Table 5.3: Total Hg (THg) levels measured in river water samples taken at three separate time points between July 21st and August 6th, 2011. Water was sampled to characterize temporal changes in water column chemistry. Mean values and standard deviations (SD) are listed.

Chemical Data	Site															
	New North Beach (NNB)				**New South Beach (NSB)**				**Site 2**				**Site 3**			
Collection Day	1	2	3	Mean (SD)	1	2	3	Mean (SD)	1	2	3	Mean (SD)	1	2	3	Mean (SD)
Total Hg (ng/L)	2.27	2.29	2.17	2.24 (0.064)	2.34	2.75	2.40	2.50 (0.221)	21.36	78.84	70.43	56.88 (31.04)	92.75	66.24	123.35	94.11 (28.58)

Table 5.4: Raw data for total Hg concentrations in sediments. The number of measurements taken for each site represents the sample size.

Project Site	Total Hg (ng/g)	Project Site	Total Hg (ng/g)
NB	3.339 3.645	Site 2	1810.9822 2384.7557 3622.8766 2480.2324 4457.5154
NNB	4.413 3.709	Site 3	555.119 665.0224 634.5902 578.2594
SB	5.415 5.337	Site 4	2050.0598 2205.1498 2133.9735 1820.3628 2499.4839
NSB	74.505 78.807 83.225 88.042 75.121 71.640 70.082 75.042 70.389 74.011 78.107	Site 5	14.9351 32.0156 16.3602 40.632 19.0305 20.3782

Table 5.5: Nucleic acid extract concentrations used to normalize gene and transcript copy numbers as determined through qPCR assays. Separate DNA extracts were used for *mer*-operon gene and reference gene assays. RNA concentrations reflect the amount of input RNA used in cDNA synthesis reactions. RNA was extracted from five of the eight project sites.

Site	[DNA] (ng/uL)		[RNA] (ng/uL)
	Reference Gene Assays	mer-Operon Gene Assays	
NB	12.1	6.6	
NNB	8.3	13.6	2.4
SB	15	32	
NSB	30.1	42.2	1.6
Site 2	11.7	16.8	2.24
Site 3	8.2	7	1.28
Site 4	23.5	28.5	
Site 5	13.5	8.1	2.24

Table 5.6: Conventional PCR assay primers used to target the genes of interest in this study. Primer sequences, properties of use and source of primer design are listed. Primers having high fidelity results were used in qPCR assays and are marked (*).

Primer Target	Primer Name	Primer Sequence (5' – 3')	Expected Amplicon Length (bp)	Cycling Conditions (Optimised)	Primer Design Source
Reference Genes					
Small Subunit Ribosomal RNA (*16S rRNA*)	27F*	AGA GTT TGA TCM TGG CTC AG	880	94°C-10min, (94°C-30s, 50°C-30s, 72°C-60s)×35, 72°C-5min	(Osborn & Smith, 2005)
	907R*	CCG TCA ATT CAT TTG AG			
Glutamine synthetase (*glnA*)	GS2γ*	AAG ACC GCG ACC TTP ATG CC	153-156	94°C-10min, (94°C-30s, 60°C-60s, 72°C-60s)×35, 72°C-7min	(Hurt, *et al.*, 2001)
	GS1β*	GAT GCC GCC GAT GTA GTA			
RNA Polymerase β-Subunit (*rpoB*)	rpoB1698f*	AAC ATC GGT TTG ATC AAC	343	94°C-5min, (94°C-30s, 52°C-90s, 72°C-90s)×35, 72°C-10min	(Dahllof, *et al.*, 2000)
	rpoB2041r*	CGT TGC ATG TTG GTA CCC AT			
Catalase-Peroxidase (*KatG*)	katG1 F50	TCATCCGCATGGCCTGGCAC	900	94°C-2min, (94°C-30s, 61°C-30s, 72°C-60s)×35, 72°C-10min	(Godocikova, *et al.*, 2010)
	katG1 R50	TCAGCTTGAACCAGGCGCGG			
	katG1 F75*	TBA TYC GYA TGG CST GGC AY	900	94°C-2min, (94°C-30s, 58°C-30s, 72°C-60s)×35, 72°C-10min	(Godocikova, *et al.*, 2010)
	katG1 R75*	TCA RYT TGA ACC AGG CR CGR			
mer *Operon Genes*					
Cytosolic membrane Hg-transport protein (*merT*)	merT1d F*	RGT GGC GYT GTT YTT CGC CT	128	94°C-2min, (94°C-20s, 60°C-20s,	In-house design
	merT1d R*	CCA GCR CGG CCA CGA YCC AG			

				72°C-30s)×35, 72°C-5min	
Cytosolic membrane Hg-transport protein (*merT*)	merT2d F* merT2d R*	TGG CGY TGT TYT TCG CCT GG RAC CAG CRC GGC CAC GAY CC	128	94°C-2min, (94°C-20s, 60°C-20s, 72°C-30s)×35, 72°C-5min	In-house design
	merT3d F merT3d R	RGT GGC GYT GTT YTT CGC CT RAC CAG CRC GGC CAC GAY CC	130	94°C-2min, (94°C-20s, 60°C-20s, 72°C-30s)×35, 72°C-5min	In-house design
	merT4d F merT4d R	GAA CCA CAA AAC GGG CGC GG AGG CGA ARA ACA RCG CCA CY	190	94°C-2min, (94°C-30s, 61.5°C-30s, 72°C-45s)×35, 72°C-5min	In-house design
	merT5d F merT5d R	GAA CCA CAA AAC GGG CGC GG CCA GCR CGG CCA CGA YCC AG	298	94°C-2min, (94°C-30s, 62.3°C-30s, 72°C-45s)×35, 72°C-5min	In-house design
Periplasmic Hg-binding protein (*merP*)	merP1d F merP1d R	GTT TGC CKC CCT YGC CCT CG GAC WGT GAT CGG RCA RGC GG	109	94°C-2min, (94°C-30s, 61.5°C-30s, 72°C-45s)×35, 72°C-5min	In-house design
	merP2d F* merP2d R*	CCG CYT GYC CGA TCA CWG TC TGG ACG GAT AGC CSG CGT CY	162	94°C-2min, (94°C-20s, 60°C-20s, 72°C-30s)×35, 72°C-5min	In-house design
	merP3d F* merP3d R*	CCG CYT GYC CGA TCA CWG TC CGG ATA GCC SGC GTC YKC GG	158	94°C-2min, (94°C-20s, 60°C-20s, 72°C-30s)×35,	In-house design

				72°C-5min	
Periplasmic Hg-binding protein (*merP*)	merP4d F	GTT TGC CKC CCT YGC CCT CG	251	94°C-2min, (94°C-30s, 61.5°C-30s, 72°C-45s)×35, 72°C-5min	In-house design
	merP4d R	TGG ACG GAT AGC CSG CGT CY			
	merP5d F	GTT TGC CKC CCT YGC CCT CG	247	94°C-2min, (94°C-30s, 61.5°C-30s, 72°C-45s)×35, 72°C-5min	In-house design
	merP5d R	CGG ATA GCC SGC GTC YKC GG			
Mercuric Reductase (*merA*)	qmerA1 F*	CAT GAC GGT GCA GGA ACT G	101	94°C-2min, (94°C-20s, 60°C-20s, 72°C-30s)×35, 72°C-5min	In-house design
	qmerA1 R*	GCT GCT TCA CAT CCT TGT TG			
	Nlf F	CCA TCG GCG GCA CYT GCG TYA A	1249	94°C-10min, (94°C-30s, 61.5°C-30s, 72°C-90s)×35, 72°C-5min	T. Barkay, (unpublished data)
	Nlf R	CGC YGC RAG CTT YAA YCY YTC RRC CAT YGT			
	Nsf F	ATC CGC AAG TNG CVA CBG TNG G	310	94°C-10min, (94°C-30s, 61.5°C-30s, 72°C-30s)×35, 72°C-5min	T. Barkay, (unpublished data)
	Nsf R	CGC YGC RAG CTT YAA YCY YTC RRC CAT YGT			

Table 5.7: qPCR conditions and standard curve data for assays applied to sediment metagenome extracts.

Assay Target	Assay Cycling Conditions	Melt Curve Conditions	NTC C_T Values	Standard Curve Results			
				Reaction Efficiency (%)	y-Intercept	Slope	R^2 Value
glnA	98°C-120s, (98°C-5s, 60°C-20s) x 35, 60°C-15s	60°C to 95°C	33.54 N/A N/A	87.49439771	41.36184862	-3.663160714	0.985432468
katG1 75	98°C-120s, (98°C-5s, 58°C-40s) x 35, 58°C-15s	58°C to 95°C	N/A N/A N/A	49.2157737	59.02230473	-5.75325216	0.98196501
rpoB	98°C-120s, (98°C-5s, 55°C-20s) x 35, 55°C-15s	55°C to 95°C	N/A N/A N/A	99.46814064	36.91732525	-3.33473904	0.99267019
merT1d	98°C-120s, (98°C-5s, 60°C-20s) x 35, 60°C-15s	60°C to 95°C	33.52 N/A N/A	99.92175425	37.77053782	-3.323804496	0.994810117
merT2d	98°C-120s, (98°C-5s, 60°C-20s) x 35, 60°C-15s	60°C to 95°C	34.11 N/A N/A	103.0439283	36.64359108	-3.251080909	0.993036286
merP2d	98°C-120s, (98°C-5s, 60°C-20s) x 35, 60°C-15s	60°C to 95°C	N/A N/A N/A	92.46124211	41.13495134	-3.516875745	0.99719997
merP3d	98°C-120s, (98°C-5s, 60°C-20s) x 35, 60°C-15s	60°C to 95°C	29.46 N/A N/A	96.55242962	37.56527927	-3.4074056	0.99737024
qmerA1	98°C-120s, (98°C-5s, 60°C-20s) x 35, 60°C-15s	60°C to 95°C	18.90 N/A N/A	106.0054331	37.46709016	-3.185944383	0.99706242

Table 5.8: qPCR metagenome assay results corresponding to those listed in Table 5.6. Extracts from samples were assayed in triplicate. The results are normalized to the concentration of DNA (ng/uL) in sediment metagenome extracts.

Site	qPCR Assay							
	glnA	**katG1**	**rpoB**	**merT1d**	**merT2d**	**merP2d**	**merP3d**	**qmerA1**
NB	268897	319852.5	18277.29	10116.19	1684.182	1971.351	710.0606	155.0367
	201612.8	288467.6	17784.96	8285.574	1499.432	1932.376	627.4327	120.3788
	301950.3	259017.1	16202.41	11350.06	1493.635	1968.296	485.8385	165.6226
NNB	134713	285258	3833.594	11532.69	1977.063	981.0288	360.9938	63.43499
	174071.4	284429.7	3273.585	11066.79	2023.019	1219.986	357.8859	112.9958
	209413.4	256040.9	4259.074	13566.4	2095.421	849.9071	345.6714	112.3658
SB	185824.4	159967.2	3124.504	3425.29	619.4858	157.9751	70.64603	43.73611
	204980.7	143147.2	2844.243	3410.343	556.2243	153.3475	75.13968	41.73751
	145992.6	105349.3	3361.785	2273.368	400.7137	114.7514	75.313	46.50614
NSB	156553.2	45871.84	1107.401	3672.855	483.5762	139.9853	76.39157	35.26704
	177777.8	41746.64	1272.068	2907.763	899.8713	112.8294	45.74174	44.52624
	175452.8	44578.45	904.7653	2763.858	668.3469	124.8374	54.60621	48.399
2	173488.1	200874.4	2767.035	21899.05	6407.55	5096.522	5972.322	5924.04
	187693.7	193774	2530.066	18908.92	7432.052	6553.301	4488.389	6405.88
	188058	178503.9	2722.769	20827.63	7301.214	6626.315	5003.191	6613.367
3	267879.8	372078.6	2760.512	29896.76	10322.03	10867.66	7564.705	13808.63
	268831.2	329684	3168.803	32923.67	8769.287	14437.49	7136.905	15373.82
	306463.8	330687.7	2969.306	34166.16	11609.03	13934.89	7448.055	14418.5
4	170158.3	86202.4	1956.624	13376.34	4951.702	1816.051	2888.363	3386.575
	180151.3	88164.88	2125.809	13510.97	4954.751	2348.945	2995.099	3325.152
	179269.2	80652.02	1996.025	14066.48	4690.659	2072.041	2969.038	2838.948
5	209404.5	191933.9	2802.895	23461.99	3834.853	3081.106	1143.398	470.3773
	178264.3	179445.1	2588.865	15246.42	4304.001	2977.86	1018.226	477.5312
	187469.2	185527.1	2629.337	19131.04	4629.841	2696.956	1187.366	506.573

Table 5.9: Results from statistical tests used to assess pooled data set distributions (Affected and Control) for normality (Shapiro-Wilk) and homoscedasticity (Levene's). T-tests were applied to determine significant differences between distributions.

Data Set	*Shapiro-Wilk* Statistic ***W*** (p-Value)		T-test p-Values		Levene's Test F-Ratio (p-Value)
	Affected Sites	Control Sites	Student's T-test	Wilcoxon T-test	
THg	0.939 (0.648)	0.645 (**0.002**)*		**0.0433***	28.063 (**0.0018**)*
glnA	0.744 (**0.034**)*	0.709 (**0.015**)*		0.2482	0.097 (0.7659)
katG	0.935 (0.622)	0.890 (0.383)	0.4266		0.401 (0.5501)
rpoB	0.882 (0.348)	0.768 (0.056)	0.8238		7.376 (**0.0348**)*
merT1d	0.922 (0.546)	0.828 (0.163)	**0.0098***		0.385 (0.558)
merT2d	0.913 (0.496)	0.904 (0.452)	**0.0042***		4.646 (0.0745)
merP2d	0.872 (0.307)	0.867 (0.287)	**0.0424***		3.913 (0.0953)
merP3d	0.988 (0.948)	0.880 (0.338)	**0.0147***		10.430 (**0.0179**)*
qmerA1	0.931 0.601)	0.871 (0.301)	**0.0471***		5.808 (0.0526)

Table 5.10: Coefficients of determination (R^2) and significance values (p) for regression curves where log transformed gene copy data was regressed upon log transformed sediment Hg data. Curve properties were compared between regression groups including and excluding NSB site sediment gene copy numbers. Significant associations between variables involved in the regression are marked (*).

	Log THg			
PCR Assay	Including **NSB** Outlier		Excluding **NSB** Outlier	
	R^2	p-Value	R^2	p-Value
glnA	0.0003	0.967	0.006	0.960
katG1	0.0482	0.601	0.102	0.485
rpoB	0.2515	0.205	0.346	0.165
merT1d	0.226	0.234	0.358	0.156
merT2d	0.460	0.065	0.624	**0.035***
merP2d	0.254	0.203	0.407	0.123
merP3d	0.475	0.059	0.721	**0.016***
qmerA1	0.682	**0.012***	0.849	**0.003***

Table 5.11: Real time PCR conditions and standard curve data for assays applied to sediment metatranscriptome extracts. Template material used for each assay was cDNA that was reverse transcribed from RNA extracted from sediment metatranscriptomes.

Assay Target	Assay Cycling Conditions	Melt Curve Conditions	NTC C_T Values	Standard Curve Results			
				Reaction Efficiency (%)	y-Intercept	Slope	R^2 Value
16S rRNA	98°C-120s, (98°C-5s, 48°C-40s) x 35, 48°C-15s	48°C to 95°C	N/A N/A N/A	74.01592151	47.46224707	-4.15646625	0.99810243
glnA	98°C-120s, (98°C-5s, 60°C-20s) x 35, 60°C-15s	60°C to 95°C	34.02 N/A N/A	107.72075772	36.39257674	-3.14980572	0.99172645
merT1d	98°C-120s, (98°C-5s, 60°C-20s) x 35, 60°C-15s	60°C to 95°C	N/A N/A N/A	97.81866884	37.76956942	-3.3753306	0.99632223
merT2d	98°C-120s, (98°C-5s, 60°C-20s) x 35, 60°C-15s	60°C to 95°C	34.15 33.83 22.25	97.92025302	37.42757641	-3.37279233	0.99855174
merP2d	98°C-120s, (98°C-5s, 60°C-20s) x 35, 60°C-15s	60°C to 95°C	32.59 N/A N/A	94.34830579	39.61441202	-3.46523449	0.99773556
qmerA1	98°C-120s, (98°C-5s, 60°C-20s) x 35, 60°C-15s	60°C to 95°C	33.96 31.88 N/A	109.83744319	37.00057374	-3.10671904	0.99330455

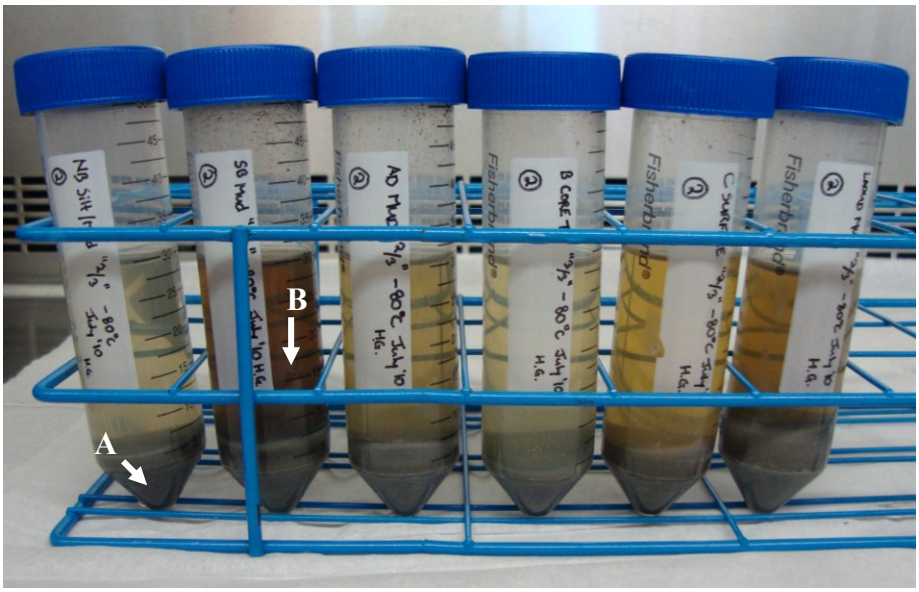

Figure 5.1: Illustration of an intermediate step in the salt-buffer sediment wash technique. The six tubes contain washed and centrifuged sediment samples (A) which lie under the wash buffer supernatant (B). The removal of humic substances is made apparent by the resultant colour of the wash buffer.

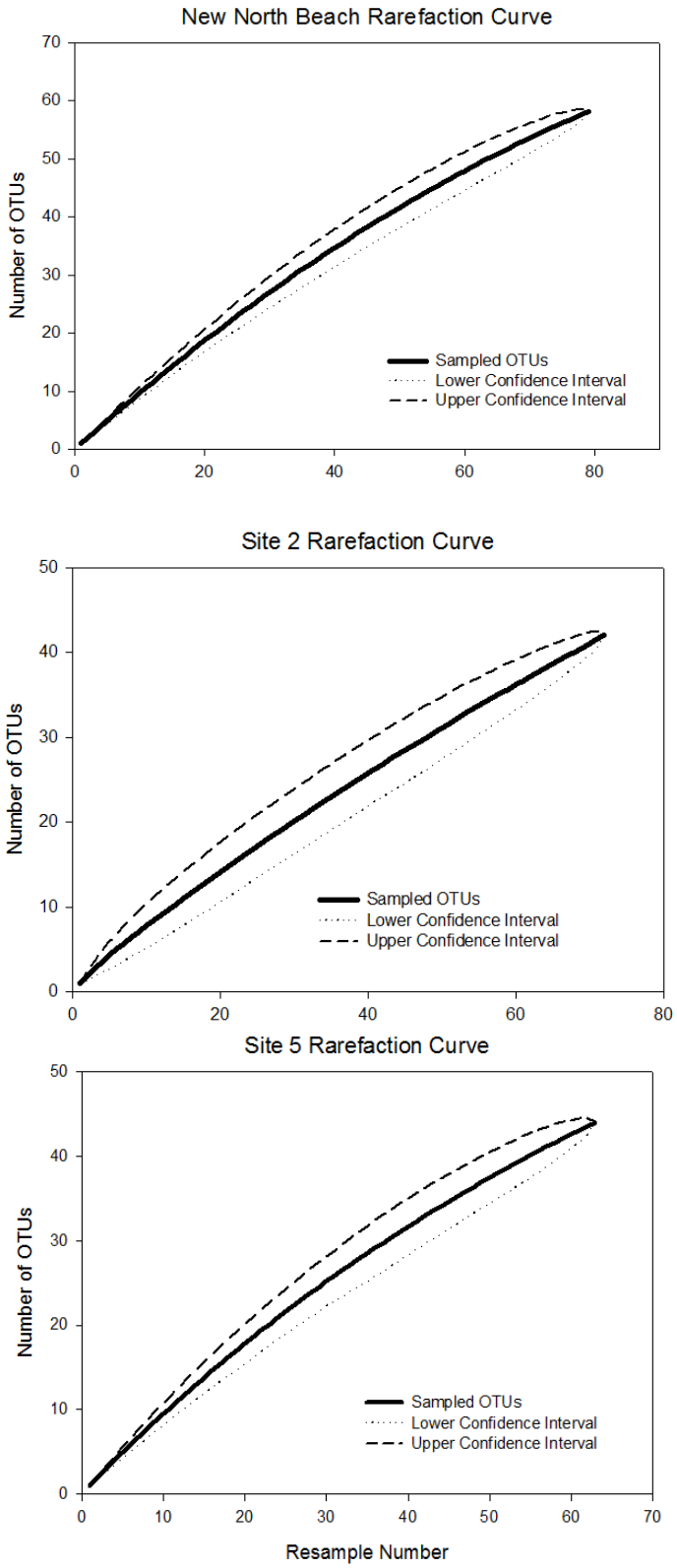

Figure 5.2: *16SrRNA* gene clone library rarefaction curves and their associated 95% confidence intervals. Libraries were constructed for three of the eight project sites: NNB, Site 2 and Site 5.

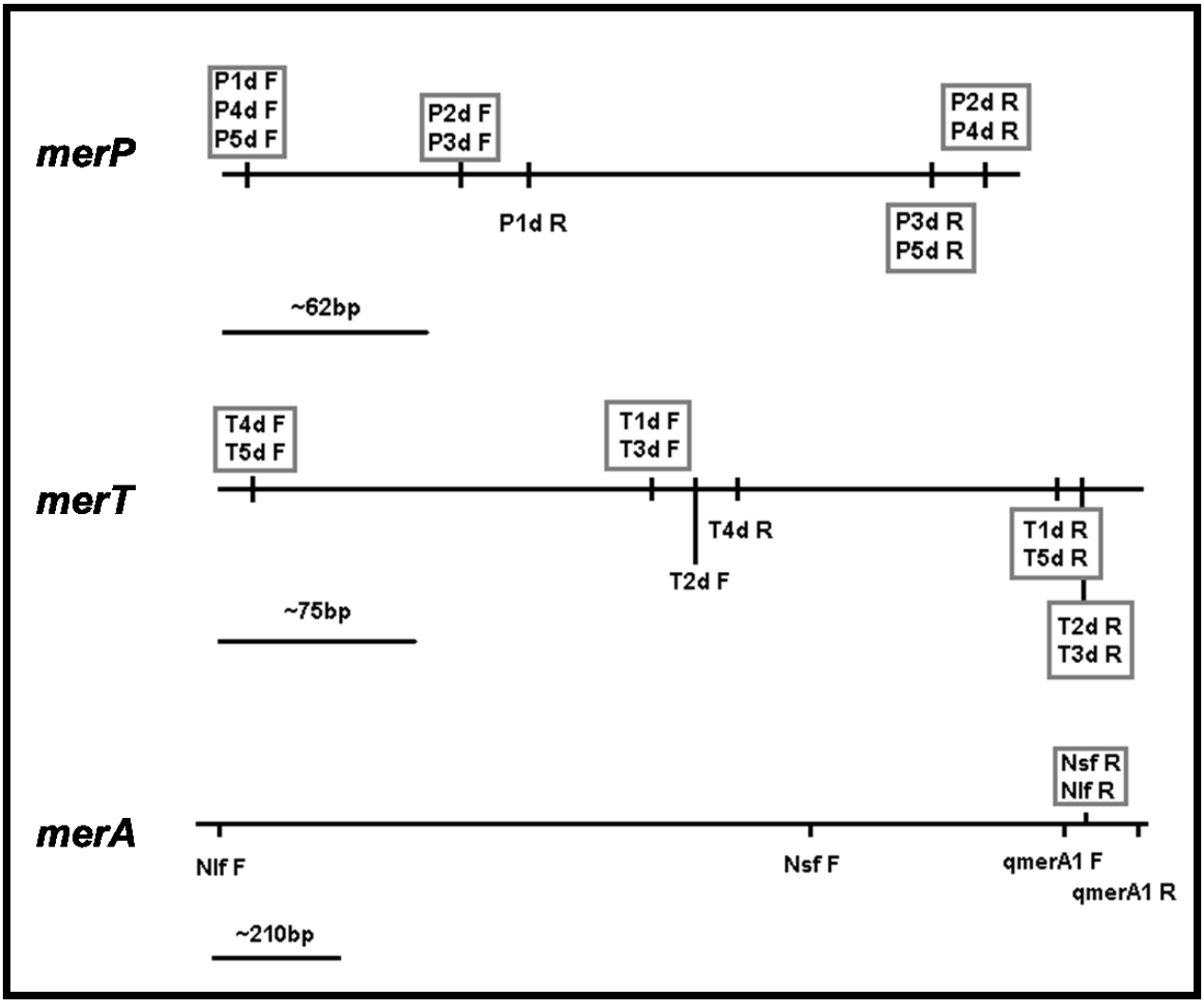

Figure 5.3: Binding site schematic for various PCR primer sets targeting mer-operon genes, *merP*, *merT* and *merA*. Base pair scales are indicated for each gene. Some sets use identical primers and are grouped within grey boxes.

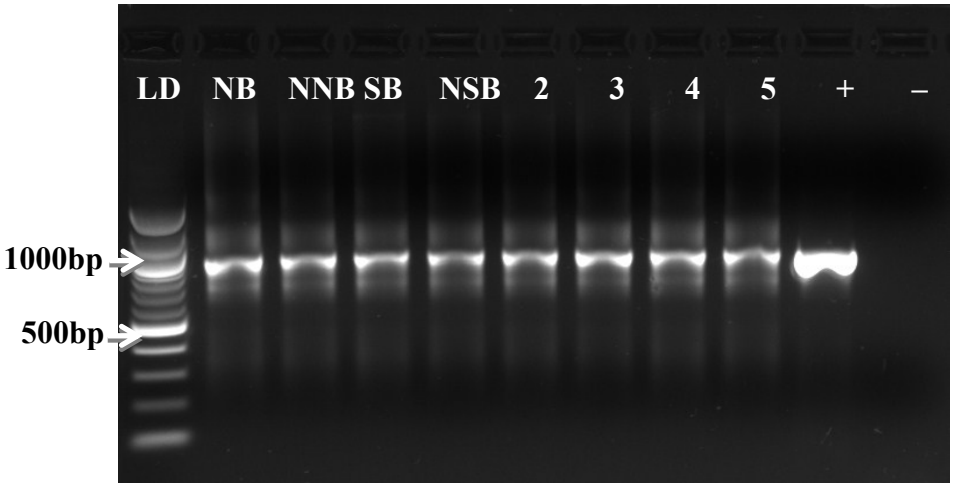

Figure 5.4: Gel electrophoresis of PCR amplicons from an assay targeting the *16S rRNA* gene using primer set **27F & 907R**. The 1.5% agarose gel was run at 100V for 50 min and imaged using an ultraviolet lamp. Sites and base pair ladder (LD) markers are listed under each well. The source of the positive (+) control was *Escherichia coli*.

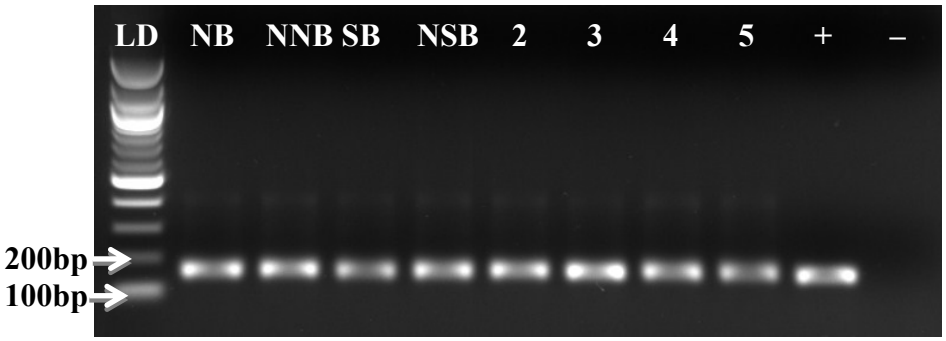

Figure 5.5: Gel electrophoresis of PCR amplicons from an assay targeting the *glnA* gene using primer set **GS2γ–GS1β**. The 1.5% agarose gel was run at 100V for 50 min and subsequently imaged using an ultraviolet lamp. Sites and base pair ladder (LD) markers are listed under each well. The source of the positive (+) control was *Escherichia coli.*

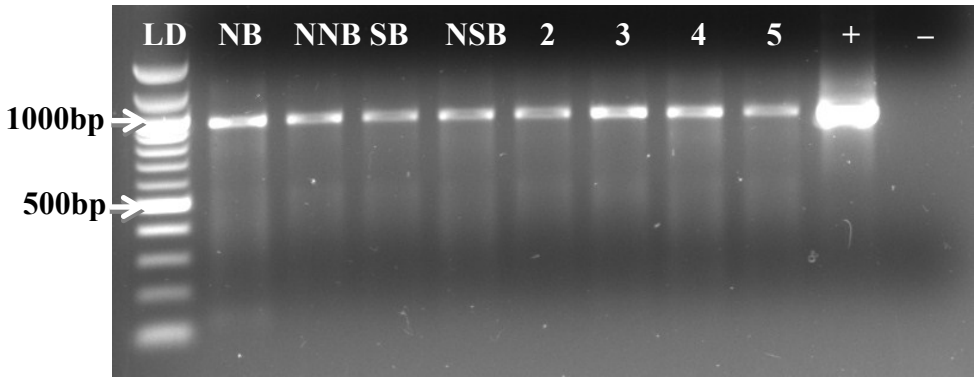

Figure 5.6: Gel electrophoresis of PCR amplicons from an assay targeting the *katG1* gene using primer set **katG1 75**. The 1.5% agarose gel was run at 100V for 70 min and subsequently imaged using an ultraviolet lamp. Sites and base pair ladder (LD) markers are listed under each well. The source of the positive (+) control was *Escherichia coli.*

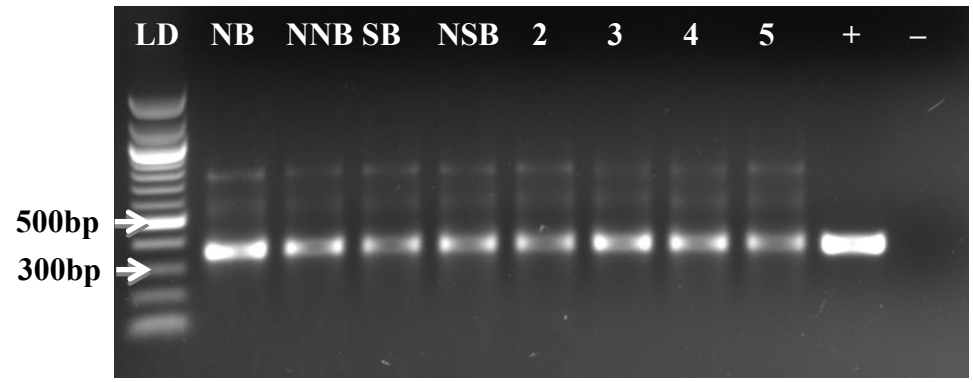

Figure 5.7: Gel electrophoresis of PCR amplicons from an assay targeting the *rpoB* gene using primer set **rpoB1698F–rpoB2041R**. The 1.5% agarose gel was run at 100V for 60 min and subsequently imaged using an ultraviolet lamp. Sites and base pair ladder (LD) markers are listed under each well. The source of the positive (+) control was *Escherichia coli.*

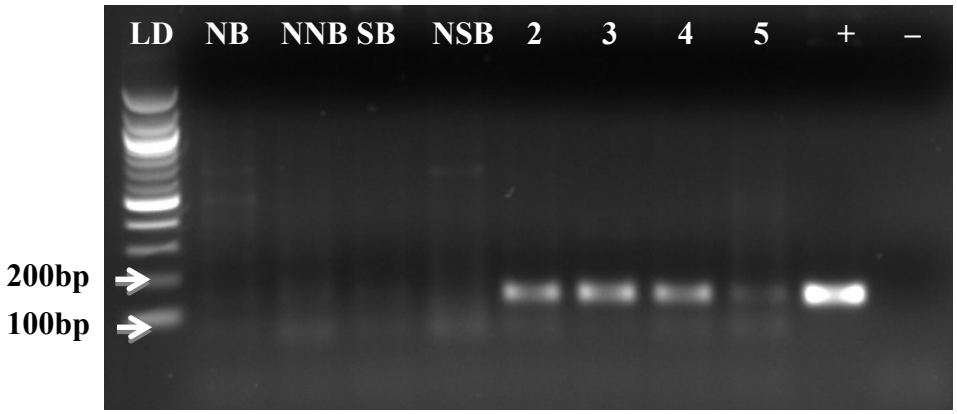

Figure 5.8: Gel electrophoresis of PCR amplicons from an assay targeting the *merT* gene using primer set **merT1d**. The 1.5% agarose gel was run at 100V for 55 min and subsequently imaged using an ultraviolet lamp. Sites and base pair ladder (LD) markers are listed under each well. The source of the positive (+) control was *Pseudomonas aeruginosa.*

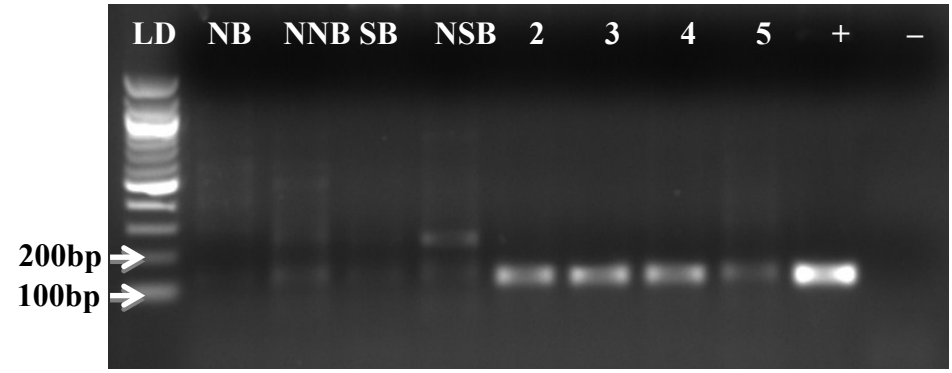

Figure 5.9: Gel electrophoresis of PCR amplicons from an assay targeting the *merT* gene using primer set **merT2d**. The 1.5% agarose gel was run at 100V for 55 min and subsequently imaged using an ultraviolet lamp. Sites and base pair ladder (LD) markers are listed under each well. The source of the positive (+) control was *Pseudomonas aeruginosa.*

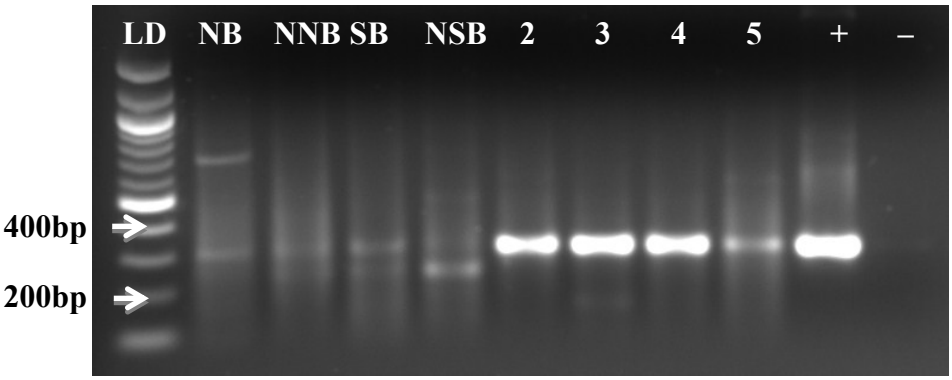

Figure 5.10: Gel electrophoresis of PCR amplicons from an assay targeting the *merT* gene using primer set **merT5d**. The 1.5% agarose gel was run at 100V for 65 min and subsequently imaged using an ultraviolet lamp. Sites and base pair ladder (LD) markers are listed under each well. The source of the positive (+) control was *Pseudomonas aeruginosa.*

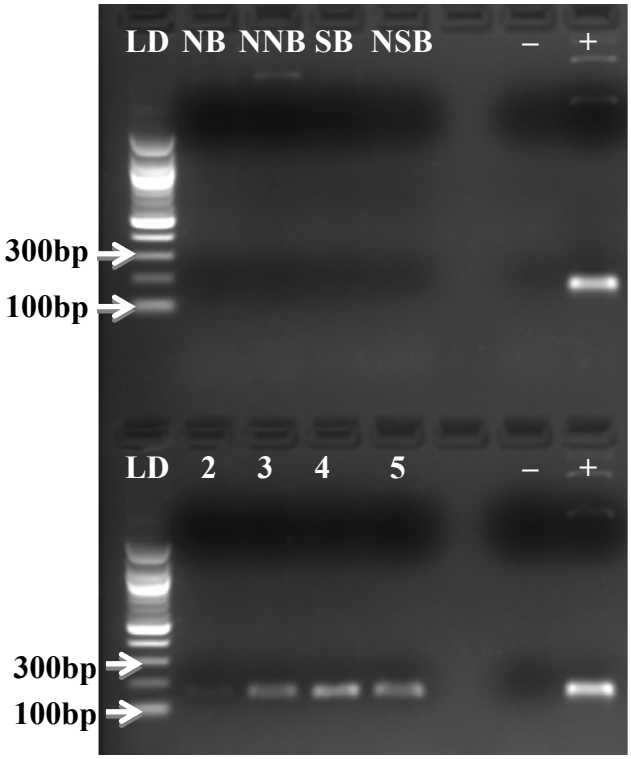

Figure 5.11: Gel electrophoresis of PCR amplicons from an assay targeting the *merP* gene using primer set **merP2d**. The 1.5% agarose gel was run at 100V for 50 min and subsequently imaged using an ultraviolet lamp. Sites and base pair ladder (LD) markers are listed under each well. The source of the positive (+) control was *Pseudomonas aeruginosa.*

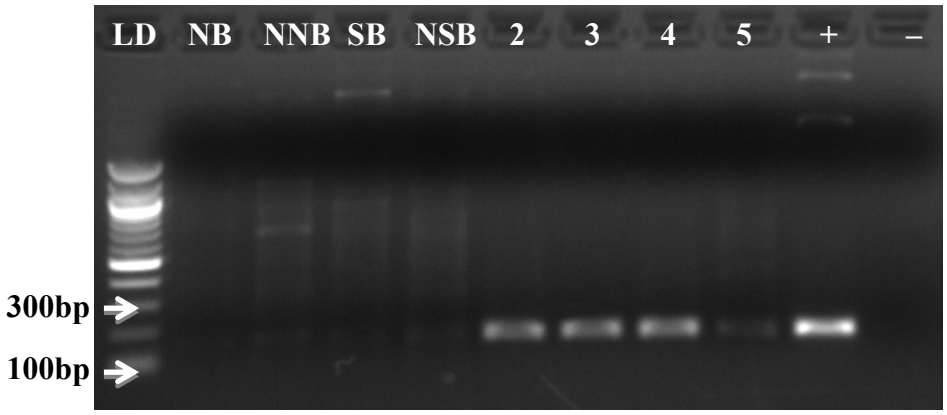

Figure 5.12: Gel electrophoresis of PCR amplicons from an assay targeting the *merP* gene using primer set **merP3d**. The 1.5% agarose gel was run at 100V for 50 min and subsequently imaged using an ultraviolet lamp. Sites and base pair ladder (LD) markers are listed under each well. The source of the positive (+) control was *Pseudomonas aeruginosa.*

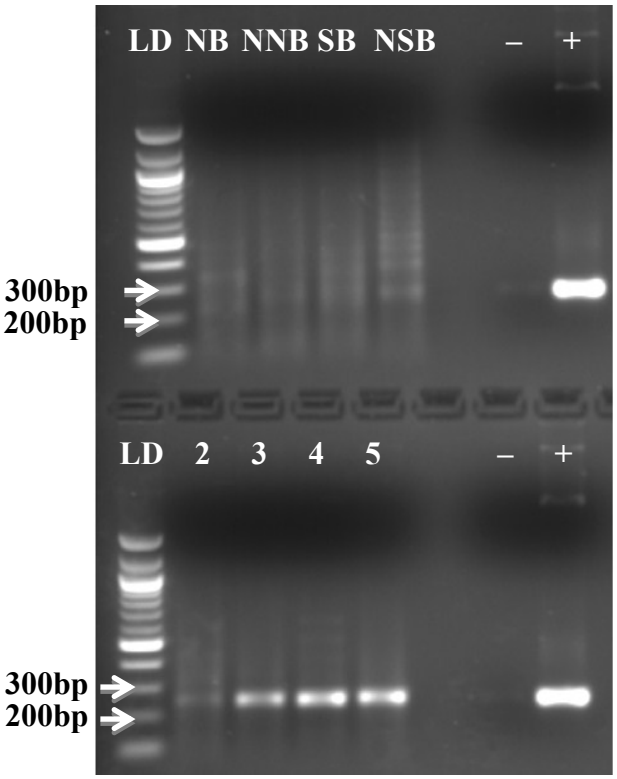

Figure 5.13: Gel electrophoresis of PCR amplicons from an assay targeting the *merP* gene using primer set **merP5d**. The 1.5% agarose gel was run at 100V for 60 min and subsequently imaged using an ultraviolet lamp. Sites and base pair ladder (LD) markers are listed under each well. The source of the positive (+) control was *Pseudomonas aeruginosa.*

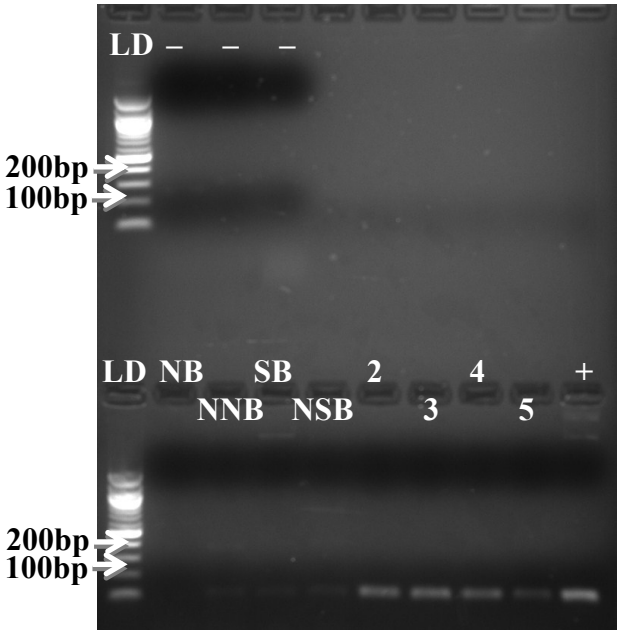

Figure 5.14: Gel electrophoresis of PCR amplicons from an assay targeting the *merA* gene using primer set **qmerA1**. The 1.5% agarose gel was run at 100V for 55 min and imaged using an ultraviolet lamp. Sites and base pair ladder (LD) markers are listed under each well. The positive (+) control source was a plasmid holding a *merA* variant from transposon Tn501.

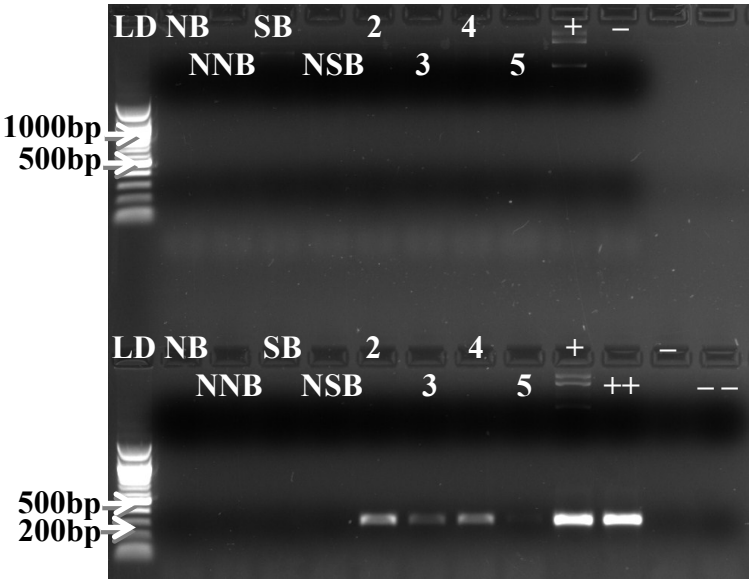

Figure 5.15: Gel electrophoresis of PCR amplicons from assays targeting *merA* using primer sets **Nlf** (A) and **Nsf** (B). The products of the Nlf PCR assay (3 cycles) were used as template for the Nsf "nested" PCR assay (B). The 1.5% agarose gel was run at 100V for 55 min and imaged using an ultraviolet lamp. Sites and base pair ladder (LD) markers are listed under each well. The positive (+) control source was a plasmid holding a *merA* variant from transposon Tn501.

6.0 References

Agrawal A, Sahu KK & Pandey BD (2004) Solid waste management in non-ferrous industries in India. *Resources, Conservation and Recycling* **42**: 99-120.

Ashelford KE, Chuzhanova NA, Fry JC, Jones AJ & Weightman AJ (2005) At least 1 in 20 16S rRNA sequence records currently held in public repositories is estimated to contain substantial anomalies. *Appl Environ Microbiol* **71**: 7724-7736.

Ashelford KE, Chuzhanova NA, Fry JC, Jones AJ & Weightman AJ (2006) New screening software shows that most recent large 16S rRNA gene clone libraries contain chimeras. *Appl Environ Microbiol* **72**: 5734-5741.

Avramescu ML, Yumvihoze E, Hintelmann H, Ridal J, Fortin D & Lean DR (2011) Biogeochemical factors influencing net mercury methylation in contaminated freshwater sediments from the St. Lawrence River in Cornwall, Ontario, Canada. *Sci Total Environ* **409**: 968-978.

Baath E (1989) Effects of Heavy Metals in Soil on Microbial Processes and Populations (A Review). *Water, Air, and Soil Pollution* **47**: 335-379.

Baldi F, Pepi M & Filippelli M (1993) Methylmercury Resistance in *Desulfovibrio desulfuricans* Strains in Relation to Methylmercury Degradation. *Appl Environ Microbiol* **59**: 2479-2485.

Barkay T (1987) Adaptation of Aquatic Microbial Communities to Hg^{2+} Stress. *Appl Environ Microbiol* **53**: 2725-2732.

Barkay T & Wagner-Dobler I (2005) Microbial Transformations of Mercury: Potentials, Challenges, and Achievements in Controlling Mercury Toxicity in the Environment. *Advances in Applied Microbiology* **57**: 1-54.

Barkay T, Miller SM & Summers AO (2003) Bacterial mercury resistance from atoms to ecosystems. *FEMS Microbiology Reviews* **27**: 355-384.

Barkay T, Kritee K, Boyd E & Geesey G (2010) A thermophilic bacterial origin and subsequent constraints by redox, light and salinity on the evolution of the microbial mercuric reductase. *Environ Microbiol* **12**: 2904-2917.

Barkay T, Turner RR, Rasmussen LD, Kelly CA & Rudd JW (1998) Luminescence-facilitated detection of bioavailable mercury in natural waters. *Bioluminescence Methods and Protocols 102,*(LaRossa RA, ed.^eds.), p.^pp. 231-246. Humana Press Inc., NJ.

Bouskill NJ, Barker-Finkel J, Galloway TS, Handy RD & Ford TE (2010) Temporal bacterial diversity associated with metal-contaminated river sediments. *Ecotoxicology* **19**: 317-328.

Brock TD & Gustavson J (1976) Ferric Iron Reduction by Sulphur- and Iron-Oxidizing Bacteria. *Appl Environ Microbiol* **32**: 567-571.

Brookes PC (1995) The use of microbial parameters in monitoring soil pollution by heavy metals. *Biol. Fertil. Soils* **19**: 269-279.

Bruce KD, Osborn AM, Pearson AJ, Strike P & Ritchie DA (1995) Genetic diversity within mer genes directly amplified from communities of noncultivated soil and sediment bacteria. *Mol Ecol* **4**: 605-612.

Bustin SA (2000) Absolute quantification of mRNA using real-time reverse transcription polymerase chain reaction assays. *Journal of Molecular Endocrinology* **25**: 169-193.

Carson RL (1962) *Silent Spring* Houghton Mifflin Company, New York, New York, USA.

Case RJ, Boucher Y, Dahllof I, Holmstrom C, Doolittle WF & Kjelleberg S (2007) Use of 16S rRNA and rpoB genes as molecular markers for microbial ecology studies. *Appl Environ Microbiol* **73**: 278-288.

Clark G (2007) *A Farewell to Alms: A Brief Economic History of the World* Princeton University Press, Princeton, New Jersey, USA.

Clarkson TW (1997) The Toxicology of Mercury. *Critical reviews in Clinical Laboratory Sciences* **34**: 369-403.

Cole JR, Wang Q, Cardenas E*, et al.* (2009) The Ribosomal Database Project: improved alignments and new tools for rRNA analysis. *Nucleic Acids Res.* **37**: D141-145.

Compeau GC & Bartha R (1985) Sulfate-Reducing Bacteria: Principal Methylators of Mercury in Anoxic Estuarine Sediment. *Appl Environ Microbiol* **50**: 498-502.

Costa DL (2007) Air Pollution. *Casarett and Doull's Toxicology: The Basic Science of Poisons* ed.^eds.), p.^pp. 1331. McGraw-Hill Professional Publishing, Blacklick, OH, USA.

Dahllof I, Baillie H & Kjelleberg S (2000) rpoB-Based Microbial Community Analysis Avoids Limitations Inherent in 16S rRNA Gene Intraspecies Heterogeneity. *Appl. Environ. Microbiol.* **66**.

DeCoste NJ, Gadkar VJ & Filion M (2011) Relative and absolute quantitative real-time PCR-based quantifications of hcnC and phlD gene transcripts in natural soil spiked with Pseudomonas sp. strain LBUM300. *Appl Environ Microbiol* **77**: 41-47.

Delongchamp TM, Lean DR, Ridal JJ & Blais JM (2009) Sediment mercury dynamics and historical trends of mercury deposition in the St. Lawrence River area of concern near Cornwall, Ontario, Canada. *Sci Total Environ* **407**: 4095-4104.

Delongchamp TM, Ridal JJ, Lean DR, Poissant L & Blais JM (2010) Mercury transport between sediments and the overlying water of the St. Lawrence River area of concern near Cornwall, Ontario. *Environ Pollut* **158**: 1487-1493.

Di-Giulio RT & Newman MC (2007) Ecotoxicology. *Casarett and Doull's Toxicology: The Basic Science of Poisons* ed.^eds.), p.^pp. 1331. McGraw-Hill Professional Publishing, Blacklick, OH, USA.

Diaz-Ravina M & Baath E (1996) Development of metal tolerance in soil bacterial communities exposed to experimentally increased metal levels. *Appl Environ Microbiol.* **62**: 2970-2977.

EPA US (1996) Method 1669: Sampling Ambient Water for Trace Metals at EPA Water Quality Criteria Levels. (Agency EP, ed.^eds.), p.^pp. U.S. Government, Washington, DC, U.S.A.

EPA US (2002) Method 1631, Revision E: Mercury in Water by Oxidation, Purge and Trap, and Cold Vapor Atomic Fluorescence Spectrometry. (Agency EP, ed.^eds.), p.^pp. U.S. Government, Washington, DC, U.S.

Ercal N, Gurer-Orhan H & Aykin-Burns N (2001) Toxic Metals and Oxidative Stress Part I: Mechanisms Involved in Metal-induced Oxidative Damage. *Current Topics in Medicinal Chemistry* **1**: 557-568.

Farr S & Kogoma T (1991) Oxidative Stress Responses in Escherichia coli and Salmonella typhimurium. *Microbiological Reviews* **55**: 561-585.

Fortin N, Beaumier D, Lee K & Greer CW (2004) Soil washing improves the recovery of total community DNA from polluted and high organic content sediments. *Journal of Microbiological Methods* **56**: 181-191.

Fredrickson JK, Hicks RJ, Li SW & Brockman FJ (1988) Plasmid Incidence in Bacteria from Deep Subsurface Sediments. *Appl Environ Microbiol* **54**: 2916-2923.

Frias-Lopez J, Shi Y, Tyson GW, Coleman ML, Schuster SC, Chisholm SW & Delong EF (2008) Microbial community gene expression in ocean surface waters. *Proc Natl Acad Sci U S A* **105**: 3805-3810.

Friesen MC, Demers PA, Spinelli JJ, Lorenzi MF & Le ND (2007) Comparison of two indices of exposure to polycyclic aromatic hydrocarbons in a retrospective aluminium smelter cohort. *Occup Environ Med* **64**: 273-278.

Fritsche J, Obrist D & Alewell C (2008) Evidence of microbial control of Hg^0 emissions from uncontaminated terrestrial soils. *J. Plant Nutr. Soil Sci.* **170**: 200-209.

Frostegard A, Tunlid A & Baath E (1993) Phospholipid Fatty Acid Composition, Biomass, and Activity of Microbial Communities from Two Soil Types Experimentally Exposed to Different Heavy Metals. *Appl Environ Microbiol* **59**: 3605-3617.

Gagnon C, Pelletier E & Mucci A (1997) Behaviour of anthropogenic mercury in coastal marine sediments. *Marine Chemistry* **59**: 159-176.

Gelencser A, Kovats N, Turoczi B*, et al.* (2011) The Red Mud Accident in Ajka (Hungary): Characterization and Potential Health Effects of Fugitive Dust. *Environ Sci Technol*.

Gihring TM, Green SJ & Schadt CW (2012) Massively parallel rRNA gene sequencing exacerbates the potential for biased community diversity comparisons due to variable library sizes. *Environ Microbiol* **14**: 285-290.

Giller KE, Witter E & McGrath SP (1998) Toxicity of Heavy Metals to Microorganisms and Microbial Processes in Agricultural Soils: A Review. *Soil Biology & Biochemistry* **30**: 1389-1414.

Godocikova J, Zamocky M, Buckova M, Obinger C & Polek B (2010) Molecular diversity of katG genes in the soil bacteria Comamonas. *Arch Microbiol* **192**: 175-184.

Goldman CR (1988) Primary productivity, nutrients, and transparency during the early onset of eutrophication in ultra-oligotrophic Lake Tahoe, California-Nevada. *Limnol. Oceanogr.* **33**: 1321-1333.

Good I (1953) The Population Frequencies of Species and the Estimation of Population Parameters. *Biometrika* **40**: 237-364.

Gough HL & Stahl DA (2011) Microbial community structures in anoxic freshwater lake sediment along a metal contamination gradient. *ISME J* **5**: 543-558.

Gupta RS (2000) The phylogeny of proteobacteria: relationships to other eubacterial phyla and eukaryotes. *FEMS Microbiol Ecol* **24**: 367-402.

Habashi F (1998) *Amalgam and Electrometallurgy*. Métallurgie Extractive Québec, Sainte-Foy, Québec.

Habashi F (2005) A short history of hydrometallurgy. *Hydrometallurgy* **79**: 15-22.

Hamilton WP, Turner RR & Ghosh MM (1995) Effect of pH and Iodide on the Adsoprtion of Mercury (II) by Illite. *Water, Air, and Soil Pollution* **80**: 483-486.

Haritha A, Sagar KP, Tiwari A, Kiranmayi P, Rodrigue A, Mohan PM & Singh SS (2009) MrdH, a novel metal resistance determinant of Pseudomonas putida KT2440, is flanked by metal-inducible mobile genetic elements. *J Bacteriol* **191**: 5976-5987.

Harris-Hellal J, Vallaeys T, Garnier-Zarli E & Bousserrhine N (2009) Effects of mercury on soil microbial communities in tropical soils of French Guyana. *Applied Soil Ecology* **41**: 59-68.

HealthCanada (1986) Water Quality - Mercury. Vol. September 2012 ed.^eds.), p.^pp. Government of Canada.

HealthCanada (1992) Water Quality - Lead. Vol. September 2012 ed.^eds.), p.^pp. Government of Canada.

Hill MO (1973) Diversity and Evenness: A Unifying Notation and Its Consequences. *Ecology* **54**: 427-432.

Holland HD (2006) The oxygenation of the atmosphere and oceans. *Philos Trans R Soc Lond B Biol Sci* **361**: 903-915.

Huber R, Wilharm T, Huber D*, et al.* (1992) Aquifex pyrophilus gen. nov. sp. nov., Represents a Novel Group of Marine Hyperthermophilic Hydrogen-Oxidizing Bacteria. *Systematic and Applied Microbiology* **15**: 340-351.

Hughes JB, Hellmann JJ, Ricketts TH & Bohannan BJM (2001) Counting the Uncountable: Statistical Approaches to Estimating Microbial Diversity. *Appl Environ Microbiol* **67**: 4399-4406.

Hurt RA, Qiu X, Wu L, Roh Y, Palumbo AV, Tiedje JM & Zhou J (2001) Simultaneous Recovery of RNA and DNA from Soils and Sediments. *Appl Environ Microbiol* **67**: 4495-4503.

Hydro-Québec (2011) Annual Report 2010. ed.^eds.), p.^pp. 122. Government of Quebec, Montreal, Canada.

Hynninen A (2010) Zinc, cadmium and lead resistance mechanisms in bacteria and their contribution to biosensing. Ph.D Thesis, University of Helsinki, Helsinki.

Hynninen A, Touze T, Pitkanen L, Mengin-Lecreulx D & Virta M (2009) An efflux transporter PbrA and a phosphatase PbrB cooperate in a lead-resistance mechanism in bacteria. *Mol Microbiol* **74**: 384-394.

Jones BEH & Haynes RJ (2011) Bauxite Processing Residue: A Critical Review of Its Formation, Properties, Storage, and Revegetation. *Critical Reviews in Environmental Science and Technology* **41**: 271-315.

Jordan D, Kremer RJ, Bergfield WA, Kim KY & Cacnio VN (1995) Evaluation of microbial methods as potential indicators of soil quality in historical agricultural fields. *Biol. Fertil. Soils* **19**: 297-302.

Kim M, Morrison M & Yu Z (2011) Evaluation of different partial 16S rRNA gene sequence regions for phylogenetic analysis of microbiomes. *J Microbiol Methods* **84**: 81-87.

Lanave C, Preparata G, Saccone C & Serio G (1984) A New Method for Calculating Evolutionary Substitution Rates. *J. Mol. Evol.* **20**: 86-93.

Larsen RF & Anon MC (1989) Effect of Water Activity a_w of Milk on acid Production by *Streptococcus thermophilus* and *Lactobacillus bulgaricus*. *Journal of Food Science* **54**: 917-921.

Lee PK, Macbeth TW, Sorenson KS, Jr., Deeb RA & Alvarez-Cohen L (2008) Quantifying genes and transcripts to assess the in situ physiology of "Dehalococcoides" spp. in a trichloroethene-contaminated groundwater site. *Appl Environ Microbiol* **74**: 2728-2739.

Legault G (1996) Fact Sheet No. 48: Alcan Smelters and Chemicals Ltd., Jonquière Works. Vol. 48 ed.^eds.), p.^pp. Minister of the Environment - Minister of Supply and Services Canada, Environment Canada.

Lewen N, Mathew S, Schenkenberger M & Raglione T (2004) A rapid ICP-MS screen for heavy metals in pharmaceutical compounds. *Journal of Pharmaceutical and Biomedical Analysis* **35**: 739-752.

Liang Y, Van Nostrand JD, Deng Y*, et al.* (2011) Functional gene diversity of soil microbial communities from five oil-contaminated fields in China. *ISME J* **5**: 403-413.

Liebert CA, Wireman J, Smith T & Summers AO (1997) Phylogeny of Mercury Resistance (mer) Operons of Gram-Negative Bacteria Isolated from the Fecal Flora of Primates. *Applied and Environmental Microbiology* **63**: 1066-1076.

Loring DH, Rantala RTT & Smith JN (1983) Response Time of Saguenay Fjord Sediments to Metal Contamination. *Environ. Biogeochem. Ecol. Bull.* **35**: 59-72.

Lovley JRLDR (2001) Microbial detoxification of metals and radionuclides. *Current Opinion in Biotechnology* **12**: 248-253.

Lozupone C & Knight R (2005) UniFrac: a new phylogenetic method for comparing microbial communities. *Appl Environ Microbiol* **71**: 8228-8235.

Lydy MJ, Lohner TW & Fisher SW (1990) Influence of pH, temperature and sediment type on the toxicity, accumulation and degredation of parathion in aquatic systems. *Aquat Toxicol* **17**: 27-44.

MacNaughton SJ, Stephen JR, Venosa AD, Davis GA, Chang Y-J & White DC (1999) Microbial Population Changes during Bioremediation of an Experimental Oil Spill. *Appl Environ Microbiol* **65**: 3566-3576.

Margulies M, Egholm M, Altman WE*, et al.* (2005) Genome sequencing in microfabricated high-density picolitre reactors. *Nature* **437**: 376-380.

Miller LL, Rasmussen JB, Palace VP & Hontela A (2009) The physiological stress response and oxidative stress biomarkers in rainbow trout and brook trout from selenium-impacted streams in a coal mining region. *J Appl Toxicol* **29**: 681-688.

Mimna R, Kildea J, Phillips EC, Carlson W, Keiser B & Meier J (2011) Opportunities for Improved Environmental Control in the Alumina Industry. (Lindsay SJ, ed.^eds.), p.^pp. 185-190. John Wiley & Sons, Inc.

Muller AK, Westergaard K, Christensen S & Sorensen SJ (2002) The diversity and function of soil microbial communities exposed to different disturbances. *Microb Ecol* **44**: 49-58.

Muller$_a$ AK, Rasmussen LD & Sorensen SJ (2001) Adaptation of the bacterial community to mercury contamination. *FEMS Microbiology Letters* **204**: 49-53.

Muller$_b$ AK, Westergaard K, Christensen S & Sorensen SJ (2001) The effect of long-term mercury pollution on the soil microbial community. *FEMS Microbiol Ecol* **36**: 11-19.

Niederberger TD, Perreault NN, Tille S*, et al.* (2010) Microbial characterization of a subzero, hypersaline methane seep in the Canadian High Arctic. *ISME J* **4**: 1326-1339.

Nies DH (1999) Microbial heavy-metal resistance. *Appl Microbiol Biotechnol* **51**: 730-750.

Nies DH (2003) Efflux-mediated heavy metal resistance in prokaryotes. *FEMS Microbiology Reviews* **27**: 313-339.

Orell A, Navarro CA, Arancibia R, Mobarec JC & Jerez CA (2010) Life in blue: copper resistance mechanisms of bacteria and archaea used in industrial biomining of minerals. *Biotechnol Adv* **28**: 839-848.

Osborn AM & Smith CJ (2005) Molecular Microbial Ecology. ed.^eds.), p.^pp. 381. Taylor & Francis Group, 270 Madison Avenue, New York, NY 10016.

Osborn AM, Bruce KD, Strike P & Ritchie DA (1997) Distribution, diversity and evolution of the bacterial mercury resistance (mer) operon. *FEMS Microbiol Ecol* **19**: 239-262.

P. D. Schloss, Westcott SL, Ryabin T*, et al.* (2009) Introducing Mothur: Open-Source, Platform-Independent, Community-Supported Software for Describing and Comparing Microbial Communities. *Appl Environ Microbiol* **75**: 7537-7541.

Pan-Hou$_a$ HSK & Imura N (1981) Role of Hydrogen Sulfide in Mercury Resistance Determined by Plasmid of *Clostridium cochlearium* T-2. *Arch Microbiol* **129**: 49-52.

Pan-Hou$_b$ HS, Nishimoto M & Imura N (1981) Possible Role of Membrane Proteins in Mercury Resistance of *Enterobacter aerogenes*. *Arch Microbiol* **130**: 93-95.

Perales-Vela HV, Pena-Castro JM & Canizares-Villanueva RO (2006) Heavy metal detoxification in eukaryotic microalgae. *Chemosphere* **64**: 1-10.

Posada D (2008) jModelTest: Phylogenetic model averaging. *Mol. Biol. Evol.* **25**: 1253-1256.

Poulain AJ, Ni Chadhain SM, Ariya PA*, et al.* (2007) Potential for mercury reduction by microbes in the high arctic. *Appl Environ Microbiol* **73**: 2230-2238.

Price MN, Dehal PS & Arkin AP (2010) FastTree 2 -- Approximately Maximum-Likelihood Trees for Large Alignments. *PLoS ONE* **5**: e9490.

Raphael E, Wong LK & Riley LW (2011) Extended-spectrum Beta-lactamase gene sequences in gram-negative saprophytes on retail organic and nonorganic spinach. *Appl Environ Microbiol* **77**: 1601-1607.

Rasmussen LD & Sørensen SJ (1998) The Effect of Longterm Exposure to Mercury on the Bacterial Community in Marine Sediment. *Current Microbiology* **36**: 291-297.

Rasmussen LD, Sorensen SJ, Turner RR & Barkay T (2000) Application of a mer-lux biosensor for estimating bioavailable mercury in soil. *Soil Biology & Biochemistry* **32**: 639-646.

Rasmussen LD, Zawadsky C, Binnerup SJ, Oregaard G, Sorensen SJ & Kroer N (2008) Cultivation of hard-to-culture subsurface mercury-resistant bacteria and discovery of new merA gene sequences. *Appl Environ Microbiol* **74**: 3795-3803.

RéseauTransAl I (2007) Canadian Alumnium Transformation Technology Roadmap. (Canada NRC, ed.^eds.), p.^pp. 124.

Roose-Amsaleg CL, Garnier-Sillam E & Harry M (2001) Extraction and purification of microbial DNA from soil and sediment samples. *Applied Soil Ecology* **18**: 47-60.

Ruyters S, Mertens J, Vassilieva E, Dehandschutter B, Poffijn A & Smolders E (2011) The Red Mud Accident in Ajka (Hungary): Plant Toxicity and Trace Metal Bioavailability in Red Mud Contaminated Soil. *Environ Sci Technol*.

Sandaa R-A, Torsvik V, Enger O, Daae FL, Castberg T & Hahn D (1999) Analysis of bacterial communities in heavy metal-contaminated soils at different levels of resolution. *FEMS Microbiol Ecol* **30**: 237-251.

Sass P (2009) Canadian Minerals Yearbook (CMY) - 2009 - Aluminum. (Canada NR, ed.^eds.), p.^pp. Government of Canada, Ottawa, Canada.

Schaefer JK, Yagi J, Reinfelder JR, Cardona T, Ellickson KM, Tel-Or S & Barkay T (2004) Role of the Bacterial Organomercury Lyase (MerB) in Controlling Methylmercury Accumulation in Mercury-Contaminated Natural Waters. *Environ. Sci. Technol.* **38**: 4304-4311.

Sessitsch A, Gyamfi S, Stralis-Pavese N, Weilharter A & Pfeifer U (2002) RNA isolation from soil for bacterial community and functional analysis: evaluation of different extraction and soil conservation protocols. *Journal of Microbiological Methods* **51**: 171-179.

Shapiro B, Rambaut A & Drummond AJ (2006) Choosing appropriate substitution models for the phylogenetic analysis of protein-coding sequences. *Mol Biol Evol* **23**: 7-9.

Silver$_a$ S & Phung LT (2005) Genes and enzymes involved in bacterial oxidation and reduction of inorganic arsenic. *Appl Environ Microbiol* **71**: 599-608.

Silver$_b$ S & Phung LT (2005) A bacterial view of the periodic table: genes and proteins for toxic inorganic ions. *J Ind Microbiol Biotechnol* **32**: 587-605.

Smith T, Pitts K, McGarvey JA & Summers AO (1998) Bacterial Oxidation of Mercury Metal Vapor, Hg(0). *Appl Environ Microbiol* **64**: 1328-1332.

StatsCan (2012) Saguenay--Lac-Saint-Jean, Quebec (Code 2475) and Quebec (Code 24) (table). Census Profile. (Statistics-Canada, ed.^eds.), p.^pp. Ottawa, Canada.

Steffen A, Douglas T, Amyot M*, et al.* (2008) A synthesis of atmospheric mercury depletion event chemistry in the atmosphere and snow. *Atmos. Chem. Phys.* **8**: 1445-1482.

Sugarman B (1983) Zinc and Infection. *Reviews of Infectious Diseases* **5**: 137-147.

Sylvan JB, Toner BM & Edwards KJ (2012) Life and death of deep-sea vents: bacterial diversity and ecosystem succession on inactive hydrothermal sulfides. *MBio* **3**: e00279-00211.

Tamaki H, Tanaka Y, Matsuzawa H*, et al.* (2011) Armatimonas rosea gen. nov., sp. nov., of a novel bacterial phylum, Armatimonadetes phyl. nov., formally called the candidate phylum OP10. *Int J Syst Evol Microbiol* **61**: 1442-1447.

Thomas F, Hehemann JH, Rebuffet E, Czjzek M & Michel G (2011) Environmental and gut bacteroidetes: the food connection. *Front Microbiol* **2**: 93.

Trelawny P & Pearce P (2009) Canadian Minerals Yearbook (CMY) - 2009. (Canada NR, ed.^eds.), p.^pp. Government of Canada, Ottawa, Canada.

Truhaut R (1977) Ecotoxicology: Objectives, Principles and Perspectives. *Ecotoxicol Environ Saf* **1**: 151-173.

Turekian KK & Wedepohl KH (1961) Distribution of the Elements in Some Major Units of the Earth's Crust. *Geological Society of America Bulletin* **72**: 175-192.

UNEP (2002) Global Mercury Assessment. (UNEP-Chemicals, ed.^eds.), p.^pp. 270. United Nations Environment Programme - Chemicals, Geneva, Switzerland.

UNEP (2008) The Global Atmospheric Mercury Assessment: Sources, Emissions, and Transport. (UNEP-Chemicals, ed.^eds.), p.^pp. 44. United Nations Environment Programme - Chemicals, Geneva, Switzerland.

Valavanidis A, Vlahogianni T, Dassenakis M & Scoullos M (2006) Molecular biomarkers of oxidative stress in aquatic organisms in relation to toxic environmental pollutants. *Ecotoxicol Environ Saf* **64**: 178-189.

Valko M, Morris H & Cronin MTD (2005) Metal, Toxicity and Oxidative Stress. *Current Medicinal Chemistry* **12**: 1161.

Van-Straalen NM (2003) Ecotoxicology becomes stress ecology. *Environ. Sci. Technol.* 324A-330A.

Ventura M, Canchaya C, Tauch A, Chandra G, Fitzgerald GF, Chater KF & van Sinderen D (2007) Genomics of Actinobacteria: tracing the evolutionary history of an ancient phylum. *Microbiol Mol Biol Rev* **71**: 495-548.

Wedepohl KH (1995) The composition of the continental crust. *Geochimica et Cosmochimica Acta* **59**: 1217-1232.

Yoshida M, Yoshida T, Kashima A, Takashima Y, Hosoda N, Nagasaki K & Hiroishi S (2008) Ecological dynamics of the toxic bloom-forming cyanobacterium Microcystis aeruginosa and its cyanophages in freshwater. *Appl Environ Microbiol* **74**: 3269-3273.

Zhang H (2006) Photochemical Redox Reactions of Mercury Recent Developments in Mercury Science. **120**: 37-79.

Zhou J, Bruns MA & Tiedje JM (1996) DNA Recovery from Soils of Diverse Composition. *Appl Environ Microbiol* **62**: 316-322.